CalVal Jason-2

Jason-2 validation and cross calibration activities

Contract No 60453/00 - lot2.C

Reference : CLS.DOS/NT/10-004

Nomenclature : SALP-RP-MA-EA-21794-CLS

Issue : 1rev 0

Date : January 26, 2010

SALP Service Altimetrie & Localisation Precise

CLS Collecte Localisation Satellites

cnes Centre National d'Études Spatiales

CLS - 8-10 Rue Hermès - Parc Technologique du Canal - 31520 Ramonville St-Agne - FRANCE
Telephone 33 5 61 39 47 00 / Fax 33 5 61 75 10 14

Chronology Issues:		
Issue:	Date:	Reason for change:
1rev0	January 22, 2010	Creation

People involved in this issue:		
Written by:	S. Philipps M. Ablain	CLS CLS
Checked by:	DT/AQM	CLS
Approved by:	JP. Dumont	CLS
Application authorized by:		

Index Sheet :	
Context:	
Keywords:	
Hyperlink:	

Distribution:		
Company	Means of distribution	Names
CLS/DOS	1 electronic copy	G.DIBARBOURE
	1 electronic copy	V.ROSMORDUC
	1 electronic copy	P.ESCUDIER
	1 electronic copy	J.DORANDEU
DT/AQM (DOC/CLS)	1 printed copy + 1 cd-rom	DOCUMENTATION
CNES	1 cd-rom	E.BRONNER
CNES	1 cd-rom	T.GUINLE
CNES	1 cd-rom	T. AL ARISS
CNES	1 cd-rom	D.CHERMAIN
CNES	1 cd-rom	T.CORREALE
CNES	via gestion doc CNES	J.LAMBIN
CNES	via gestion doc CNES	A.LOMBARD
CNES	via gestion doc CNES	N.PICOT
CNES	via gestion doc CNES	J.NOUBEL

List of tables and figures

List of Tables

List of Figures

Contents

1. Introduction

This document presents the synthesis report concerning validation activities of Jason-2 GDRs under SALP contract (N° 60453/00 Lot2.C) supported by CNES at the CLS Space Oceanography Division. It is divided into two parts: CAL/VAL Jason-2 activities - Jason-2 / Jason-1 cross-calibration.
The OSTM/Jason-2 satellite was successfully launched on June, 20th 2008. Since July, 4th, Jason-2 is on its final orbit. Until January 2009, it was flying in tandem with Jason-1, only 55s apart. Since the beginning of the mission, Jason-2 data have been analyzed and monitored in order to assess the quality of Jason-2 products. Cycle per cycle reports are available on AVISO webpage.
This present report assesses the Jason-2 data quality. Missing and edited measurements are monitored. Furthermore relevant parameters derived from instrumental measurements and geophysical corrections are analyzed.
Analyzes are focused on Jason-1/Jason-2 cross-calibration since both missions were on the same orbit during the Calibration/Validation phase until the 26th of January 2009. This allows to precisely assess parameter discrepancies between both missions in order to detect geographically correlated biases, jumps or drifts. The SLA performances and consistency with Jason-1 are also described. Even if only low order statistics are mainly presented here, other analyzes including histograms, plots and maps are continuously produced and used in the quality assessment process. Indeed, it is now well recognized that the usefulness of any altimeter data only makes sense in a multi-mission context, given the growing importance of scientific needs and applications, in particular for operational oceanography. One major objective of the Jason-2 mission is to continue the Jason-1 and T/P high precision altimetry and to allow combination with other missions (ENVISAT, Jason-1). This kind of comparisons between different altimeter missions flying together provides a large number of estimations and consequently efficient long term monitoring of instrument measurements.

2. Processing status

2.1. Processing

End of 2008 Jason-2 data were already available to end users in OGDR (3h data latency) and IGDR (1-2 days data latency). They are available in version "c", the same version as Jason-1 data (for better compatibility). GDR data were released in version T during August 2009. In this report, GDRs from cycle 1 to 50 are used (till 19/11/2009). A description of the different Jason-2 products is available in the OSTM/Jason-2 Products handbook ([17]), as well as in the GDR version T product disclaimer ([15])
The purpose of this document is to report the major features of the data quality from the Jason-2 mission. As Jason-2 was in tandem flight formation with Jason-1 (only 55 s apart) till January 2009, this report focuses on intercalibration with Jason-1.

2.2. CAL/VAL status

2.2.1. List of events

The following table shows the major plannified events during the beginning of Jason-2 mission.

Dates	Events	Impacts
4 July 2008 5h57	Start of Jason-2 Cycle 0	
4 July 2008 12h15	Start of Poseidon3 altimeter. Tracking mode : autonomous acquisition, median	Start of level2 product generation.
04 July 2008 13:47:52 to 04 July 2008 14:13:36	Poseidon3 altimeter. Tracking mode : Diode acquisition, median	
04 July 2008 14:14:39 to 17 July 2008 15:30:22	Poseidon3 altimeter. Tracking mode : Diode acquisition, SGT	
8 July 2008 4h45 - 5h25	Poseidon3 altimeter. Dedicated period for validation of tracking mode performances	small data gaps on corresponding passes [Cycle 0]
11 July 2008 13h00-13h01 and 13h04-13h12	Poseidon3 altimeter. Tracking mode : Diode-DEM (functional)	Functional test of DIODE-DEM tracking mode while onboard DEM was not correct, leading to wrong waveforms and so impacts on altimeter retracking outputs.
12 July 2008 1h20	Start of Jason-2 Cycle 1	
		.../...

Dates	Events	Impacts
16 July 2008 7h10-17h08	upload POS3 - DEM	Data gap on corresponding passes [Cycle 1, Pass 108-144]
17 July 2008 7h29-11h30	upload POS3 - DEM	Data gap on corresponding passes [Cycle 1, Pass 108-144]
17 July 2008 15:30:22 to 31 July 2008 21:17:08 UTC	Poseidon3 altimeter. Tracking mode : Diode acquisition, median	
21 July 2008 23h18	Start of Jason-2 Cycle 2	
31 July 2008 21:17:09 to 10 August 2008 19:15:39	Jason-2 Cycle 3: Poseidon3 altimeter. Tracking mode : Diode-DEM	
10 August 2008 19:15:40 to 20 August 2008 17:14:10	Jason-2 Cycle 4: Poseidon3 altimeter. Tracking mode : Diode acquisition, median	
20 August 2008 17:14:11 to 30 August 2008 15:12:43	Jason-2 Cycle 5: Poseidon3 altimeter. Tracking mode : Diode-DEM	
30 August 2008 15:12:43 to 9 September 2008 13:11:15	Jason-2 Cycle 6: Poseidon3 altimeter. Tracking mode : Diode acquisition, median	
9 September 2008 13:11:15 to 19 September 2008 11:09:47	Jason-2 Cycle 7: Poseidon3 altimeter. Tracking mode : Diode-DEM	
19 September 2008 11:09:47 to 29 September 2008 09:08:19	Jason-2 Cycle 8: Poseidon3 altimeter. Tracking mode : Diode acquisition, median	
11 Mai 2009 12:09 to 14 Mai 2009 13:09	Upload POS3 (new DEM)	data gaps (northern hemisphere) for passes 154 to 231
2 February 2009 06:55:11 to 15:58:05	software upload to Poseidon-3	data gap between passes 204 and 213
4 June 2009 06:31:27 to 14 June 2008 04:29:59	Jason-2 Cycle 34: Poseidon3 altimeter. Tracking mode : Diode-DEM	

Table 1: *P*lannified events

2.2.2. Missing measurements

This section presents a summary of major satellite or ground segment events that occurred from cycle 0 to 50. Table 2 gives a status about the number of missing passes (or partly missing) for GDRs, as well as the associated events for each cycle.
Up to now, Jason-2 has little missing measurements. They were mainly caused by station acquisition problems, ground processing anomalies or plannified events (like upload of DEM software).

Jason-2 Cycles/Pass	Dates	Events
000/222-224	10/07/2008 - 18:28:02 to 20:25:04	Missing telemetry (Usingen station pb)
000/232	11/07/2008 - 03:57:08 to 04:30:30	Partly missing due to altimeter calibration (long LPF)
000/235	11/07/2008 - 07:01:28 to 07:27:41	Partly missing due to altimeter calibration (CNG step)
001/44-46	13/07/2008 - 17:40:00 to 19:37:30	Missing telemetry (Usingen station pb)
001/48-50	13/07/2008 - 21:37:02 to 23:30:00	Missing telemetry (NOAA station pb)
001/108-144		several passes partly missing due to upload of new DEM (plannified unavailability)
003/032-035	02/08/2008 - 02:23:45 to 05:46:30	Passes 32 and 35 are partly missing, passes 33 and 34 are completely missing due to missing telemetry (Usingen)
005/236-241	29/08/2008 - 21:44:56 to 30/08/2008 02:52:07	Missing telemetry (Usingen station pb): passes 237 to 240 completely missing, passes 236 and 241 partly missing
006/232	08/09/2008 - 15:48:00 to 16:21:22	pass 232 partially missing due to altimeter calibration (long LPF)
006/235	08/09/2008 - 18:53:00 to 19:19:10	pass 235 partially missing due to altimeter calibration (CNG step)
016/73	10/12/2008 - 15:11:19 to 15:13:27	pass 73 partially missing due to 1) upload of correction for low signal tracking anomaly and 2) memory dumps (planned unavailability)
026/33	18/03/2009 - 05:09:15 to 05:10:44	pass 33 has approximatly 90 seconds of missing ocean measurements in gulf of guinea (probably due to missing telemetry)
.../...		

Jason-2 Cycles/Pass	Dates	Events
029/209-210	23/04/2009 - 20:18:36 to 20:35:11	data gap over land (on transition between passes 209 and 210) due to missing telemetry
031/154-231	11/05/2009 12:09 to 14/05/2009 13:09	Upload of new DEM leading to missing portions (northern hemisphere) for passes 154 to 231
033/204-213	02/06/2009 - 06:55:11 to 15:58:05	Passes 205 to 212 are completely missing. Passes 204 and 213 are partly missing with respectively 100% and 96% of missing measurements over ocean. This is due to software upload to Poseidon-3.
034/232	13/06/2009 - 07:07:03 to 07:40:23	Due to long calibration, pass 232 is partly missing with 65% of missing measurements over ocean.
034/235	13/06/2009 - 10:11:41 to 10:37:50	Due to calibration CNG step, pass 235 is partly missing with 8% of missing measurements over ocean.
037/54	06/07/2009 - 02:33:12 to 02:34:33	pass 054 has a small data gap due to missing PLTM

Table 2: *M*issing pass status

2.2.3. Edited measurements

Table 3 indicates particular high editing periods (see section 3.2.1.). Most of the occurrences correspond to radiometer wet troposphere correction at default value (due to processing anomalies) or altimeter low signal tracking anomaly (AGC anomaly), though the latter concerns only few measurements and was corrected during cycle 16 (see section 7.1.).

Jason-2 Cycles/Passes	Date	Comments
000/89	05/07/08 - 14:22:07 to 14:23:38	Partly edited by several parameters out of threshold (AGC anomaly)
000/134	07/07/08 - 08:06:37 to 08:28:57	Partly edited by several parameters out of threshold (AGC anomaly)
000/156	08/07/08 - 04:35:12 to 05:31:01	rain flag is set (dotted), probably related to start/stop sequence (from 04:45 to 05:24)
000/234	11/07/08 - 05:45:12 to 05:49:03	Partly edited by several parameters out of threshold (AGC anomaly)
.../...		

Jason-2 Cycles/Passes	Date	Comments
000/241	11/07/08 - 13:04:27 to 13:09:11	Partly edited by ice flag (number of elementary Ku-band measurements at 0, AGC=16.88) due to test of altimeter DEM mode
001/		several passes partly edited by several parameters out of threshold (AGC anomaly)
002/		several passes partly edited by several parameters out of threshold (AGC anomaly)
004/		several passes partly edited by several parameters out of threshold (AGC anomaly)
006/		several passes partly edited by several parameters out of threshold (AGC anomaly)
008/		several passes partly edited by several parameters out of threshold (AGC anomaly)
009/		several passes partly edited by several parameters out of threshold (AGC anomaly)
010/		several passes partly edited by several parameters out of threshold (AGC anomaly)
011/		several passes partly edited by several parameters out of threshold (AGC anomaly)
012/		several passes partly edited by several parameters out of threshold (AGC anomaly)
013/		several passes partly edited by several parameters out of threshold (AGC anomaly)
014/		several passes partly edited by several parameters out of threshold (AGC anomaly)
015/		several passes partly edited by several parameters out of threshold (AGC anomaly)
019/024-042	07/01/ 11:00:35 to 08/01/2009 03:23:34	radiometer wet troposphere correction at default value due to AMR unavailability
019/119-161	11/01/ 03:56:38 to 12/01/2009 19:26:14	radiometer wet troposphere correction at default value due to AMR unavailability

Table 3: *E*dited measurement status

2.3. Models and Standards History

Two versions of the Jason-2 Operational Geophysical Data Records (OGDRs) and Interim Geophysical Data Records (IGDRs) have been generated to date. These two versions are identified by the version numbers "T" (for test) and "c" in the product filename. For example, version "T" IGDRs are named "JA2_IPN_2PT" and version "c" IGDRs are named "JA2_IPN_2Pc". Both versions adopt an identical data record format as described in Jason-2 User Handbook ([17]) and differ only sligthly (names of variables are corrected and 3 variables added). Version "T" O/IGDRs were the first version released soon after launch and was disseminated only to OSTST community. Version "c" O/IGDRs were first implemented operationally from data segment 141 of cycle 15 for the OGDRs (3rd December 2008) and cycle 15 for the IGDRs. Version "c" of Jason-2 data is consistent with version "c" of Jason-1 data. Note that up to now only one GDR product version is available (version T). The table 4 below summarizes the models and standards that are adopted for versions "T" and "c" of Jason-2 data. More details on some of these models are provided in Jason-2 User Handbook document ([17]).

Model	Product version "T" and "c"
Orbit	Based on Doris onboard navigator solution for OGDRS. DORIS tracking data for IGDRs DORIS+SLR+GPS tracking data for GDRs.
Altimeter Retracking	"Ocean" retracking: MLE4 fit from 2nd order Brown model: MLE4 simultaneously retrieves the 4 parameters that can be inverted from the altimeter waveforms: • Epoch (tracker range offset) → altimeter range • Composite Sigma → SWH • Amplitude → Sigma0 • Square of mispointing angle "Ice" retracking: Geometrical analysis of the altimeter waveforms, which retrieves the following parameters: • Epoch (tracker range offset) → altimeter range • Amplitude → Sigma0
Altimeter Instrument Corrections	Consistent with MLE4 retracking algorithm.
Jason-2 Advanced Microwave Radiometer (AMR) Parameters	Using calibration parameters derived from long term calibration tool developed and operated by NASA/JPL.
	.../...

Model	Product version "T" and "c"
Dry Troposphere Range Correction	From ECMWF atmospheric pressures and model for S1 and S2 atmospheric tides
Wet Troposphere Range Correction from Model	From ECMWF model
Sea State Bias Model	Empirical model derived from 3 years of MLE4 Jason-1 altimeter data with version "b" geophysical models.
Mean Sea Surface Model	CLS01
Geoid	EGM96
Bathymetry Model	DTM2000.1
Inverse Barometer Correction	Computed from ECMWF atmospheric pressures after removing S1 and S2 atmospheric tides
Non-tidal High-frequency De-aliasing Correction	Mog2D high resolution ocean model on I/GDRs. None on OGDRs. Ocean model forced by ECMWF atmospheric pressures after removing S1 and S2 atmospheric tides.
Tide Solution 1	GOT00.2 + S1 ocean tide . S1 load tide ignored
Tide Solution 2	FES2004 + S1 and M4 ocean tides. S1 and M4 load tides ignored
Equilibrium long-period ocean tide model.	From Cartwright and Taylor tidal potential.
Non-equilibrium long-period ocean tide model.	Mm, Mf, Mtm, and Msqm from FES2004
Solid Earth Tide Model	From Cartwright and Taylor tidal potential.
Pole Tide Model	Equilibrium model
Wind Speed from Model	ECMWF model
Altimeter Wind Speed	Derived from TOPEX/POSEIDON data

Table 4: *M*odels and standards adopted for the Jason-2 products. Taken from [17]

3. Data coverage and edited measurements

3.1. Missing measurements

3.1.1. Over land and ocean

Determination of missing measurements relative to the theoretically expected orbit ground pattern is an essential tool to detect missing telemetry or satellite events for instance. Applying the same procedure for Jason-1 and Jason-2, the comparison of the percentage of missing measurements has been performed. Jason-2 can use several onboard tracking modes: Split Gate Tracker (ie the Jason-1 tracking mode, and used for cycle 0 and half of cycle 1), Diode/DEM (used for cycles 3, 5, 7, and 34) and median tracker (used for the other cycles). These different tracking modes are described by [12]. Thanks to the new modes of onboard tracking (median tracker and especially Diode/DEM), the data coverage over land surface was dramatically increased in comparison with Jason-1 depending on the tracker mode and the period. Figure 1 shows the percentage of missing measurements for Jason-2 and Jason-1 (all surfaces) computed with respect to a theoretical possible number of measurements. Due to differences between altimeter tracking algorithms, the number of available data is greater for Jason-2 than for Jason-1. Differences appear on land surfaces as shown in figure 2. Since cycle 16, percentage of missing measurements of Jason-2 has slightly increased due to the correction of the low signal tracking anomaly (see section 7.1.), but also due to an annual cycle. The missing data are highly correlated with the mountains location.

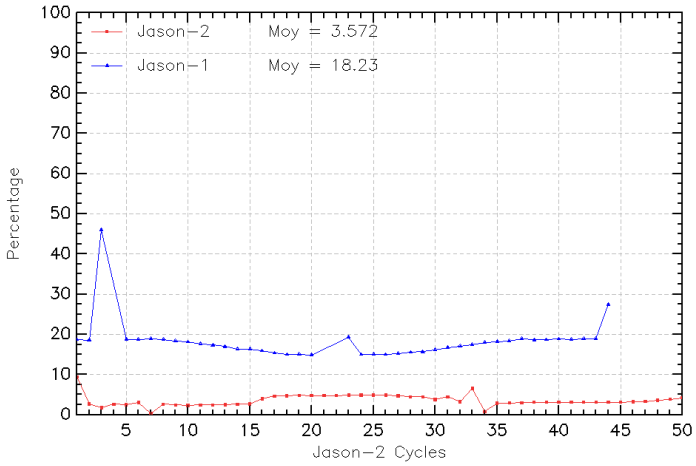

Figure 1: *Percentage of missing measurements over ocean and land for JA2 and JA1*

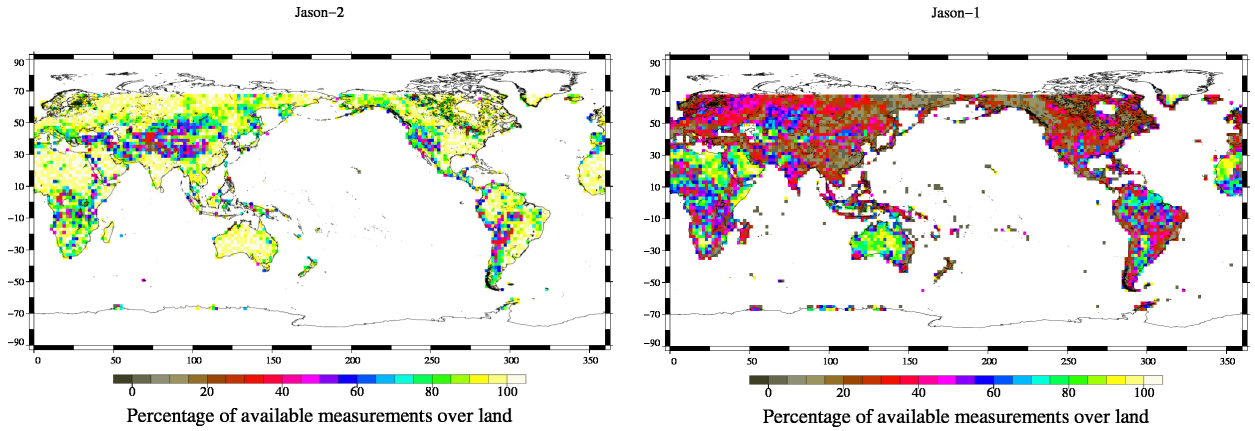

Figure 2: *Map of percentage of available measurements over land for Jason-2 on cycle 43 (left) and for Jason-1 on cycle 282 (right)*

3.1.2. Over ocean

When considering ocean surface, the same analysis method leads also to an improvement of Jason-2 data coverage, as plotted on the top left figure 3. It represents the percentage of missing measurements relative to the theory, when limited to ocean surfaces. The mean value is about 0.3% for Jason-2 and 3.2% for Jason-1, but this figure is not significant due to several events where the measurements are missing. All these events are described on table 2.
On figure 3 on the top right, the percentage of missing measurements is plotted without taking into account the cycles where instrumental events or other anomalies occurred. The mean value of missing measurements lowers down to 0.03% for Jason-2 and 2.0% for Jason-1. These additional Jason-1 missing measurements are mainly located over sea ice and near the coasts and are related to the altimeter tracking method. Indeed, selecting latitudes lower than 50° and bathymetry area lower than -1000m (see bottom of figure 3), the Jason-1 percentage becomes very weak (close to 0.02%) which represents less than 100 missing measurements per cycle over open ocean. For Jason-2, the same statistic is comparable but slightly smaller with around 0.01% of missing measurements over open oean. This weak percentage of missing measurements is mainly explained by the rain cells and sigma0 blooms. These sea states can disturb significantly the Ku band waveform shape leading to an altimeter lost of tracking. Discontinuities at the border between the reception stations (NOAA and Usingen) may also lead to missing measurements.

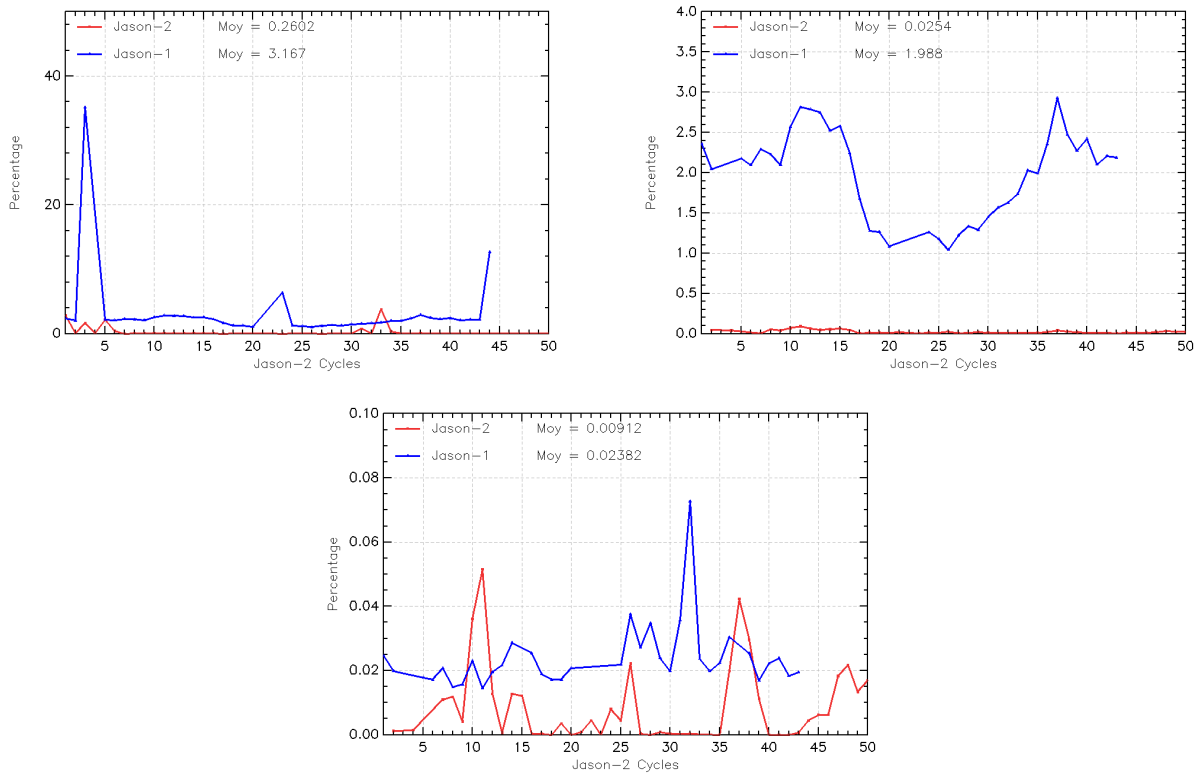

Figure 3: *Cycle per cycle percentage of missing measurements over ocean (top left), without anomalies (top right), without anomalies and with geographical selections (bottom).*

3.2. Edited measurements

3.2.1. Editing criteria definition

Editing criteria are used to select valid measurements over ocean. The editing process is divided into 4 parts. First, only measurements over ocean and lakes are kept (see section 3.2.2.). Second, some flags are used as described in section 3.2.3.. Note that the rain flag is not usable in the current release of GDR, but measurements corrupted by rain are well detected by other altimeter parameter criteria. Then, threshold criteria are applied on altimeter, radiometer and geophysical parameters and are described in the table 5. Except for the dual frequency ionosphere correction, only Ku-band measurements are used in this editing procedure, as they mainly represent the end user dataset. Moreover, a spline criterion is applied to remove the remaining spurious data. For each criterion, the cycle per cycle percentage of edited measurements has been monitored. This allows detection of anomalies in the number of removed data, which could come from instrumental, geophysical or algorithmic changes.

Parameter	Min thresholds	Max thresholds	mean edited
Sea surface height	$-130\,m$	$100\,m$	0.32%
			.../...

Parameter	Min thresholds	Max thresholds	mean edited
Sea level anomaly	$-10\,m$	$10.0\,m$	1.08%
Number measurements of range	10	*Not applicable*	0.43%
Standard deviation of range	0	$0.2\,m$	1.47%
Squared off-nadir angle	$-0.2\,deg^2$	$0.64\,deg^2$	0.83%
Dry troposphere correction	$-2.5\,m$	$-1.9\,m$	0.00%
Inverted barometer correction	$-2.0\,m$	$2.0\,m$	0.00%
AMR wet troposphere correction	$-0.5m$	$-0.001\,m$	0.56%
Ionosphere correction	$-0.4\,m$	$0.04\,m$	1.08%
Significant wave height	$0.0\,m$	$11.0\,m$	0.49%
Sea State Bias	$-0.5\,m$	$0.0\,m$	0.22%
Number measurements of Ku-band Sigma0	10	*Not applicable*	0.42%
Standard deviation of Ku-band Sigma0	0	$1.0\,dB$	2.38%
Ku-band Sigma0 [1]	$7.0\,dB$	$30.0\,dB$	0.34%
Ocean tide	$-5.0\,m$	$5.0\,m$	0.09%
Equilibrium tide	$-0.5\,m$	$0.5\,m$	0.00%
Earth tide	$-1.0\,m$	$1.0\,m$	0.00%
Pole tide	$-15.0\,m$	$15.0\,m$	0.00%
Altimeter wind speed	$0\,m.s^{-1}$	$30.0\,m.s^{-1}$	0.70%
All together	-	-	4.02%

Table 5: *E*diting criteria

3.2.2. Selection of measurements over ocean and lakes

In order to remove data over land, a land-water mask is used. Only measurements over ocean or lakes are kept. This allows to keep data near the coasts and so to detect potential anomalies in these areas. Furthermore, there is no impact on global performance estimations since the most significant results are derived from analyzes in deep ocean areas. Figure 4 shows the cycle per cycle percentage of measurements eliminated by this selection. The signal reflects the impact of the different altimeter tracking modes: SGT (split gate tracking), Median and DIODE/DEM (digital elevation model). SGT mode, the nominal mode for Jason-1, was used for Jason-2 during cycle

[1] The thresholds used for the Ku-band Sigma0 are the same than for Jason-1 and T/P, but the same sigma0 bias as between Jason-1 and T/P (about 2.4 dB) is applied.

0 and half of cycle 1. This mode does not perform very well over land (as also depicted on right side of figure 2), therefore a comparable small percentage of measurements are edited over land for cycle 1 (approximately 24%). Most of Jason-2 cycles (cycles 2, 4, 6, and onwards from cycle 8) were operated in Median mode (also used by Envisat). This mode is more adapted for tracking over land than SGT and provides therefore more measurements over land (as also seen on left side of figure 2) and so more measurements are edited (between 25.5% and 27% depending on season) due to the ocean/land criteria. A new tracking mode, DEM, was used during cycles 3, 5, 7, and 34. It has been designed to provide more data over inland water surfaces and coastal areas. It provides a continuous data set over land but some are not meaningful (in areas where the DEM is not accurate enough like in the major mountains). Therefore during these cycles, almost 29% of measurements are removed by the selection. Since 10th of December, 2008 the onbord altimeter configuration was modified to correct for the low signal tracking anomaly, which led to a more strict control of acquisition gain loop (to avoid the tracking of low signal anomalies). This explains the quite steep decrease of land measurements edited around cycle 16 (section 7.1.).

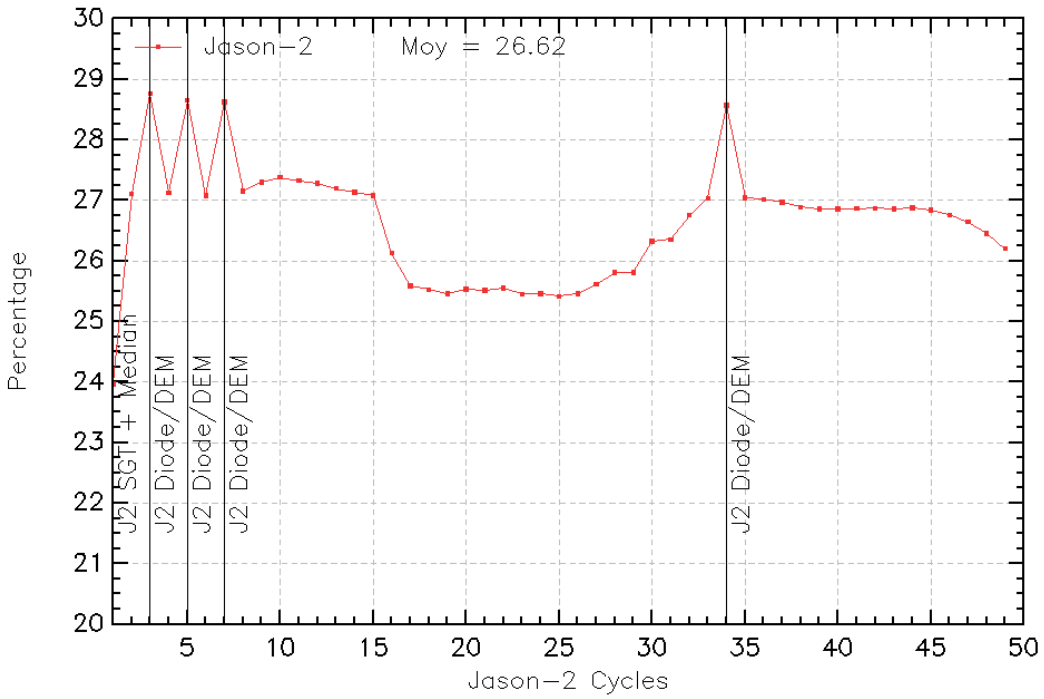

Figure 4: *Cycle per cycle percentage of eliminated measurements during selection of ocean/lake measurements.*

3.2.3. Flagging quality criteria: Ice flag

The ice flag is used to remove the sea ice data. Figure 5 shows the cycle per cycle percentage of measurements edited by this criterion. Over the shown period, no anomalous trend is detected (figure 5 left) but the nominal annual cycle is visible. Indeed, the maximum number of points over ice is reached during the southern winter (ie. July - September). As Jason-2 takes measurements between 66° north and south, it does not detect thawing of sea ice (due to global warming), which takes place especially in northern hemisphere over 66°N. The percentage of measurements edited by ice flag is plotted in the right of figure 5 for a period of 1 year.

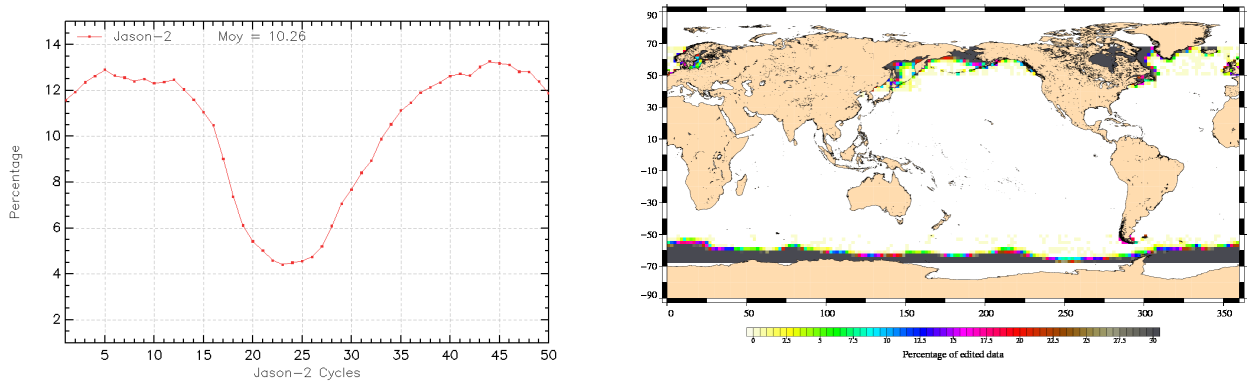

Figure 5: *Percentage of edited measurements by ice flag criterion. Left: Cycle per cycle monitoring. Right: Map over a one year period (cycles 14 to 50).*

3.2.4. Flagging quality criteria: Rain flag

The rain flag is not used for data selection since it is not yet tuned for Jason-2. Indeed rain flag was tuned on Jason-1 automatic gain control loop measurements. As automatic gain control loop is different for Jason-2 and Jason-1 the rain flag currently does not work and is currently set to default values in Jason-2 GDR products.

3.2.5. Threshold criteria: Global

Instrumental parameters have also been analyzed from comparison with thresholds, after having selected only ocean/lakes measurements and applied flagging quality criteria (ice flag). Note that no measurement is edited by the following corrections : dry troposphere correction, inverted barometer correction (including DAC), equilibrium tide, earth and pole tide. Indeed these parameters are only verified in order to detect data at default values, which might happen during a processing anomaly.
The percentage of measurements edited using each criterion is monitored on a cycle per cycle basis (figure 6). The mean percentage of edited measurements is about 4.0%.

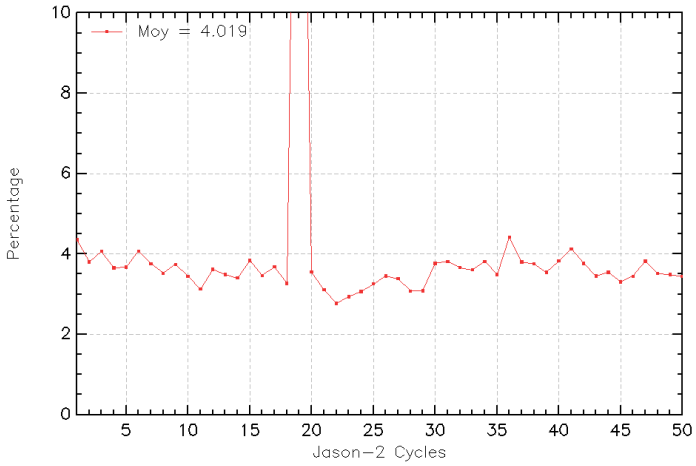

Figure 6: *Cycle per cycle percentage of edited measurements by threshold criteria*

3.2.6. Threshold criteria: 20-Hz measurements number

The percentage of edited measurements because of a too low number of 20-Hz measurements is represented on left side of figure 7. No trend neither any anomaly has been detected, except for cycle 19, where percentage of edited measuremetns is slightly higher than usual. This is related to unavailability of Jason-2 Advanced Microwave Radiometer (see section 7.3.).
The map of measurements edited by 20-Hz measurements number criterion is plotted on right side of figure 7 and shows correlation with heavy rain and wet areas. Indeed waveforms are distorted by rain cells, which makes them often meaningless for SSH calculation. As a consequence, edited measurements due to several altimetric criteria are often correlated with wet areas.

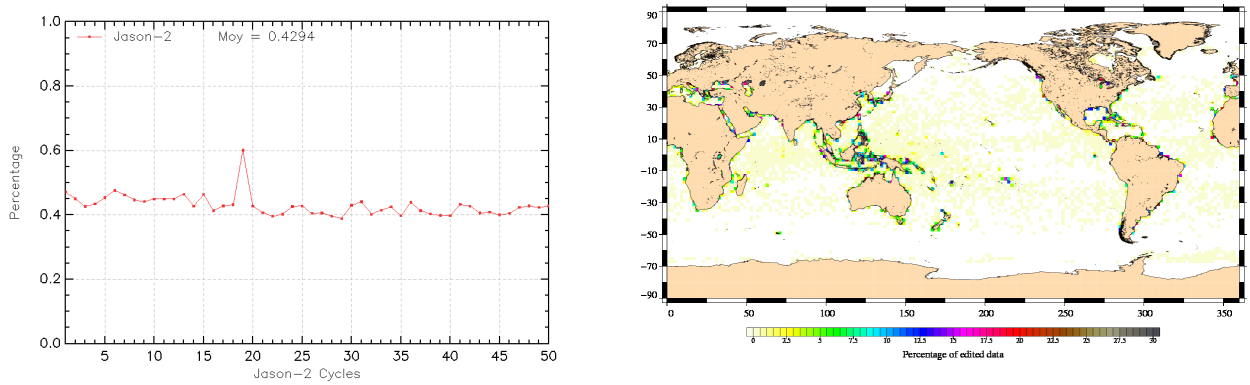

Figure 7: *Percentage of edited measurements by 20-Hz measurements number criterion. Left: Cycle per cycle monitoring. Right: Map over a one year period (cycles 14 to 50).*

3.2.7. Threshold criteria: 20-Hz measurements standard deviation

The percentage of edited measurements due to 20-Hz measurements standard deviation criterion is shown in figure 8 (left). During cycle 1, slightly more measurements are edited by 20-Hz measurements standard deviation criterion than during other cycles. This is likely due to low signal tracking anomaly which impacted especially this cycle. The right side of figure 8 shows a map of measurements edited by the 20-Hz measurements standard deviation criterion. As in section 3.2.6., edited measurements are correlated with wet areas, but also in regions where ice flag probably missed detection of sea ice (near Antarctic).

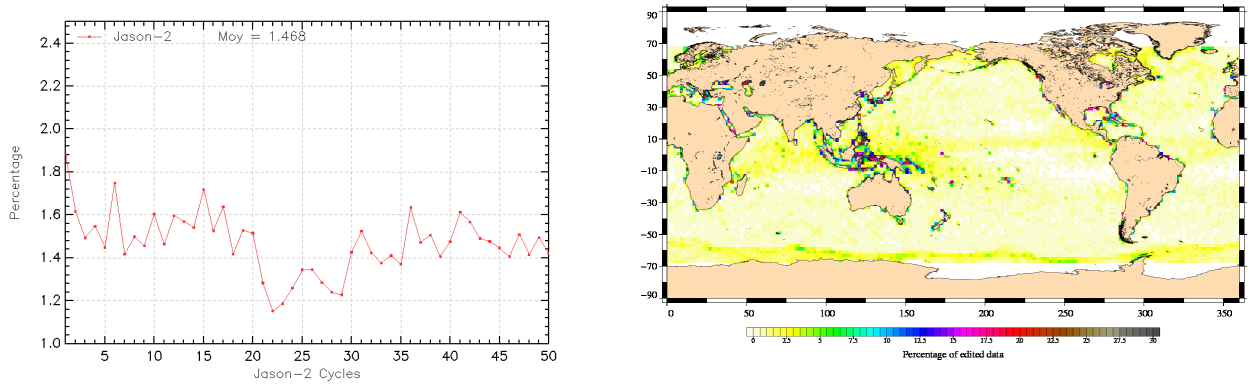

Figure 8: *Percentage of edited measurements by 20-Hz measurements standard deviation criterion. Left: Cycle per cycle monitoring. Right: Map over a one year period (cycles 14 to 50).*

3.2.8. Threshold criteria: Significant wave height

The percentage of edited measurements due to significant wave height criterion is represented in figure 9. It is about 0.50%. In the beginning of the mission, the curve of measurements edited by SWH threshold criterion is quite irregular, as low signal tracking anomalies occurred during SGT and Median tracking modes, whereas there are no low signal tracking anomalies during DEM tracking modes (cycles 3, 5, and 7). Indeed during periods of low signal tracking anomaly, parameters like significant wave height, backscattering coefficient and squared off-nadir angle from waveforms are out of thresholds and therefore edited (see section 7.1.). Figure 9 (right part) shows that measurements edited by SWH criterion are especially found near coasts in the equatorial regions.

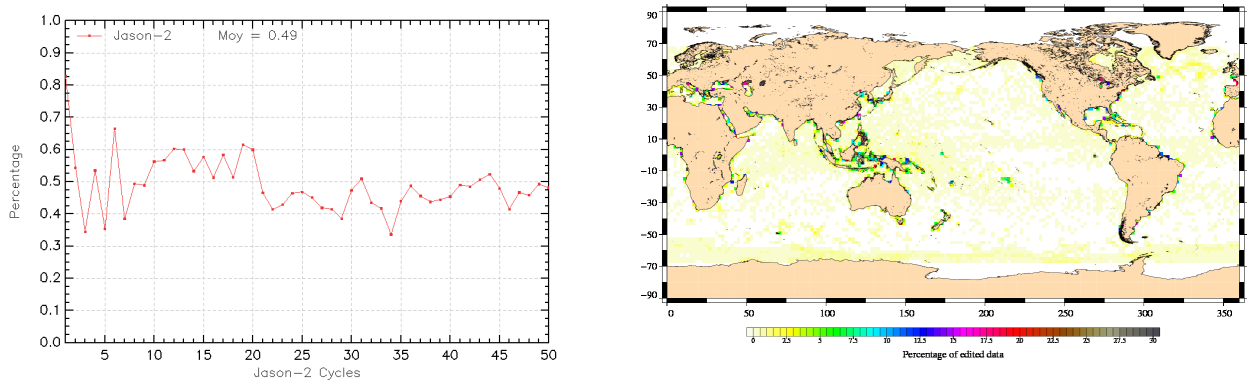

Figure 9: *Percentage of edited measurements by SWH criterion. Left: Cycle per cycle monitoring. Right: Map over a one year period (cycles 14 to 50).*

3.2.9. Backscatter coefficient

The percentage of edited measurements due to backscatter coefficient criterion is represented in figure 10. It is about 0.34% It is also impacted by low signal tracking anomalies, especially during cycle 1. The right part of figure 10 shows that measurements edited by backscatter coefficient criterion are especially found near coasts in the equatorial regions and closed sea (Mediterranean).

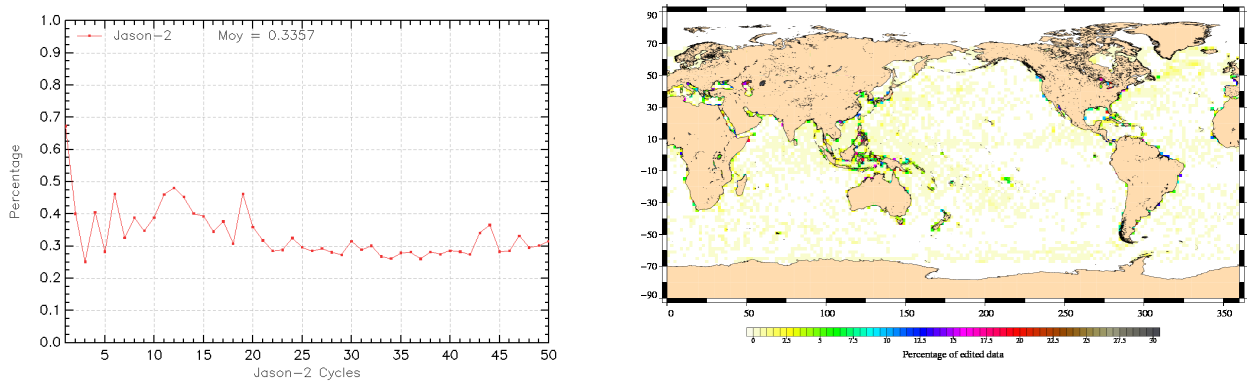

Figure 10: *Percentage of edited measurements by Sigma0 criterion. Left: Cycle per cycle monitoring. Right: Map over a one year period (cycles 14 to 50).*

3.2.10. Backscatter coefficient: 20 Hz standard deviation

The percentage of edited measurements due to 20 Hz backscatter coefficient standard deviation criterion is represented in figure 11. It is about 2.4%. It is also impacted by low signal tracking anomalies, especially during cycle 1. The right part of figure 10 shows that measurements edited by 20 Hz backscatter coefficient standard deviation criterion are especially found in regions with disturbed waveforms.

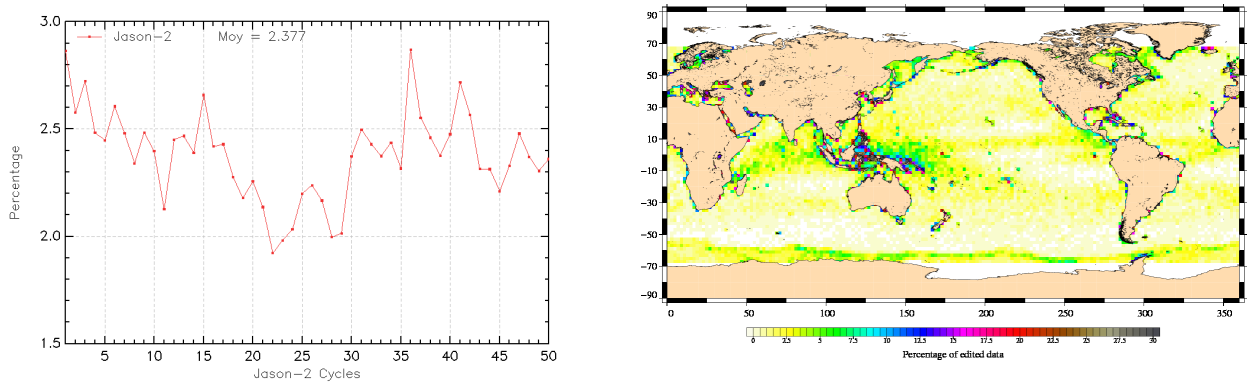

Figure 11: *Percentage of edited measurements by 20 Hz Sigma0 standard deviation criterion. Left: Cycle per cycle monitoring. Right: Map over a sixth month period (cycles 0 to 17).*

3.2.11. Radiometer wet troposphere correction

The percentage of edited measurements due to radiometer wet troposphere correction criterion is represented in figure 12. It is about 0.56%. When removing cycles which experienced problems, percentage of edited measurements drops to 0.1%. For cycle 19 the percentage of edited measurements is higher than usual. This is linked to radiometer wet troposphere correction at default value due to AMR unavailability. Passes concerned are easily detectable on right side of figure 12.

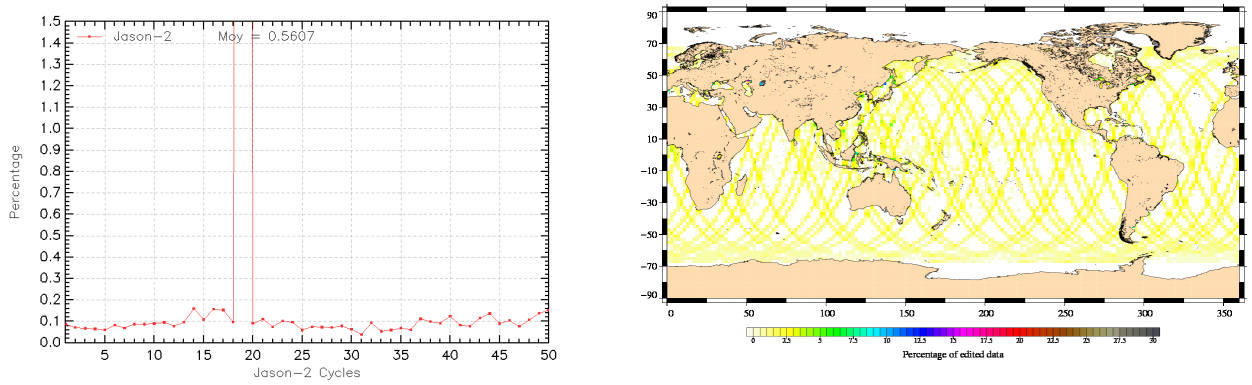

Figure 12: *Percentage of edited measurements by radiometer wet troposphere criterion. Left: Cycle per cycle monitoring. Right: Map over a one year period (cycles 14 to 50).*

3.2.12. Dual frequency ionosphere correction

The percentage of edited measurements due to dual frequency ionosphere correction criterion is represented in figure 13. It is about 1.08% and shows no drift. The map 13 shows that measurements edited by dual frequency ionosphere correction are mostly found in equatorial regions, but also near sea ice.

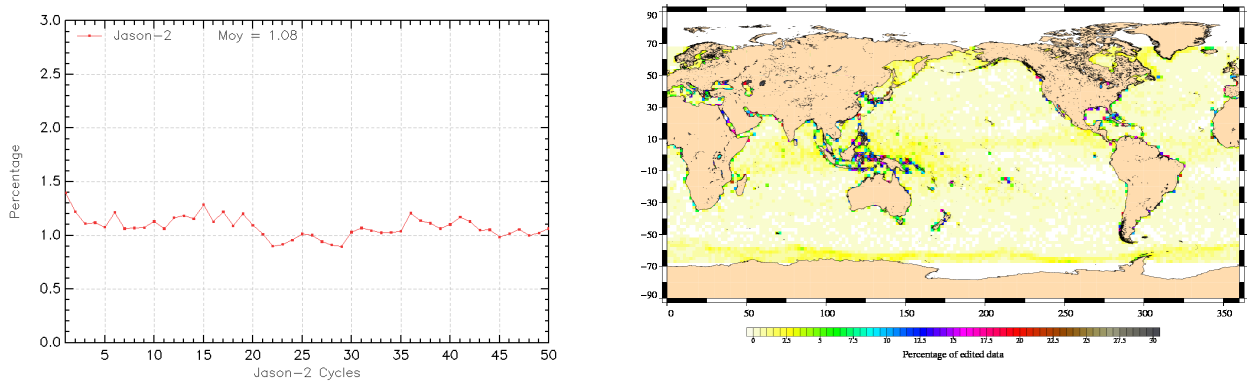

Figure 13: *Percentage of edited measurements by dual frequency ionosphere criterion. Left: Cycle per cycle monitoring. Right: Map over a one year period (cycles 14 to 50).*

3.2.13. Square off-nadir angle

The percentage of edited measurements due to square off-nadir angle criterion is represented in figure 14. It is about 0.83%. As for other parameters, impact of low signal tracking anomalies is visible especially for cycle 1. The map 14 shows that edited measurements are mostly found in coastal regions and regions with disturbed waveforms.

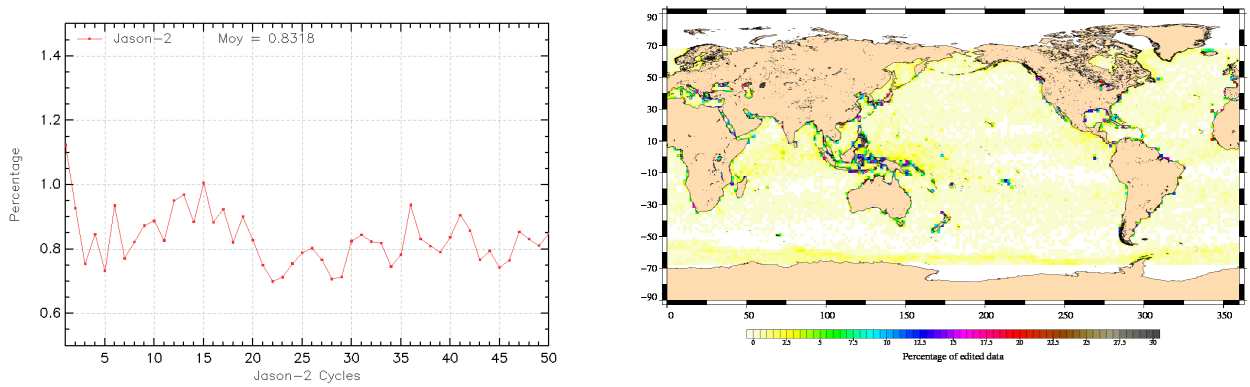

Figure 14: *Percentage of edited measurements by square off-nadir angle criterion. Left: Cycle per cycle monitoring. Right: Map over a one year period (cycles 14 to 50).*

3.2.14. Sea state bias correction

The percentage of edited measurements due to sea state bias correction criterion is represented in figure 15. The percentage of edited measurements is about 0.22% and shows no drift.
The map 15 shows that edited measurements are mostly found in equatorial regions near coasts.

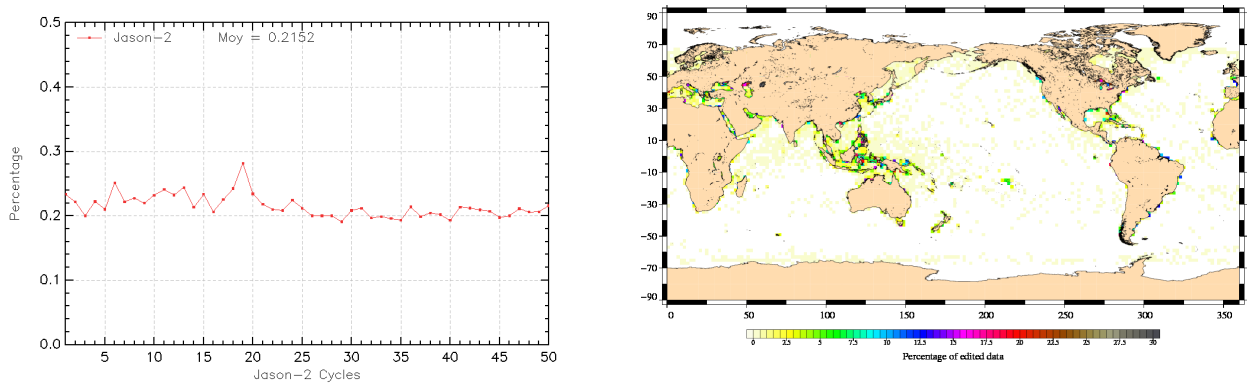

Figure 15: *Cycle per cycle percentage of edited measurements by sea state bias criterion (left). Right: Map of percentage of edited measurements by sea state bias criterion over a one year period (cycles 14 to 50).*

3.2.15. Altimeter wind speed

The percentage of edited measurements due to altimeter wind speed criterion is represented in figure 16. It is about 0.70%. The measurements are edited, because they have default values. This is the case when sigma0 itself is at default value, or when it shows very high values (higher than 25 dB), which occur during sigma bloom and also over sea ice. Indeed, the wind speed algorithm (which uses backscattering coefficient and significant wave height) can not retrieve values for sigma0 higher than 25 dB.
The map 16 showing percentage of measurements edited by altimeter wind speed criterion is correlated with maps 15 and 9.

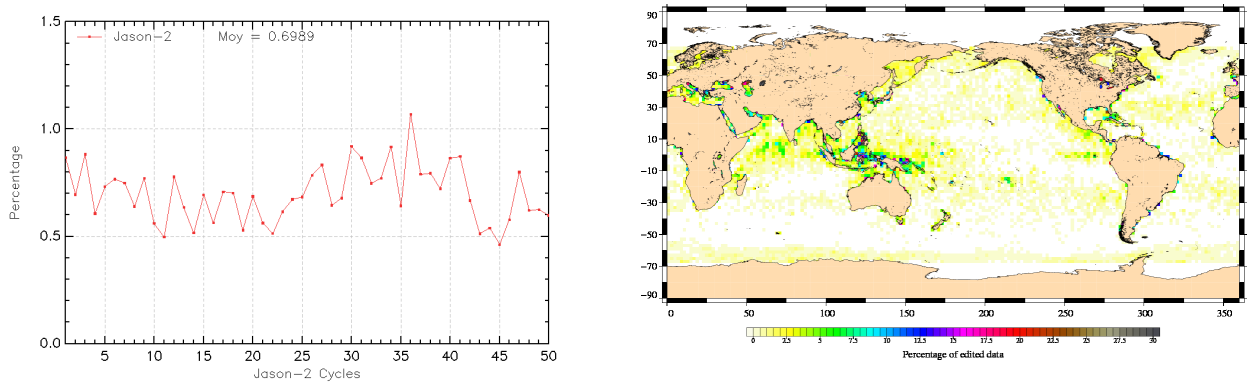

Figure 16: *Percentage of edited measurements by altimeter wind speed criterion. Left: Cycle per cycle monitoring. Right: Map over a one year period (cycles 14 to 50).*

3.2.16. Ocean tide correction

The percentage of edited measurements due to ocean tide correction criterion is represented in figure 17. It is about 0.09% and shows a small annual signal. The ocean tide correction is a model output, there should therefore be no edited measurements. Indeed there are no measurements edited in open ocean areas, but only very few near coasts or in lakes or rivers (see map 17). These measurements are mostly at default values.
Some of these lakes are in high latitudes and therefore periodically covered by ice. This explains the annual signal visible in figure 17.

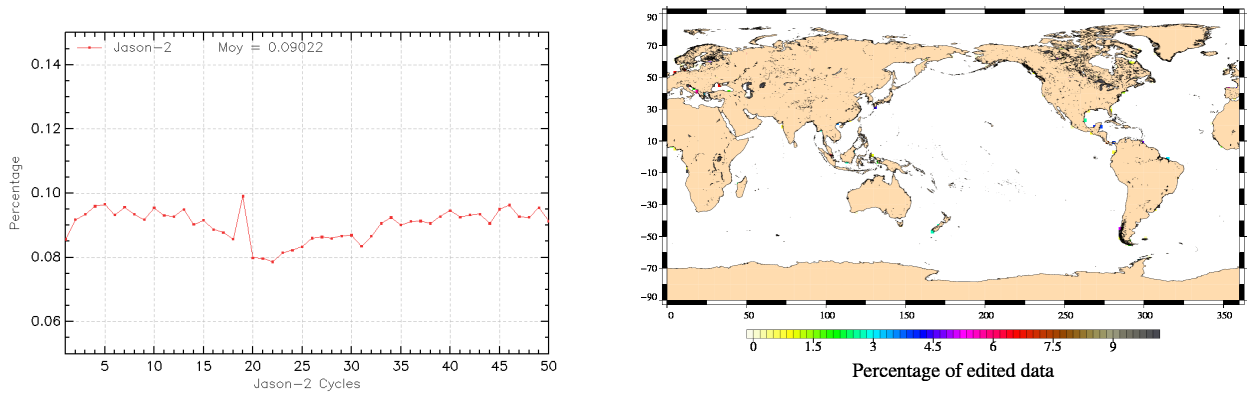

Figure 17: *Percentage of edited measurements by ocean tide criterion. Left: Cycle per cycle monitoring. Right: Map over a one year period (cycles 14 to 50).*

3.2.17. Sea surface height

The percentage of edited measurements due to sea surface height criterion is represented in figure 18. It is about 0.32% and shows no drift. The measurements edited by sea surface height criterion are mostly found near coasts in equatorial regions (see map 18)

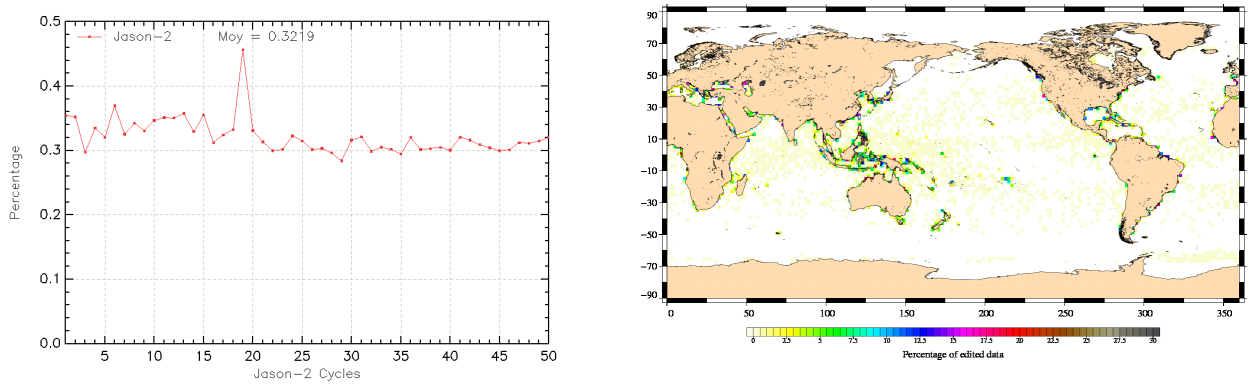

Figure 18: *Percentage of edited measurements by sea surface height criterion. Left: Cycle per cycle monitoring. Right: Map over a one year period (cycles 14 to 50).*

3.2.18. Sea level anomaly

The percentage of edited measurements due to sea level anomaly criterion is represented in figure 19. It is about 1.08% (0.6% without cycle 19) and shows no drift. The graph is quite similar to the one in figure 12 (showing the percentage of measurements edited by AMR), as the SLA clip contains, among other parameters, the radiometer wet troposphere correction.
Whereas the map in figure 19 allows us to plot the measurements edited due to sea level anomaly out of thresholds (after applying all other threshold criteria). There are only very few measurements, principally located in Caspian Sea.

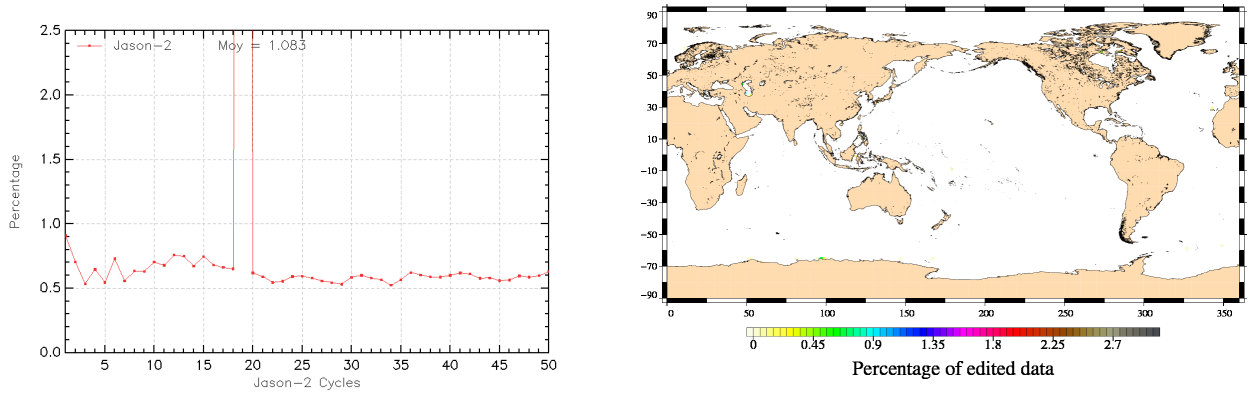

Figure 19: *Percentage of edited measurements by sea level anomaly criterion. Left: Cycle per cycle monitoring. Right: Map over a one year period (cycles 14 to 50).*

4. Monitoring of altimeter and radiometer parameters

4.1. Methodology

Both mean and standard deviation of the main parameters of Jason-2 have been monitored since the beginning of the mission. Moreover, a comparison with Jason-1 parameters has been performed: it allows us to monitor the bias between the parameters of the 2 missions. Two different methods have been used to compute the bias:

- Till Jason-2 cycle 20, Jason-2 and Jason-1 ground tracks are on the same ground track and are spaced out about 1 minute apart. The mean of the Jason-1 - Jason-2 differences can be computed using a point by point repeat track analysis.
- From Jason-2 cycle 21 (Jason-1 cycle 260), a maneuver sequence was conducted (from 26th of January to 14th of February 2009) to move Jason-1 to the new tandem mission orbit. It's the same as already used by Topex/Poseidon during its tandem phase with Jason-1, but there is a time shift of 5 days. Several maneuvers (including altitude changes of several km) were necessary to move Jason-1 to its new orbit. Geographical variations are then too strong to directly compare Jason-2 and Jason-1 parameters on a point by point basis. Therefore cycle per cycle differences have been carried out to monitor differences between the two missions. Nevertheless, data gaps on both satellites have been taken into account. These differences are quite noisy, especially for corrections which vary rapidly in time and space. Therefore occasional jumps will be covered by the noise of the differences. Nevertheless with longer time series (which can be filtered), drifts and permanent jumps can be detected.

Note that differences are done over Jason-2 cycles 1 to 44, corresponding to Jason-1 cycles 240 to 283/284. Indeed GDR products are currently only available till Jason-1 cycle 283, as computation of new JMR calibration coefficients is necessary, further to detection of a jump in radiometer wet troposphere correction (see [30].)

4.2. 20 Hz Measurements

The monitoring of the number and standard deviation of 20 Hz elementary range measurements used to derive 1 Hz data is presented here. These two parameters are computed during the altimeter ground processing. For Jason-1, before performing a regression to derive the 1 Hz range from 20 Hz data, a MQE (mean quadratic error) criterion is used to select valid 20 Hz measurements. This first step of selection consists in verifying that the 20 Hz waveforms can be approximated by a Brown echo model (Brown, 1977 [4]) (Thibaut et al. 2002 [25]). Then, through an iterative regression process, elementary ranges too far from the regression line are discarded until convergence is reached. Thus, monitoring the number of 20 Hz range measurements and the standard deviation computed among them is likely to reveal changes at instrumental level.
The Jason-1 MQE threshold are not applicable to Jason-2, using those thresholds would edit more measurements than necessary. Therefore the Jason-2 MQE threshold has been set to default, leading to no editing based on MQE values.

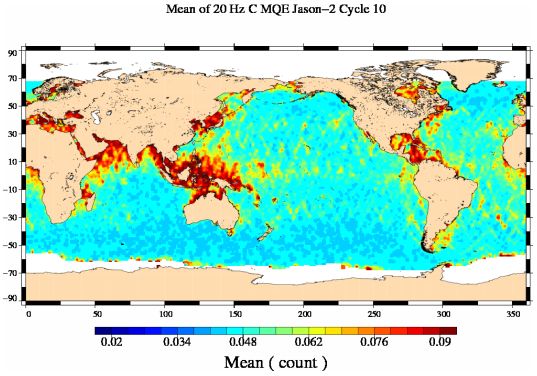

Figure 20: *Map of 20 Hz C-band MQE for Jason-2 cycle 10.*

4.2.1. 20 Hz measurements number in Ku-Band and C-Band

Jason-2 number of elementary 20 Hz range mesurements is very stable in time with an average of 19.66 for Ku-band and 19.43 as shown on figure 21, whereas Jason-1 data show a slight annual cycle (especially for C-band). Figures 22 and 23 show on the left the daily monitoring of the mean and standard deviation of Jason-1 - Jason-2 differences of 20-Hz measurements number in Ku-Band and C-band during the flight formation phase. Besides a slight variation, related to the annual cycle of Jason-1 data, they are quite stable and do not show any anomaly. Number of 20 Hz range measurements is slightly higher for Jason-2 than for Jason-1, since mean of Jason-1 - Jason-2 difference is slightly negatif (-0.1 for Ku-band and -0.19 for C-band). The regions where Jason-1 has less elementary range measurements are especially located around Indonesia, as shown on map of Jason-1 - Jason-2 differences (right side of figures 22 and 23). They seem to be correlated to high MQE values (see figure 20), especially in C-band. Since the current MQE criterium for Jason-2 does not eliminate 20 Hz measurements used for 1 Hz compression (whereas for Jason-1 this is the case), number of 20 Hz range measurements is smaller for Jason-1 than for Jason-2 in high MQE areas.

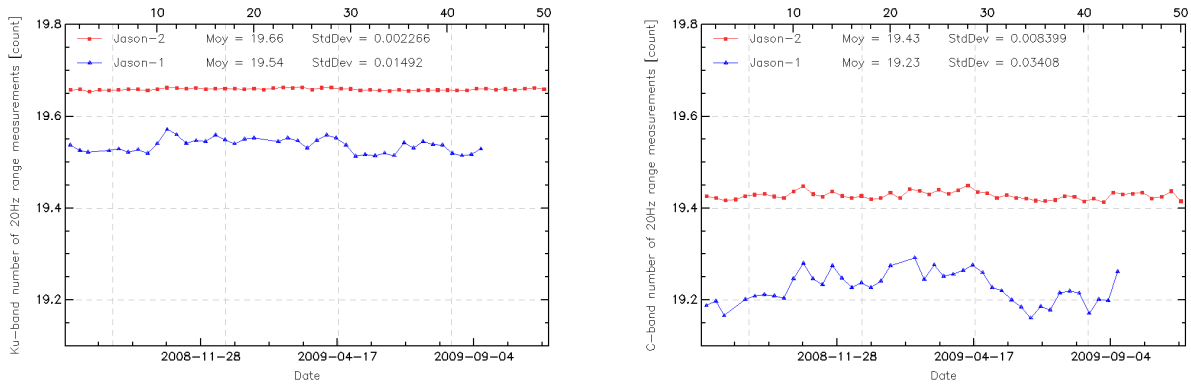

Figure 21: *Cyclic monitoring of number of elementary 20 Hz range measurements for Jason-1 and Jason-2 for Ku-band (left) and C-band (right).*

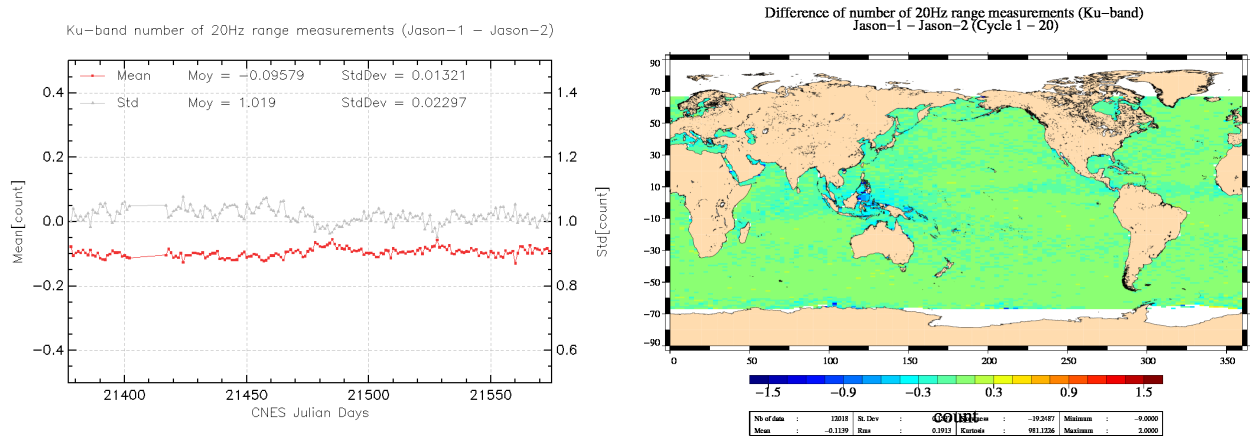

Figure 22: *Daily monitoring of mean and standard deviation of Jason-1 - Jason-2 differences for number of elementary 20 Hz Ku-band range measurements (left) and map showing mean of Jason-1 - Jason-2 differences over cycles 1 to 20.*

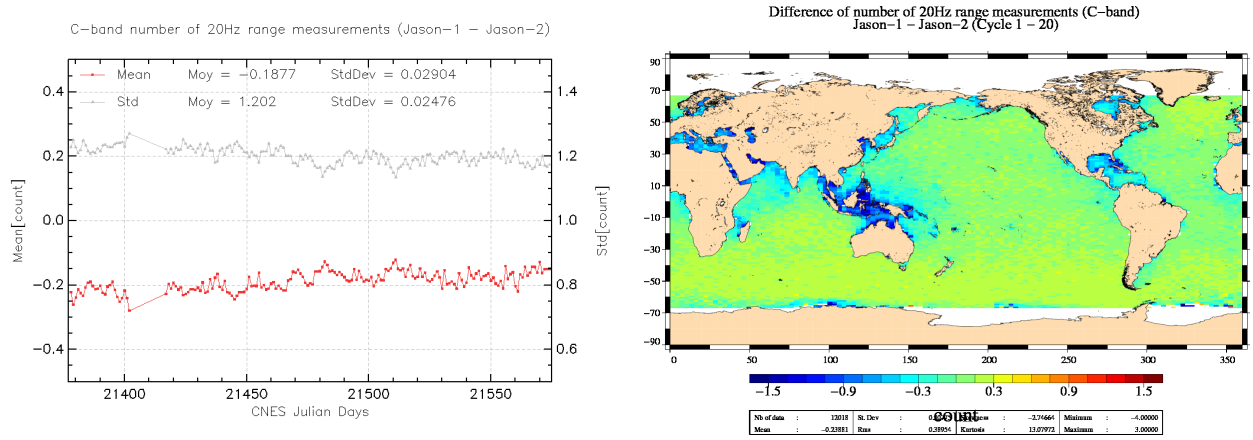

Figure 23: *Daily monitoring of mean and standard deviation of Jason-1 - Jason-2 differences for number of elementary 20 Hz C-band range measurements (left) and map showing mean of Jason-1 - Jason-2 differences over cycles 1 to 20.*

4.2.2. 20 Hz measurements standard deviation in Ku-Band and C-Band

Jason-2 standard deviation of the 20 Hz measurements is 7.9 cm for Ku-Band and 17.3 cm for C-Band (figure 24). It is very similar to Jason-1 data (especially during the formation flight phase). Figure 25 and 26, showing daily monitoring of Jason-1 - Jason-2 difference of standard deviation of the 20 Hz measurements in Ku-Band and C-Band (on the left), reveal no trend neither anomaly. C-Band standard deviation of the 20 Hz measurements rms is noisier than those of Ku-Band. This is directly linked to the C-band standard deviation which is higher than the Ku, as the onboard averaging is performed over less waveforms leading to an increased noise.

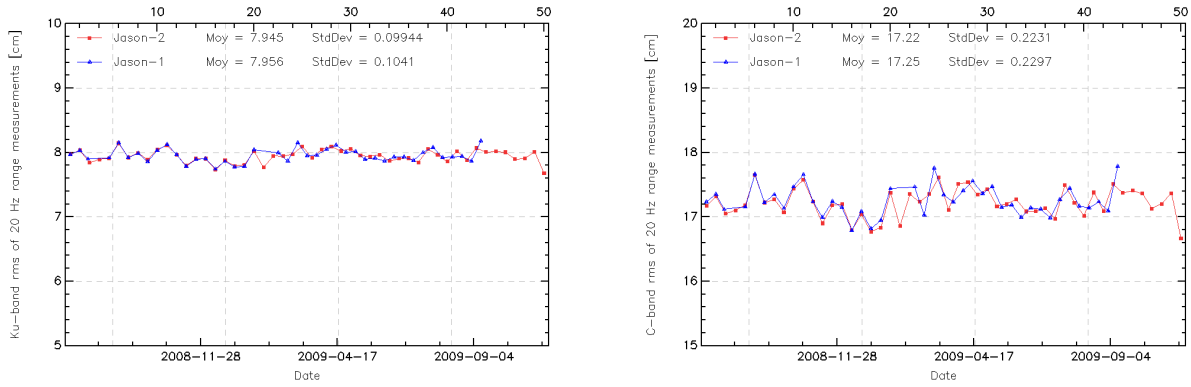

Figure 24: *Cyclic monitoring of rms of elementary 20 Hz range measurements for Jason-1 and Jason-2 for Ku-band (left) and C-band (right).*

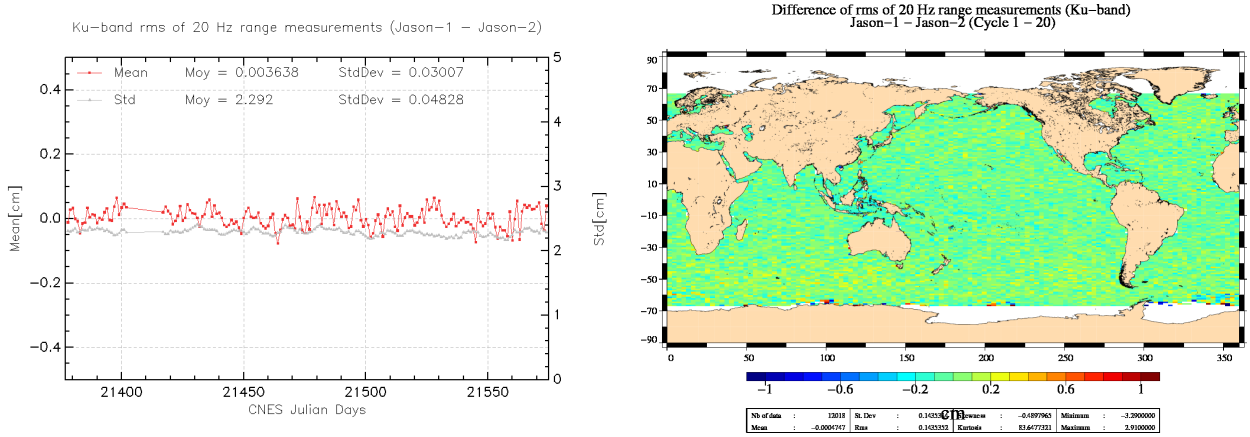

Figure 25: *Daily monitoring of mean and standard deviation of Jason-1 - Jason-2 differences for the rms of elementary 20 Hz Ku-band range measurements (left) and map showing mean of Jason-1 - Jason-2 differences over cycles 1 to 20 (right).*

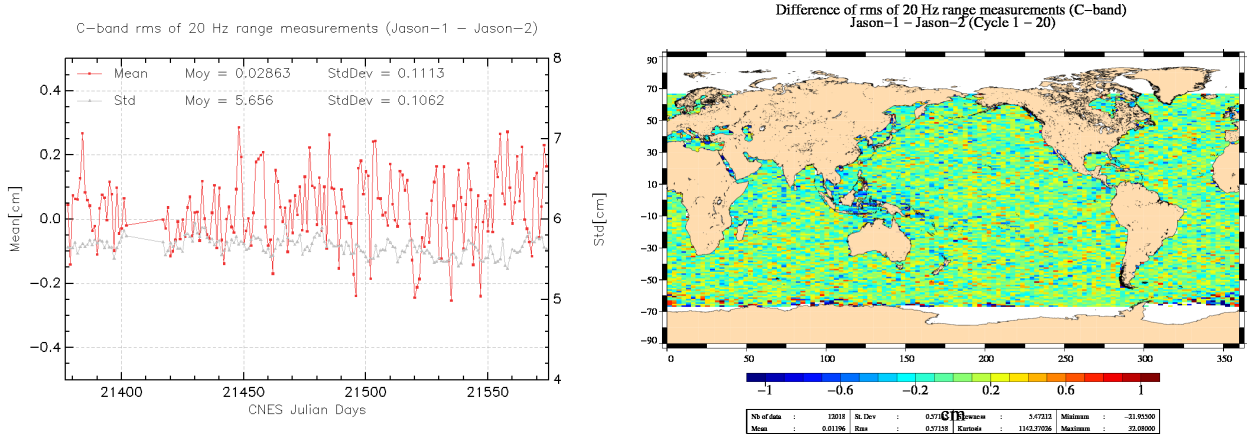

Figure 26: *Daily monitoring of mean and standard deviation of Jason-1 - Jason-2 differences for rms of elementary 20 Hz C-band range measurements (left) and map showing mean of Jason-1 - Jason-2 differences over cycles 1 to 20 (right).*

4.3. Off-Nadir Angle from waveforms

The off-nadir angle is estimated from the waveform shape during the altimeter processing. The square of the off-nadir angle, averaged on a daily basis, has been plotted for Jason-1 and Jason-2 on the left side of figure 27, whereas the right side shows the histograms over one cycle. The mean values are slightly positive. This mean value is not significant in terms of actual platform mispointing. Mispointing of Jason-2 is quite stable, close to 0.01 deg2. Whereas Jason-1 may show higher values (related to the reduced tracking performance of both star trackers, especially during fixed-yaw).
The small shift Jason-2 mispointing is related to small differences in antenna aperture values used for Jason-1 and Jason-2 processing. Indeed **??** shows, that retracking with different values of antenna aperture, changes the mean value of Jason-2 mispointing (see figure 28).

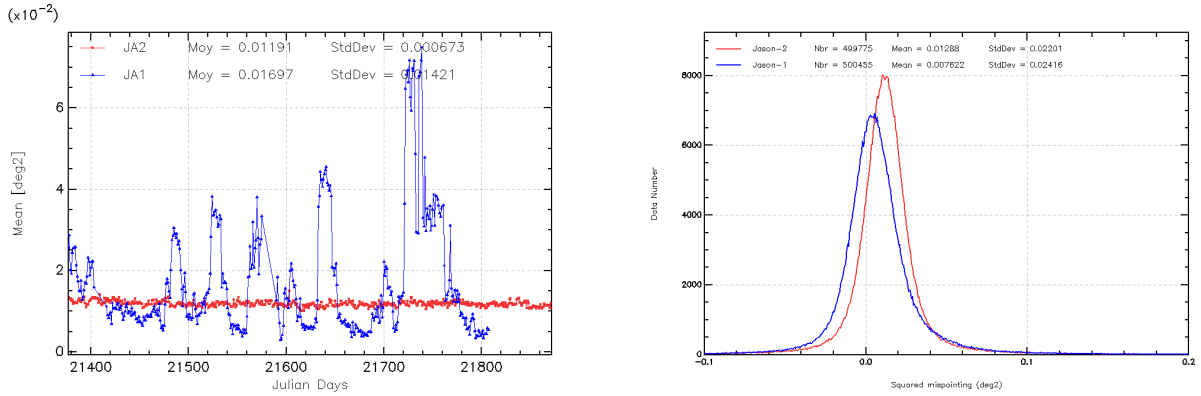

Figure 27: *Square of the off-nadir angle deduced from waveforms (deg^2) for Jason-1 and Jason-2: Daily monitoring (left), histograms for Jason-2 cycle 10 (Jason-1 cycle 249).*

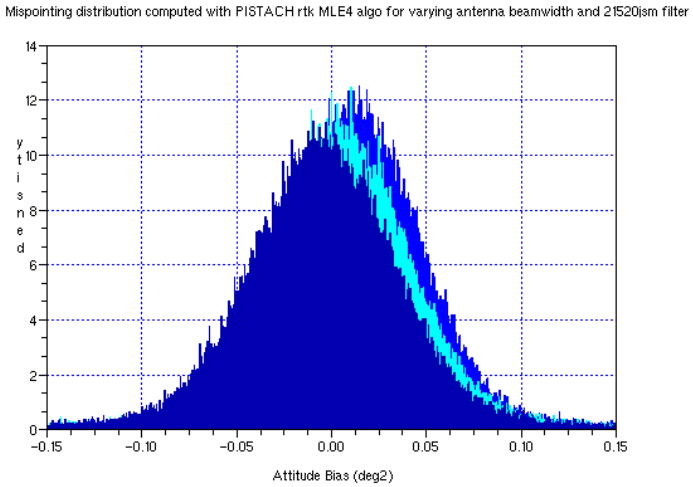

Figure 28: *Histograms of Jason-2 mispointing after retracking with different antenna beamwidth (from **??**): 1.26° (blue), 1.28° (light blue), 1.30° (dark blue).*

4.4. Backscatter coefficient

The Jason-2 Ku-band and C-band backscattering coefficient shows good agreement with Jason-1 as visible for cyclic monitoring in figure 29 (top left and right). Left sides of figures 30 and 31 show daily monitoring of mean differences during the formation flight phase. For Ku-band, a small bias close to 0.15 dB is detected, it varies slightly (+/- 0.05 dB). Indeed, Jason-1 backscattering coefficient is slightly impacted by the higher off-nadir angles (due to low star tracker availability). The average standard deviation of both Sigma0 differences (measurements by measurements) is also very low around 0.15 dB rms. C-Band sigma0 differences indicate a small bias close to 0.2 dB. In the meantime, the map of mean differences (right side of figures 30 and 31) highlights very small differences. They are mainly located in areas where waveforms can be disturbed by rain cells or sigma0 blooms for instance. As previously mentioned in edited measurements section, this is likely linked to the MQE criteria not tuned for Jason-2. The impact is stronger concerning the C-Band (right side of figure 31). During the tandem phase (from Jason-2 cycle 21 onwards), mean differences continue to be calculated but comparing only the global statistics cycle by cycle (see bottom of figure 29). Although the statistic is calculated less accurately, a similar bias is observed as during the formation flight phase, and no significant drift is detected between both missions.

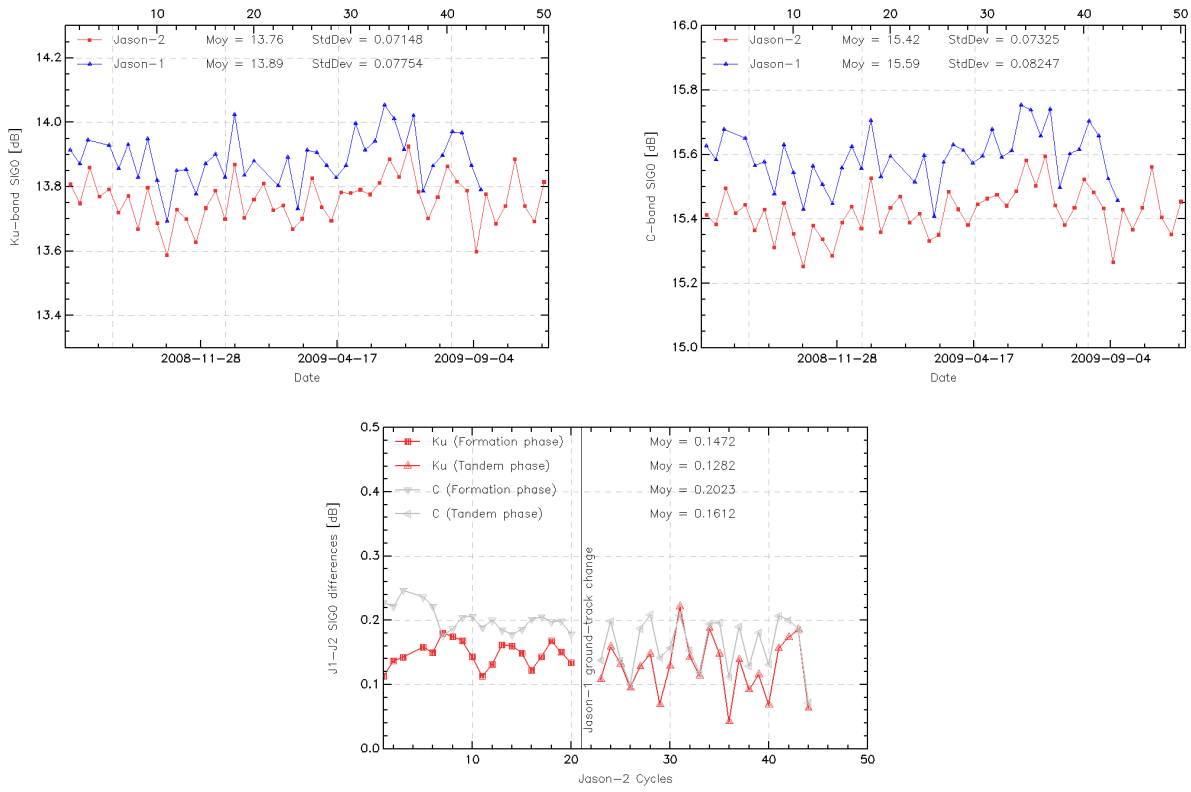

Figure 29: *Cyclic monitoring of Sigma0 for Jason-1 and Jason-2 for Ku-band (left) and C-band (right) and Jason-1 - Jason-2 differences (bottom).*

Notice that in the Jason-1 science ground processing corresponding to GDR-A release (2002), Ku-Band Sigma0 was biased by a -2.26 dB value in order to calculate correctly the altimeter wind speed derived from an algorithm ([16]) based on TOPEX Sigma0. This value corresponds approximately

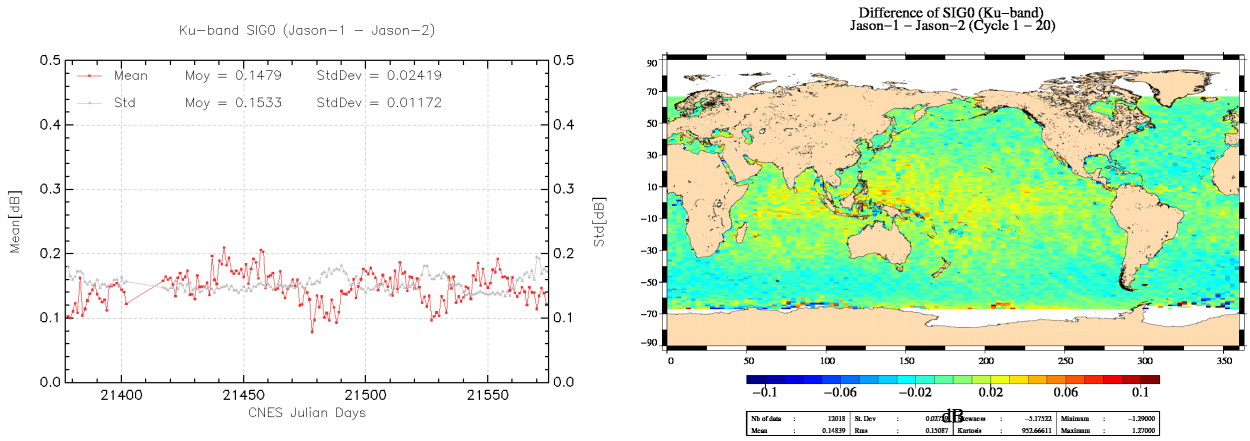

Figure 30: *Daily monitoring of mean and standard deviation of Jason-1 - Jason-2 differences for Ku-band Sigma0 (left) and map showing mean of Jason-1 - Jason-2 differences over cycles 1 to 20.*

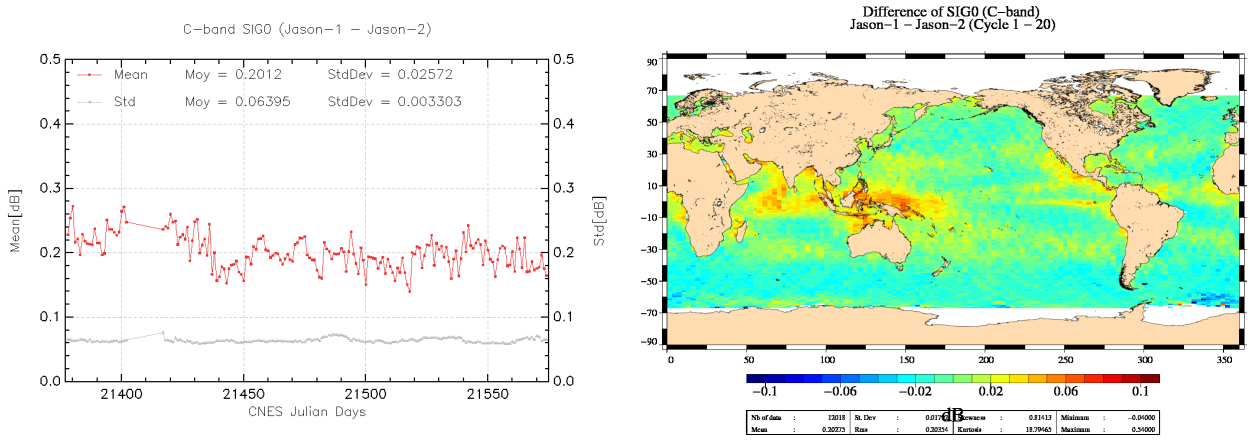

Figure 31: *Daily monitoring of mean and standard deviation of Jason-1 - Jason-2 differences for C-band Sigma0 (left) and map showing mean of Jason-1 - Jason-2 differences over cycles 1 to 20.*

to the bias between Jason-1 and TOPEX sigma0 estimated during the Jason-1/TOPEX formation flight phase ([13]). From Jason-1 GDR-B release (2006), the wind speed is calculated from the same algorithm but fitted on Jason-1 Sigma0 in order to not apply the TOPEX/Jason-1 sigma0 bias. It is the same algorithm applied for Jason-2 now, although there is a 0.15 dB bias between Jason-1 and Jason-2. So far, an error of 0.1 dB or 0.2 dB was considered negligible to estimate the altimeter wind speed. But thanks to the altimetry standard improvements since Jason-1 launch ([24], [9]), the error budget of SSH calculation has been reduced. Through the sea state bias correction, the Sigma0 bias uncertainty has thus become not inconsiderable as shown in recent study ([29]). It should be taken into account in next Jason-2 GDR release.

4.5. Significant wave height

As for Sigma0 parameter, a very good consistency between both significant wave height is shown (see top left and right of figure 32). A small bias close to around -1.2 cm is calculated over the formation flight phase. It is close to -0.7 cm in C-band (see left side of figures 33 and 34). It is stable in time and space with locally stronger differences (see difference maps in right side of figures 33 and 34). These differences are too weak to impact scientific applications. They are generally due to ground processing differences between both missions as the MQE criteria for instance, especially for C-band (see section 7.2.). As previously, extending the monitoring of SWH bias during the tandem phase (bottom of figure 32) highlights variations larger since both satellites do not measure the same SWH. However bias is still stable and no drift is detected.

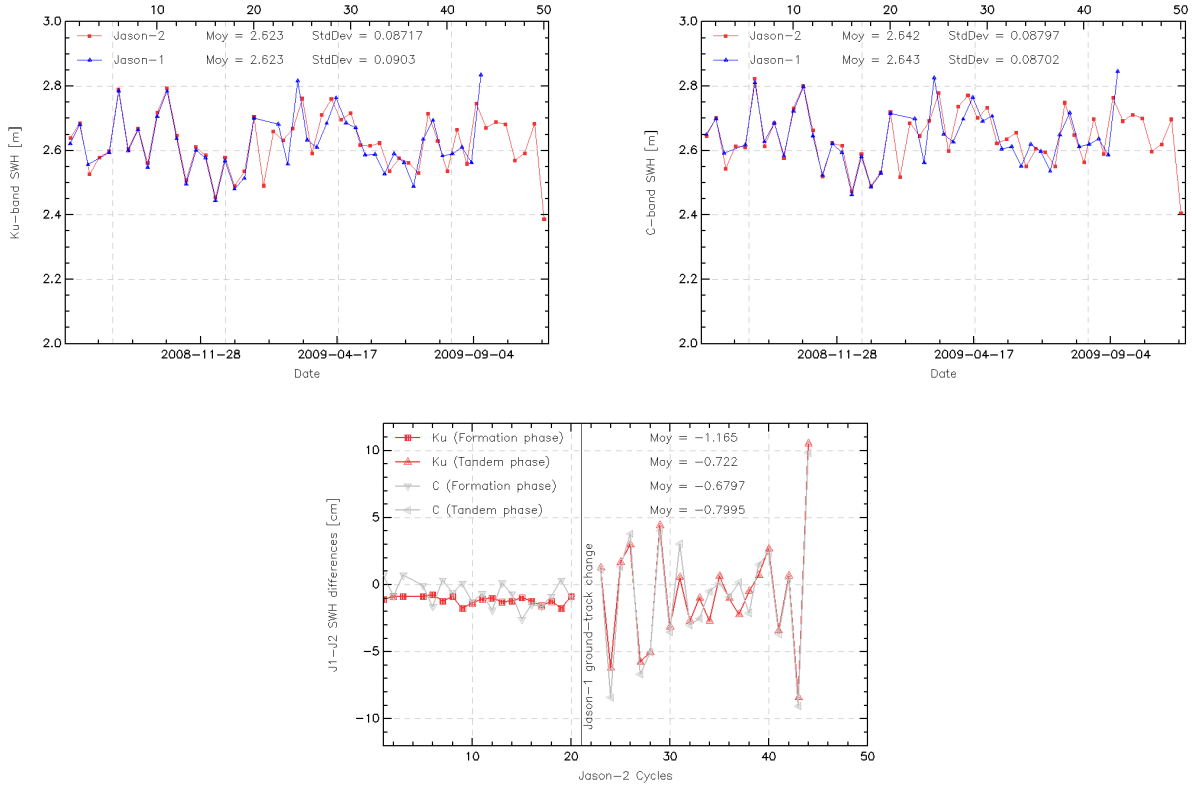

Figure 32: *Cyclic monitoring of SWH for Jason-1 and Jason-2 for Ku-band (left) and C-band (right) and Jason-1 - Jason-2 differences (bottom).*

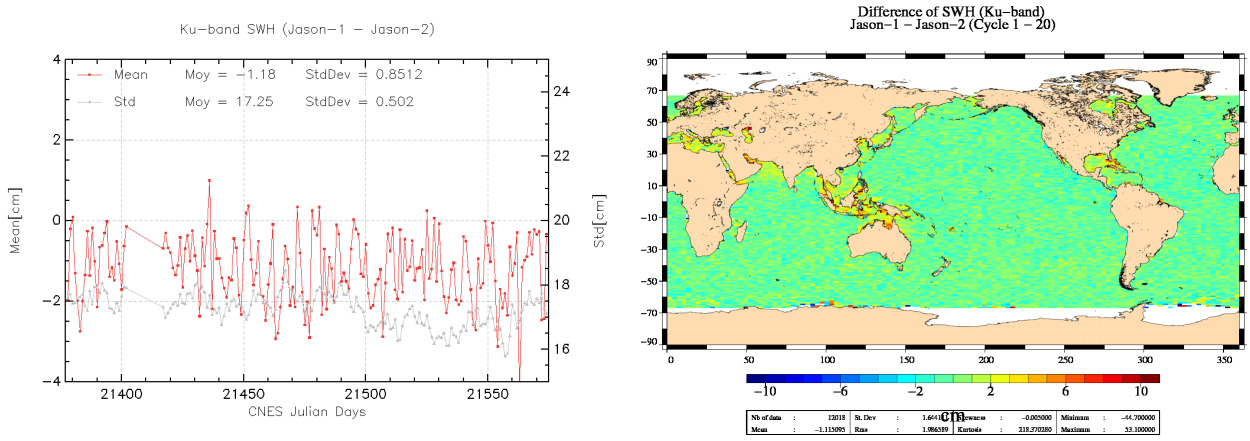

Figure 33: *Daily monitoring of mean and standard deviation of Jason-1 - Jason-2 differences for Ku-band SWH (left) and map showing mean of Jason-1 - Jason-2 differences over cycles 1 to 20.*

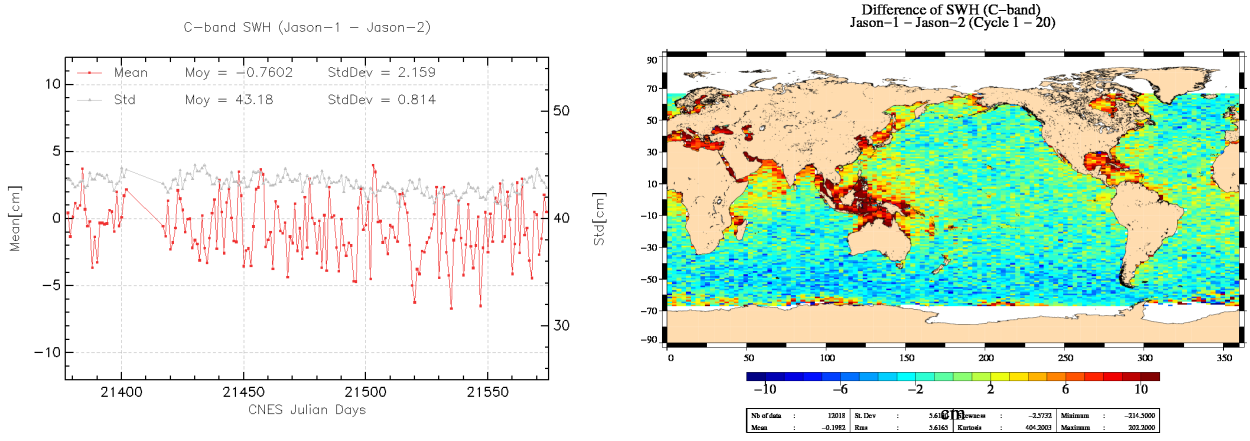

Figure 34: *Daily monitoring of mean and standard deviation of Jason-1 - Jason-2 differences for C-band SWH (left) and map showing mean of Jason-1 - Jason-2 differences over cycles 1 to 20.*

4.6. Dual-frequency ionosphere correction

The dual frequency ionosphere corrections derived from the Jason-2 and Jason-1 altimeters show a mean difference of about -0.9 cm (figure 35 (left)), with cycle to cycle variations lower than 1 mm. This bias is due to the relative Ku-band (-8.3 cm) and C-band (-13.1 cm) range difference between Jason-1 and Jason-2. As the dual-frequency ionosphere correction is derived from a combination of Ku and C band ranges, a bias of -8.5 mm between Jason-1 and Jason-2 results [10]. Apart from this bias, the two corrections are very similar and vary according to the solar activity. The map of local differences (figure 35 right) shows increased differences near Indonesia (probably correlated to high MQE values).

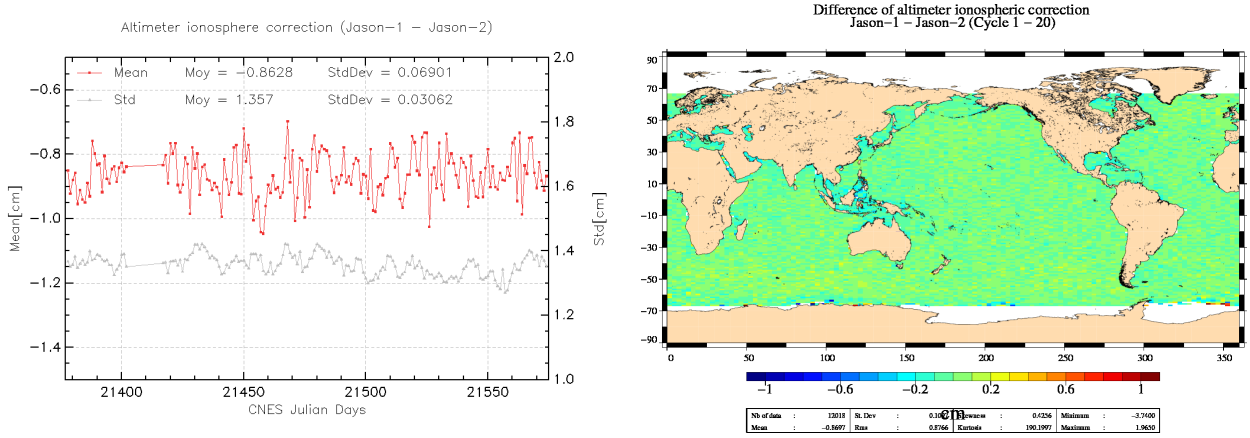

Figure 35: *Daily monitoring of mean and standard deviation of Jason-1 - Jason-2 differences for dual-frequency ionospheric correction (left) and map showing mean of Jason-1 - Jason-2 differences over cycles 1 to 20.*

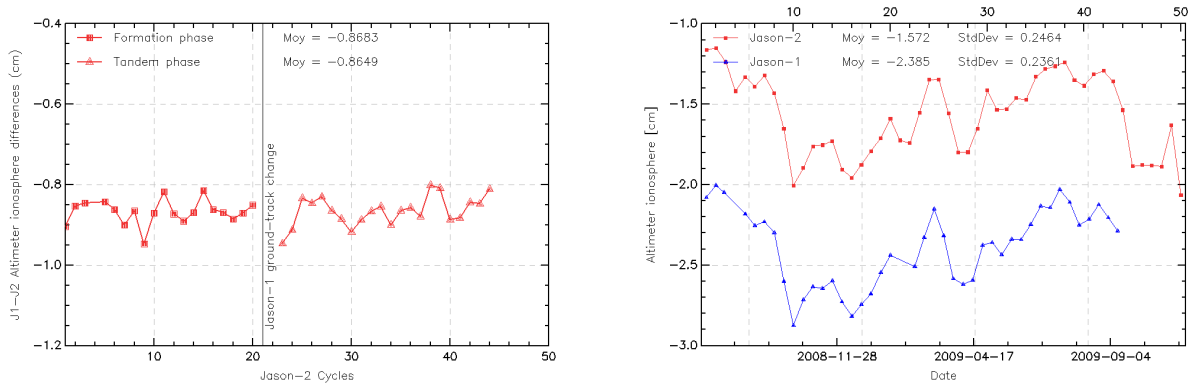

Figure 36: *Cyclic monitoring of dual-frequency ionosphere for Jason-1 and Jason-2 (right) and Jason-1 - Jason-2 differences (left).*

Notice that, as for TOPEX and Jason-1 (Le Traon et al. 1994 [20], Imel 1994 [19], Zlotnicky 1994 [31]), it is recommended to filter the Jason-2 dual frequency ionosphere correction before using it as a SSH geophysical correction (Chambers et al. 2002 [8]). A low-pass filter has thus

been used to remove the noise of the correction in all SSH results presented in the following sections. Plotting difference of non-filtered ionospheric correction between Jason-1 and Jason-2 versus Jason-2 ionospheric correction shows an apparent scale error, which disappears when using filtered data (see figure 37). As currently ionosphere correction is very low, the ionosphere noise is of the same order of magnitude as the ionosphere correction itself. Therefore plotting the difference of non-filtered dual-frequency ionospheric correction versus dual-frequency ionospheric correction induces an apparent scale error.

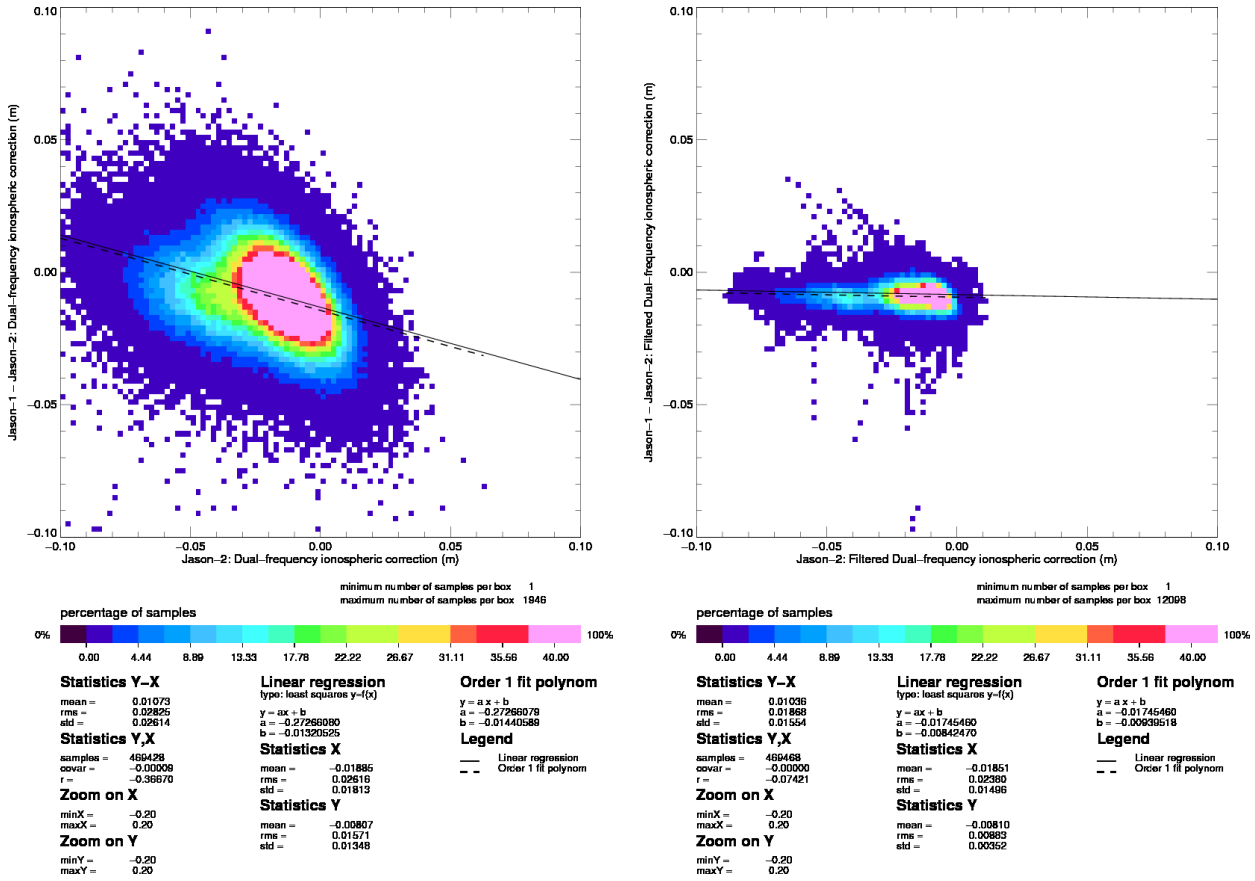

Figure 37: *Diagram of dispersion of Jason-1 - Jason-2 versus Jason-2 dual-frequency ionosphere correction for Jason-2 cycle 15. Left: non-filtered, right: filtered.*

4.7. AMR Wet troposphere correction

Figure 38 shows on the left side the daily monitoring of the difference of radiometer wet troposphere correction between the two missions (JMR - AMR). AMR is globally slightly dryer than JMR (-0.15 cm). But locally, especially near equator and coasts (right side of figure 38), AMR is wetter than JMR. In the daily monitoring, an odd behaviour is visible after the Jason-1 safehold mode in August 2008 which occured in the middle of Jason-2 cycle 3 till end of Jason-2 cycle 4: difference between JMR and AMR shows several large anomalies reaching up to 7 mm. This is due to odd behaviour of JMR, as described in the next section.

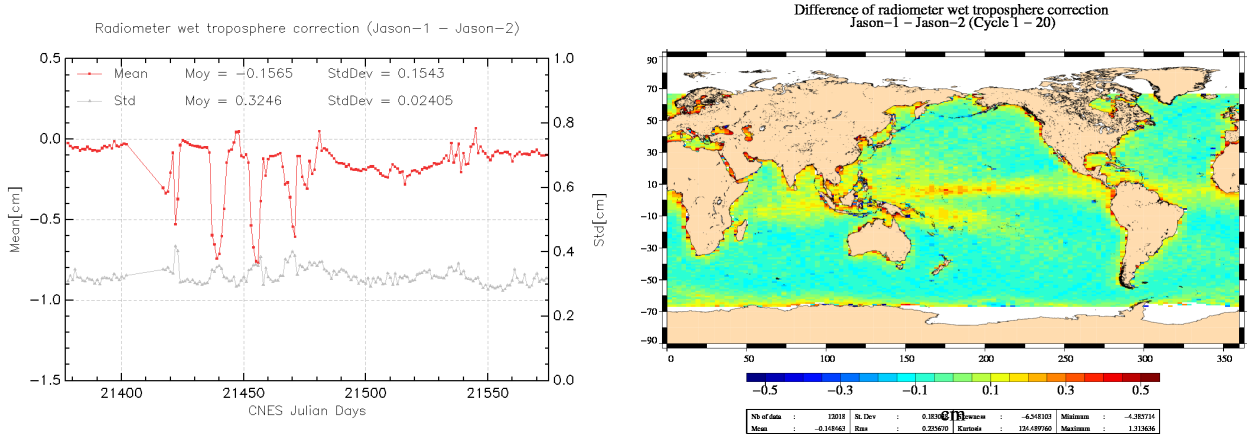

Figure 38: *Daily monitoring of mean and standard deviation (left) of Jason-1 - Jason-2 radiometer wet troposphere correction. Map showing mean of Jason-1 - Jason-2 differences over cycles 1 to 20.*

4.7.1. Comparison with the ECMWF model

The ECWMF wet troposphere correction has been used to check the Jason-1 and Jason-2 radiometer corrections. Daily differences are calculated and plotted in figure 39. It clearly appears that Jason-2 radiometer correction (AMR) from GDR products is much more stable than for Jason-1 (JMR), especially at the beginning of Jason-2 period where large oscillations (up to 7mm) are observed between JMR and model. Indeed after the safehold mode of Jason-1 in August 2008 (corresponding to Jason-2 cycle 4), JMR experienced some thermal instability. In addition, small differences linked to yaw-dependent effects (as also observed on TOPEX radiometer (Dorandeu et al., 2004, [13])) are visible. In order to take into account these effects, new JMR calibration coefficients are regularly provided and updated at least at each new Jason-1 GDR release. Now, thanks to the new ARCS (Autonomous Radiometer Calibration System) (Brown et al. 2009, [6]) calibration system set up for Jason-2, AMR radiometer correction is calibrated at each GDR cycle explaining its better stability. However, the AMR comparison with model highlights also long-term signals with Jason-2 not clearly observed with Jason-1. As a result of a poor confidence in JMR stability, Envisat wet troposphere correction (MWR) is also compared to the ECMWF model in same figure 39. Concerning the end of the period (from May 2009), Envisat and Jason-2 provide similar differences with model likely in relationship with evolutions in the ECWMF operational model. Focusing on the beginning of the Jason-2 period, MWR correction shows a negative trend with the model (3mm

over 3 months) also observed on JMR/model curve. In the meantime, this trend is not detected on AMR (GDR)/model comparisons which is much more stable over this period. This last result does not demonstrate necessarily the better stability of AMR. Indeed, there might be a risk that real geophysical signals are absorbed by the calibration method used. Finally, the cross-comparison between all radiometers and models available is a good way to analyze the stability of the each wet troposphere correction.

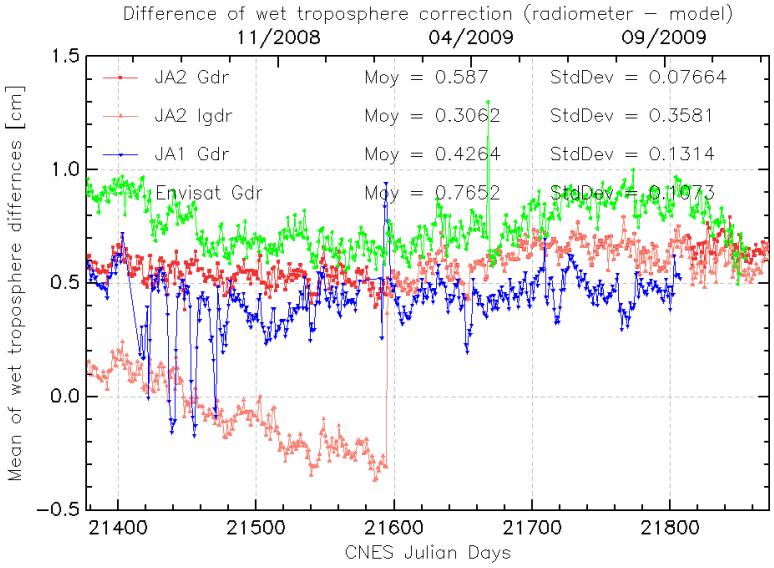

Figure 39: *Daily monitoring of radiometer and ECMWF model wet troposphere correction differences for Jason-1 (blue), Jason-2 (red) and Envisat (green).*

5. SSH crossover analysis

5.1. Overview

SSH crossover differences are the main tool to analyze the whole altimetry system performances. They allow us to analyze the SSH consistency between ascending and descending passes. However in order to reduce the impact of oceanic variability, we select crossovers with a maximum time lag of 10 days. Mean and standard deviation of SSH crossover differences are computed from the valid data set to perform maps or a cycle by cycle monitoring over all the altimeter period. In order to monitor the performances over stable surfaces, additional editing is applied to remove shallow waters (bathymetry above -1000m), areas of high ocean variability (variability above 20 cm rms) and high latitudes ($> |50|deg$). SSH performances are then always estimated with equivalent conditions.
The main SSH calculation for Jason-2 and Jason-1 are defined below.

$$SSH = Orbit - Altimeter\ Range - \sum_{i=1}^{n} Correction_i$$

with $Jason-1/Jason-2\ Orbit = POE\ CNES\ orbit$ for GDR products, and

$$\begin{aligned}\sum_{i=1}^{n} Correction_i &= Dry\ troposphere\ correction \\ &+ Dynamical\ atmospheric\ correction \\ &+ Radiometer\ wet\ troposphere\ correction \\ &+ Dual\ frequency\ ionospheric\ correction\ (filter\ 250\ km) \\ &+ Non\ parametric\ sea\ state\ bias\ correction \\ &+ GOT00\ ocean\ tide\ correction\ (including\ loading\ tide) \\ &+ Earth\ tide\ height \\ &+ Pole\ tide\ height\end{aligned}$$

5.2. Mean of SSH crossover differences

The cycle by cycle mean of SSH differences is plotted in figure 40 for Jason-1 and Jason-2. Both curves are very similar and do not highlight any strong anomaly. However, most of the time they are slightly negative (-0.55 cm for Jason-2 and -0.35 cm for Jason-1 in average) indicating a systematic ascending/descending SSH bias. The map of SSH differences calculated over all the Jason-2 period in left side of figure 41, shows that this bias is not spatially homogenous with a negative structure reaching -2 cm in the southern Atlantic, east of the southern Pacific, and west of the Indian Ocean and tropical Pacific. In inverse, a positive patch close to +2 cm is observed in the northern Atlantic. Although orbit are fully compliant with mission requirements, orbit calculation is the main source to explain these discrepancies between ascending and descending passes since they are significantly reduced using other orbits than those available in GDR products, such as orbits based only on GPS solutions provided by CNES ([7]) or JPL ([3]). The map of mean SSH

crossover differences plotted in right side of figure 41 was calculated by applying the JPL orbit (JPL09A) instead of GDR operational orbit. It just highlights a small hemispheric signal lower than 1 cm between northern and southern hemisphere. It comes from a small pseudo time tag bias (-0.28 ms) as explained further in this chapter.

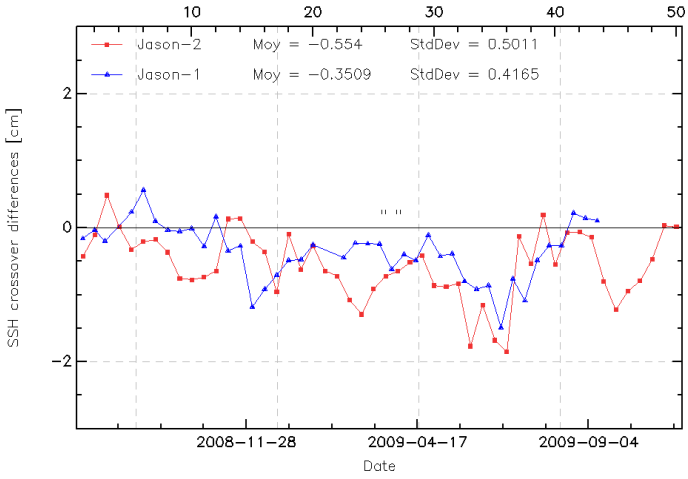

Figure 40: *Monitoring of mean of SSH crossover differences for Jason-2 and Jason-1 using official POE orbits from GDR.*

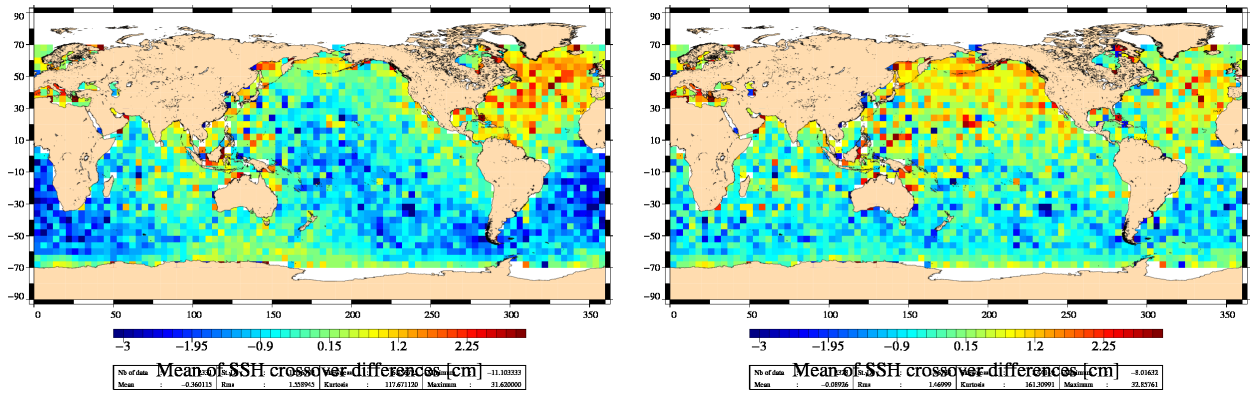

Figure 41: *Map of mean of SSH crossovers differences for Jason-2 cycle 1 to 50 using GDR orbit (left) and for cycles 1 to 40 using GPS orbit JPL09A (right).*

5.3. Standard deviation of SSH crossover differences

The cycle by cycle standard deviation of SSH crossovers differences are plotted for Jason-2 and Jason-1 in figure 42 after applying geographical criteria as defined previously. Both missions show very good performances, very similar and stable in time. No anomaly is detected. The average figure is 5.07 cm rms for both missions. Keeping in mind that during the Jason-1/TOPEX formation flight phase in 2002, the same statistic using Jason-1 GDR-A products was close to 6.15 cm (see [13]). This illustrates the improvements performed in the altimetry ground processing since the Jason-1 launch especially thanks to new retracking algorithms, new geophysical corrections (oceanic tidal, dynamic atmospheric correction, ...) and new orbit calculations implemented first in GDR-B and later in GDR-C release (see [24] concerning impact of GDR-B/GDR-A, [9] concerning impact of GDR-C/GDR-B).

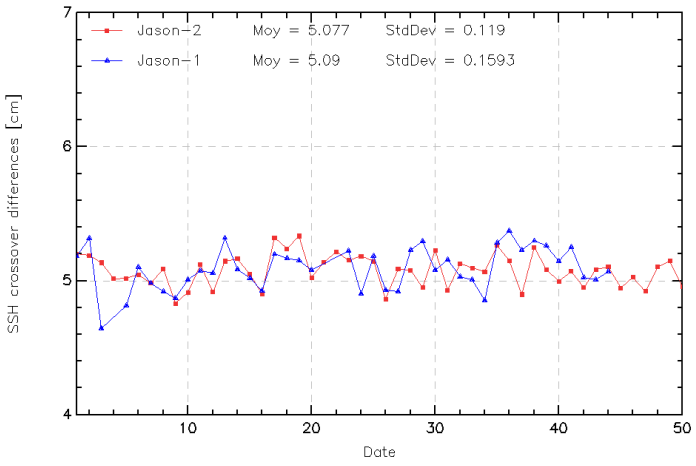

Figure 42: *Cycle by cycle standard deviation of SSH crossover differences for Jason-2 and Jason-1 over the Jason-2 period.*

5.4. Estimation of pseudo time-tag bias

The pseudo time tag bias (α) is found by computing at SSH crossovers a regression between SSH and orbital altitude rate ($\dot{H}$), also called satellite radial speed:

$$SSH = \alpha \dot{H}$$

. This empirical method allows us to estimate the potential real time tag bias but it can also absorb other errors correlated with $\dot{H}$. Therefore it is called ?pseudo? time tag bias. The monitoring of this coefficient estimated at each cycle is performed for Jason-1 and Jason-2 in figure 43. Both curves are very similar highlighting a 60-day signal and a bias close to -0.25 ms for Jason-1 and -0.28 ms for Jason-2. As mentioned just previously, this bias directly explained the small hemispheric differences observed at SSH crossover differences with maximal differences close to 8 mm where $\dot{H}$ is maximal (15 $m.s^{-1}$) at medium latitudes ($\pm 50^{\circ}$). To date, the origin of this pseudo time tag bias or the 60 day-signal is unexplained. Studies are on going to understand it, testing the impact of the orbit calculation for instance. However, a correction containing $\alpha \dot{H}$ in Jason-1 GDR-C products ([2]) has been already added to improve the Jason-1 SSH calculation. Similar improvements could be carried out in next Jason-2 GDR release.

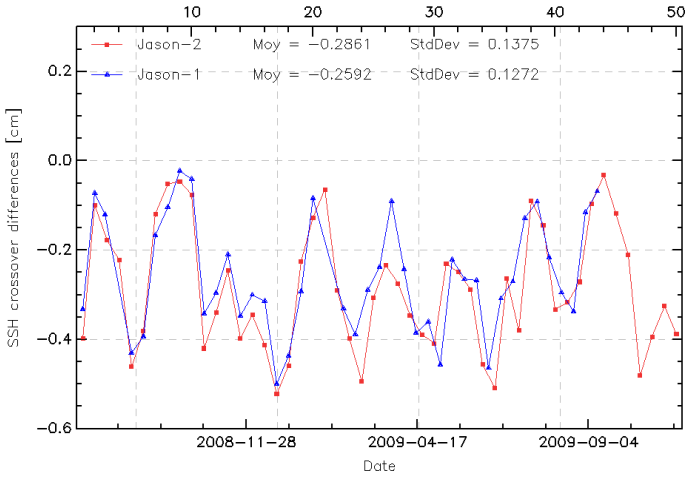

Figure 43: *Monitoring of pseudo time-tag bias estimated cycle by cycle from GDR prodcuts for Jason-2 and Jason-1*

6. Sea Level Anomalies (SLA) Along-track analysis

6.1. Overview

The Sea Level Anomalies (SLA) are computed along track from the SSH minus the mean sea surface (MSS CLS2001) with the SSH calculated as defined in previous section 5.1. :

$$SLA = SSH - MSS(CLS2001)$$

SLA analysis is a complementary indicator to estimate the altimetry system performances. It allows us to study the evolution of SLA mean (detection of jump, abnormal trend or geographical correlated biases), and also the evolution of the SLA variance highlighting the long-term stability of the altimetry system performances. In order to take advantage of the Jason-2/Jason-1 formation flight phase (cycles 1 to 20), we performed direct SLA comparisons between both missions during this period. Corrections applied in SSH calculation are theoretically the same for Jason-1 and Jason-2 since both satellites measure the same ocean. Thus, it?s possible to not apply them in order to obtain directly information on the altimeter range and the orbit calculation differences. However, as the repetetivity of both ground passes is not exact (± 1 km cross-track distance), SLA measurements have to be projected and interpolated over the Jason/TOPEX theoretical ground pass after applying the MSS in order to take into account cross-track effects on SSH.

$$\Delta SLA_{J1-J2} = [(Range_{Ku} - Orbite - MSS)_{J1}]_{\bar{T}} - [(Range_{Ku} - Orbite - MSS)_{J2}]_{\bar{T}}$$

This allows us also to select the intersection of both datasets and compare exactly the same data. After Jason-1 ground track change, direct SLA comparisons are no more possible. Thus, global statistics computed cycle by cycle are just basically compared.

6.2. Mean of SLA differences between Jason-2 and Jason-1

The cycle by cycle monitoring of mean SLA differences between Jason-1 and Jason-2 is plotted in figure 44 over all the Jason-2 period. During the formation flight phase, the SSH bias is computed with and without the SSH corrections. Both curves are very similar and stable in time with variations lower than 1 mm rms. They are just spaced out by a 0.8 cm bias resulting from differences between Jason-1 and Jason-2 ionosphere corrections and also between radiometer wet troposphere corrections as previously mentioned in this paper. The global average SSH bias is close to -7.45 cm using SSH corrections and -8.3 cm without. Recent investigations presented at Seattle OSTST in June 2009 [Zaouche, 2009], [Desjonqueres, 2009] explained the origin of most of the bias between both altimeters. The authors explain that there are 2 origins. Firstly the use of a truncated altimeter PRF (Pulse repetition frequency) in the Jason-1 and Jason-2 ground segments leads to a Jason-1 minus Jason-2 difference of 2.15 cm, and secondly a difference in the characterization parameter set for Ku-band leads to a difference of -11.70 cm, combining to a Jason-1 minus Jason-2 bias of -9.5 cm. This is very close to the observed bias of -8.3 cm. However, the more crucial point for scientific applications is to insure that there is no drift between both missions, since the global bias can be easily corrected a fortiori. The extension of the monitoring of the SSH bias after the Jason-1 ground track change is precisely a good way to check the long-term Jason-1 and Jason-2 stability. It is plotted over 44 cycles in figure 44 and does not highlight any drift.
Spatial SLA differences (only during the Jason-1 formation flight phase) show a very homogenous map between both missions as plotted in left side of figure 45. However a weak hemispheric bias

lower than 1 cm is detected in relationship with orbit calculation differences. Indeed, the use of a GSFC orbit for both Jason-1 and Jason-2, showed that this hemispheric bias is reduced (right side of figure 45).

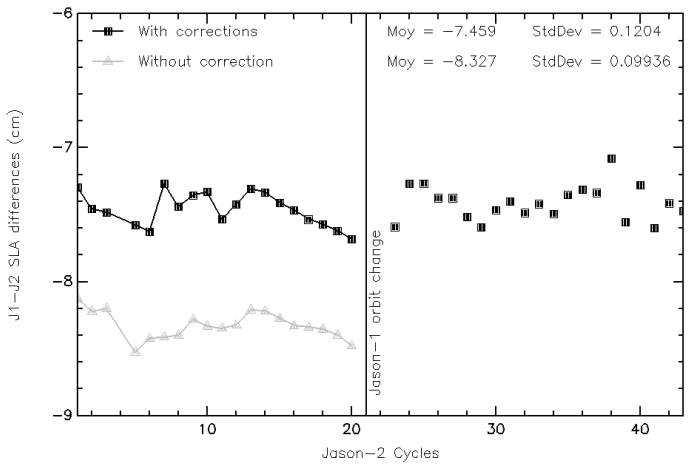

Figure 44: *Cycle by cycle monitoring of SSH bias between Jason-1 and Jason-2 before and after Jason-1 ground-track change (black curve and dots) and SSH bias without applying corrections in SSH calculation for both missions only during the formation flight phase (gray curve).*

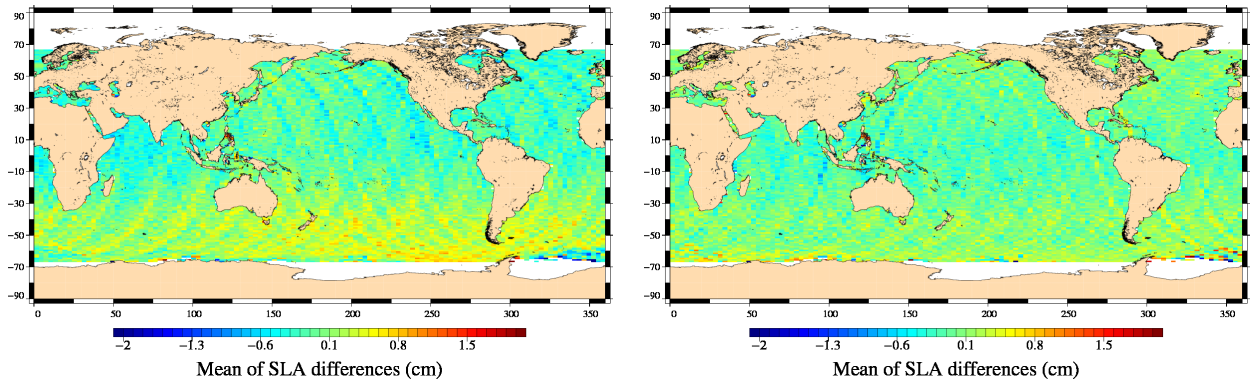

Figure 45: *Maps of SLA mean differences between Jason-1 and Jason-2 during formation flight phase (cycles 1 to 20) using official POE orbit from GDRs (left) and GSFC09 orbit (right)*

6.3. Standard deviation of SLA differences between Jason-2 and Jason-1

The monitoring of SLA standard deviation has been computed for both missions over the whole data set (plotted in figure 46). Both curves are very well correlated during the formation flight phase (close to 10.7 cm rms in average) although small differences are observed for some cycles in relationship with specific altimeter events (maneuvers, altimeter incidents) impacting the data coverage or the orbit calculation. After the Jason-1 ground track change (from Jason-2 cycle 21 onwards), Jason-1 standard deviation increases by almost 3 cm rms in average: 10.77 cm rms for Jason-1 instead of 10.44 cm rms for Jason-2. The use of the Mean Sea Surface [18] explains the Jason-1 standard deviation increase since MSS errors are higher outside the historical T/P-Jason ground track. Similar feature was observed comparing Jason-1 and TOPEX performances after T/P satellite was moved on its new ground track in August 2002 ([13]). Future MSS using all the satellite tracks including the interleaved T/P and Jason-1 ground tracks - which will be computed in the frame of the SLOOP project ([14]) - should improve the SLA calculation also for the interleaved ground tracks. Cartography of standard deviation of spatial Jason-1 minus Jason-2 SLA differences (not shown here) does not show any anomaly. It varies indeed in function of noise on measurements, which is dependant on significant wave height. Therefore, standard deviation of SLA differences is higher in regions with important significant wave heights.

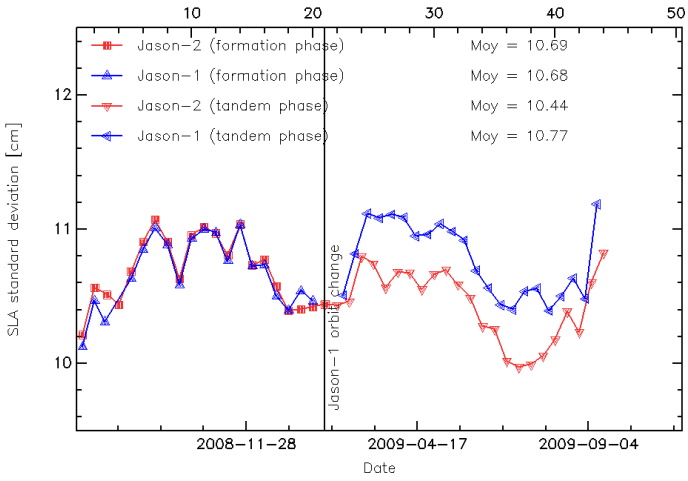

Figure 46: *Cycle by cycle monitoring of SLA standard deviation for Jason-1 and Jason-2.*

6.4. Mean sea level (MSL) calculation

The global mean level of the oceans is one of the most important indicators of climate change. Precise monitoring of changes in the mean level of the oceans, particularly through the use of altimetry satellites, is vitally important, for understanding not just the climate but also the socioeconomic consequences of any rise in sea level. Thanks to the T/P, Jason-1 and now Jason-2 altimetry missions, the global MSL has been calculated on a continual basis since January 1993 (figure 47) highlighting a trend of 3.26 mm/yr (see http://www.aviso.oceanobs.com/msl). Notice that the global isostatic adjustment (-0.3 mm/yr, [23]) is applied. We replaced Jason-1 by Jason-2 in the MSL time data series at Jason-2 cycle 11 (October 2008) applying a SSH bias between both missions of -7.45 cm as calculated previously. To calculate a precise MSL rate, it is essential to link accurately time data series together. Recent study ([1]) showed the uncertainty on the global MSL trend resulting from the impact of MSL bias uncertainties between TOPEX-A and TOPEX-B (due to altimeter change in February 1999) and between TOPEX-B and Jason-1 (in May 2002) is close to 0.2 mm/yr from 1993 onwards. As we showed just previously, the SSH consistency between Jason-1 and Jason-2 is very good in space and stable in time, the SSH bias uncertainty is consequently very weak close to 0.5 mm. It is lower than between T/P and Jason-1 (estimated close to 1 mm ([1])). Its impact on global MSL trend error budget is thus very weak: lower than 0.05 mm/yr.

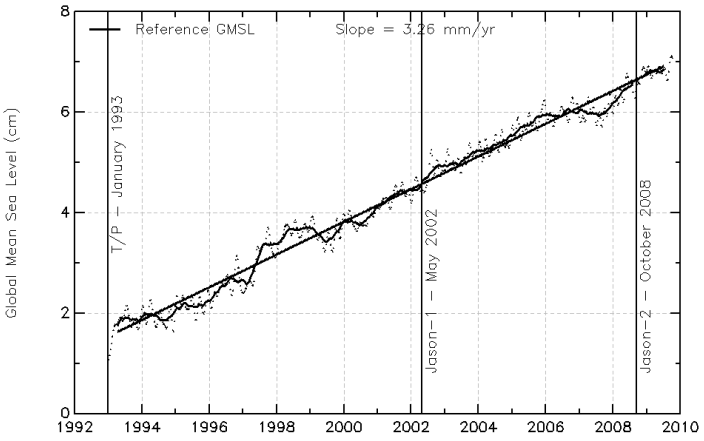

Figure 47: *MSL evolution calculated from T/P, Jason-1 and using Jason-2 data from october 2008.*

7. Particular Investigations

This sections contains some investigations led on Jason-2 data, such as on the low signal tracking anomaly, on testing the use of MQE threshold for Jason-2 1 Hz compression and an analysis of high frequency spectrums.

7.1. Low signal tracking anomaly (AGC anomaly)

During SGT and also Median tracking mode, Jason-2 altimeter could track during several minutes low signal echoes with "Brown like" but "distorted" shape (see [11]). This concerned less than 0.5% of ocean measurements. An example of waveforms during such an anomaly is visible in [26]. This anomaly was especially noticeable over ocean. These measurements were edited by several parameters out of threshold: mispointing, backscattering coefficient, significant wave height. They also showed a drop in AGC (automatic gain control). These anomalies were called "low signal tracking anomaly" or "AGC anomaly". An example of low signal tracking anomaly is shown in figure 48.

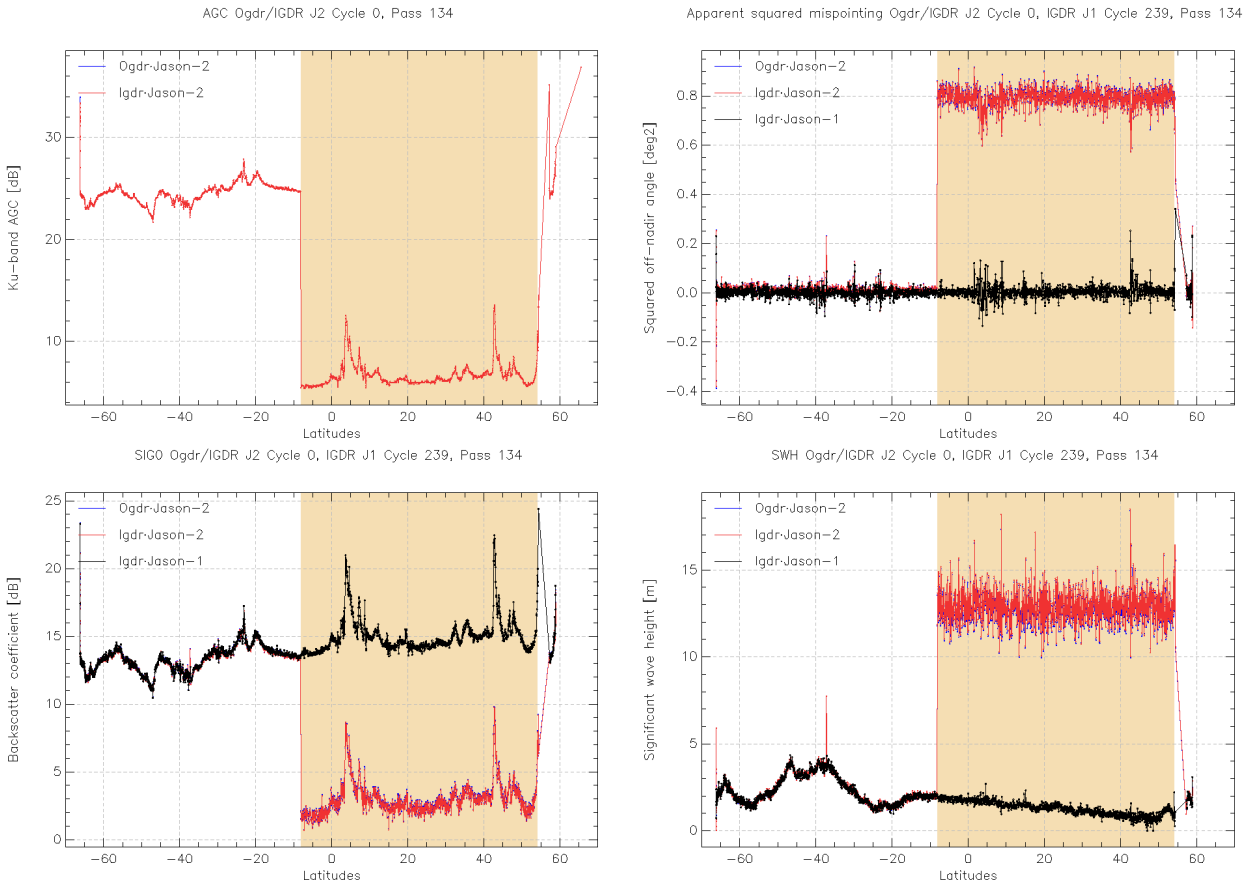

Figure 48: *Example of low signal tracking anomaly for pass 134, Jason-2 cycle 0. Several parameters are shown: AGC (top left), apparent squared mispointing (top right), Sigma0 (bottom left), and SWH (bottom right). Period of anomaly colored.*

Low signal tracking anomaly were especially severe (several tens of minutes) during SGT mode, they were shorter in median mode (at worst a couple of minutes) and never appeared during DEM modes. During cycle 16, on 10th of December, a correction for the low signal tracking anomaly (AGC anomaly) was uploaded (during pass 73). Till cycle 16, pass 70 AGC anomalies were still detected, biggest one (lasting approximately 2 minutes) on the transition Africa/ Indian ocean (pass 5). But no further AGC anomaly (on ocean) has occurred since the upload of the correction. The correction for the low signal tracking anomaly consists in more strict criteria for acquisition (to avoid that low signal echoes are tracked). This has no impact for the quantity of ocean measurements as shown on figure 49 where cycle 15 (before upload of correction for low signal tracking anomaly) and 18 (after upload of correction) show equivalent number of measurements. But number of tracked measurements over land has decreased (see figure 50 and 51).

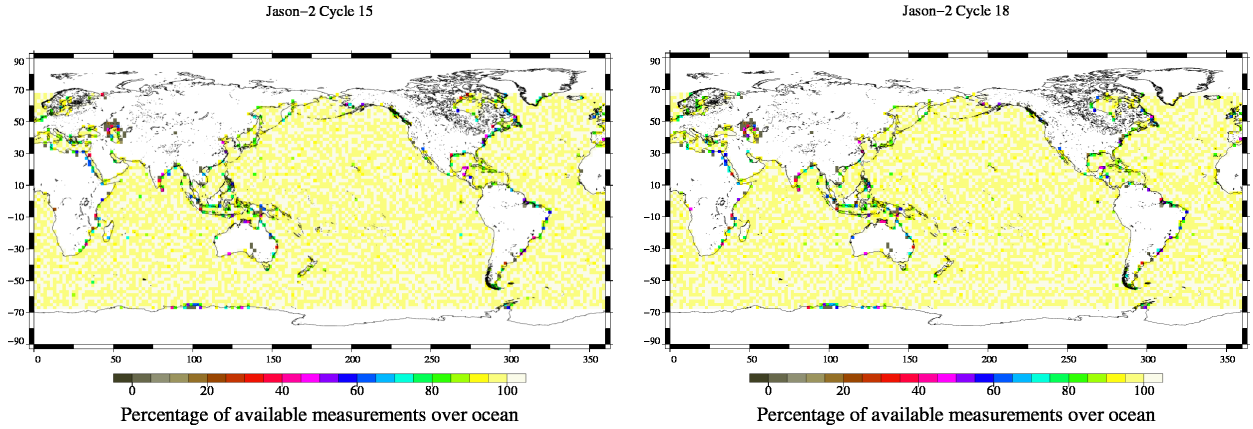

Figure 49: *Percentage of available measurements over ocean for Jason-2 cycle 15 (left) and 18 (right).*

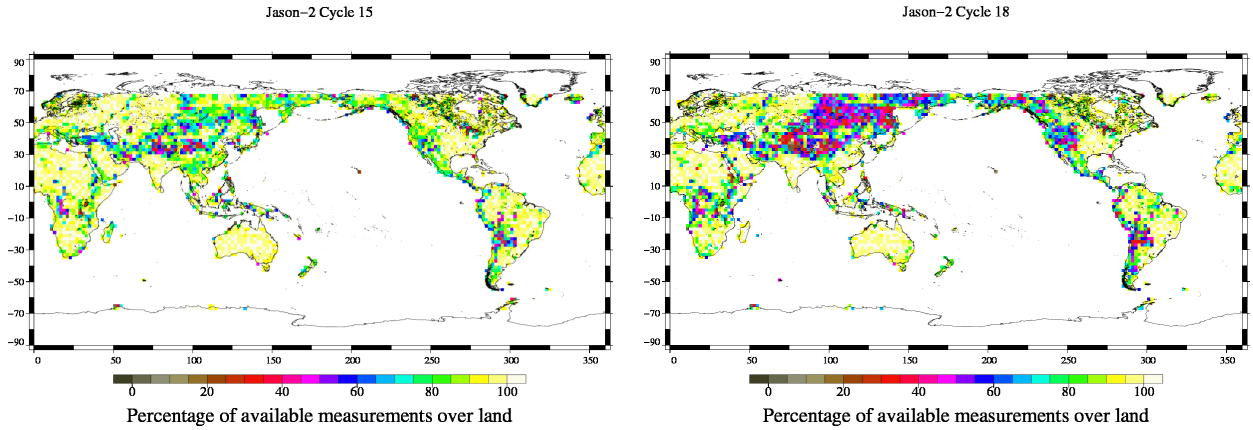

Figure 50: *Percentage of available measurements over land for Jason-2 cycle 15 (left) and 18 (right).*

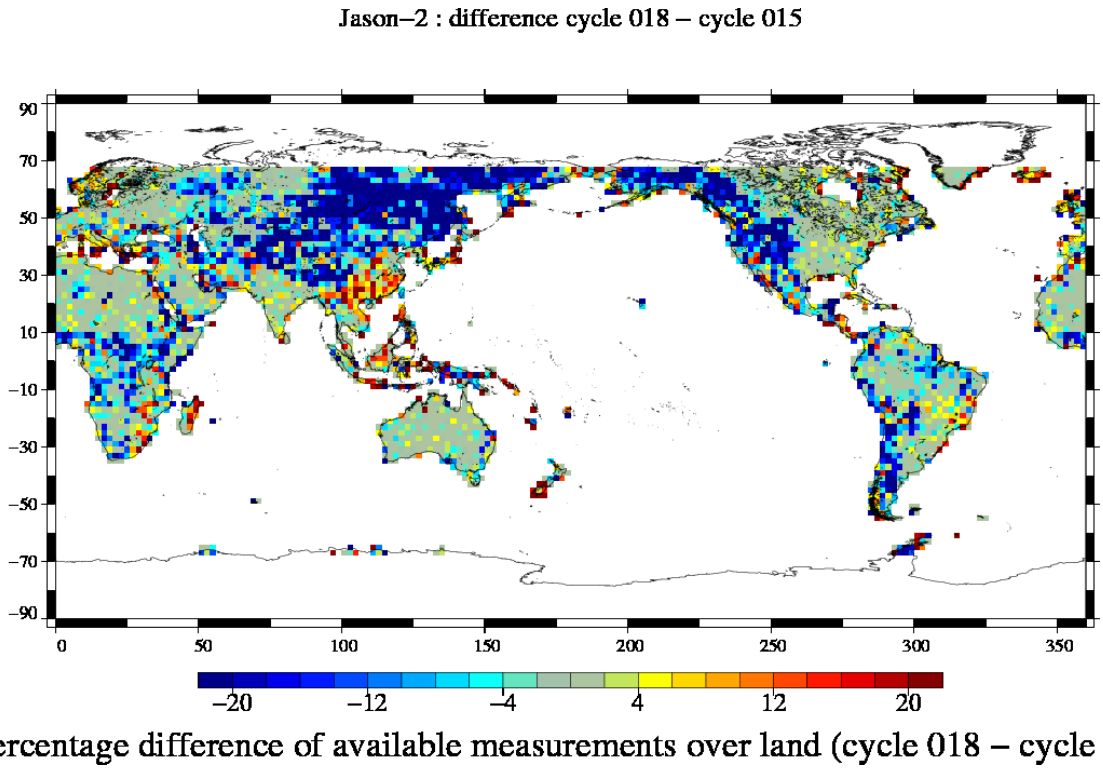

Figure 51: *Percentage difference of available measurements over land for Jason-2. Cycle 018 (after correction) - cycle 015 (before correction).*

7.2. Study applying MQE threshold during 1 Hz compression

Comparison maps of Jason-1 and Jason-2 differences (after interpolation on theoretical track) have shown regional differences around Indonesia especially for C-band parameters (number of elementary range measurements (figure 23, significant wave height (figure 34)), which seems to be correlated with MQE (Mean quadratic error) values (figure 52).

This is supposed to be due to the fact that for Jason-2 1-Hz compression, no threshold is used on MQE. This choice was made, since threshold from Jason-1 was not applicable to Jason-2 (it eliminated too much measurements).

This hypothesis was verified for Jason-2 Igdr cycle 10 by a study, using the following thresholds for MQE during compression : 0.0171 for Ku-band, and 0.1559 for C-band. These values correspond to 3 sigma (see figure 53).
The following parameters were therefore recomputed for Ku- and C-band: range, number and rms of elementary range measurements, significant wave height, rms of 20 Hz significant wave height measurements, backscattering coefficient, number and rms of 20 Hz backscattering coefficient. Dual-frequency ionospheric correction was recomputed using new range and (old) sea state bias.
Only a simple editing procedure was used, based on threshold editing, to keep valid measurements.

7.2.1. Comparison residus differences

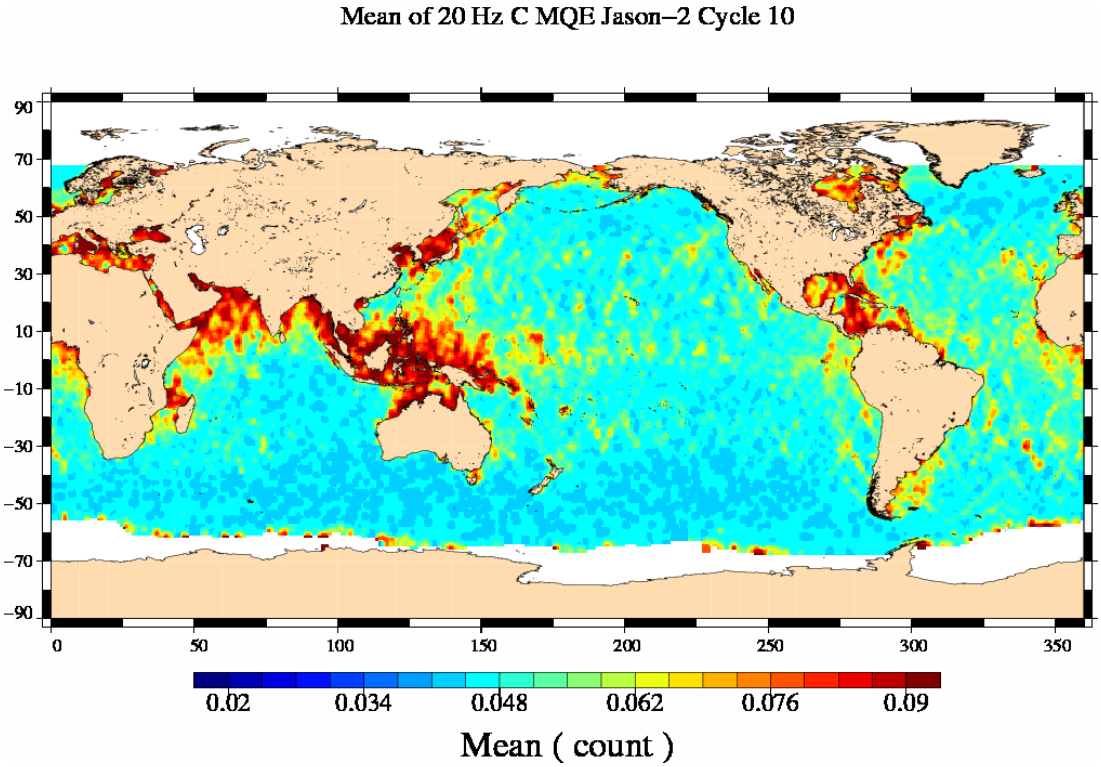

Figure 52: *Map showing C-Band MQE for Jason-2 cycle 10.*

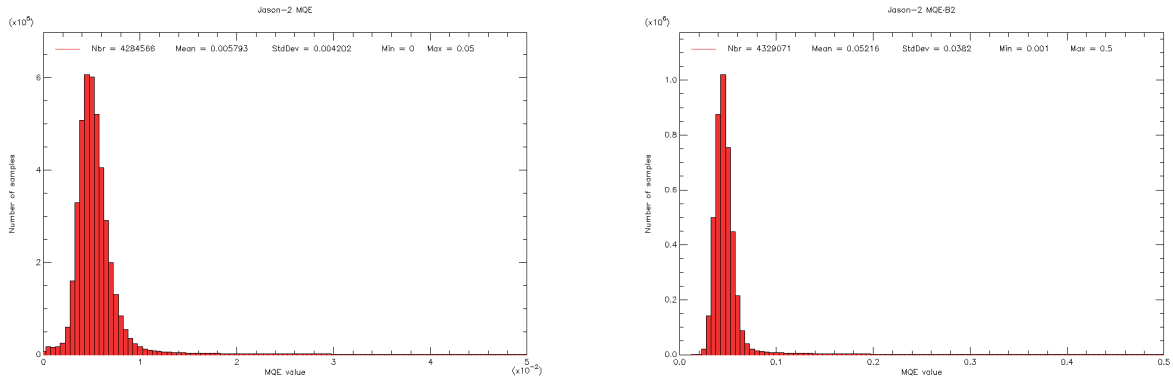

Figure 53: *Histogram of Jason-2 MQE for Ku-band (left) and C-band (right).*

In the following, residus differences (JA1-JA2) are shown for Jason-2 cycle 10 (Jason-1 cycle 249). These are differences of Jason-1 and Jason-2 measurements after interpolation on theoretical ground pass (as real ground passes of both satellites may deviate up to ±1km from theoretical ground pass). On the left side figures difference is made using variables from original Jason-2 products. On the right side Jason-2 variables were recomputed using the MQE threshold.

7.2.1.1. Ku - C band range difference

MQE threshold changes only slightly the bias of Ku - C-band range differences between Jason-1 and Jason-2. It goes from -4.75 cm (without MQE threshold) to -4.60 cm (with MQE threshold).

Nevertheless the differences visible in Mediterranean Sea, around Indonesia and in the Gulf of Mexico seem to be attenuated.

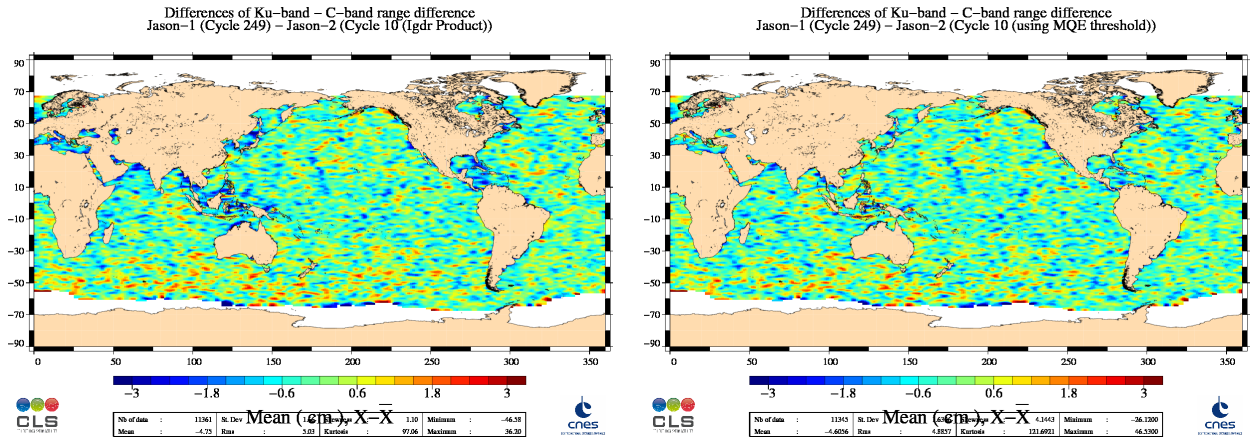

Figure 54: *Map showing mean of JA1-JA2 residus difference of Ku-band - C-band range difference. Left: original JA2 product, right recomputed JA2.*

7.2.1.2. Number of elementary C-band range measurements

Comparing elementary number of 20Hz C-band range measurements showed a mean bias of 0.2 counts, meaning that number of 20Hz C-band range measurements are in average lower for Jason-1 than for Jason-2, as some elementary measurements were eliminated by MQE threshold criterion active for Jason-1. Differences are especially visible for regions with high MQE values, as Mediterranean Sea and around Indonesia (left side of figure 55). Using also a MQE threshold for Jason-2, eliminates elementary 20 Hz C-band range measurements for Jason-2, so in average between the two satellites there is only a difference of 0.02 count. The large differences in high MQE regions have also disappeared (right side of figure 55).

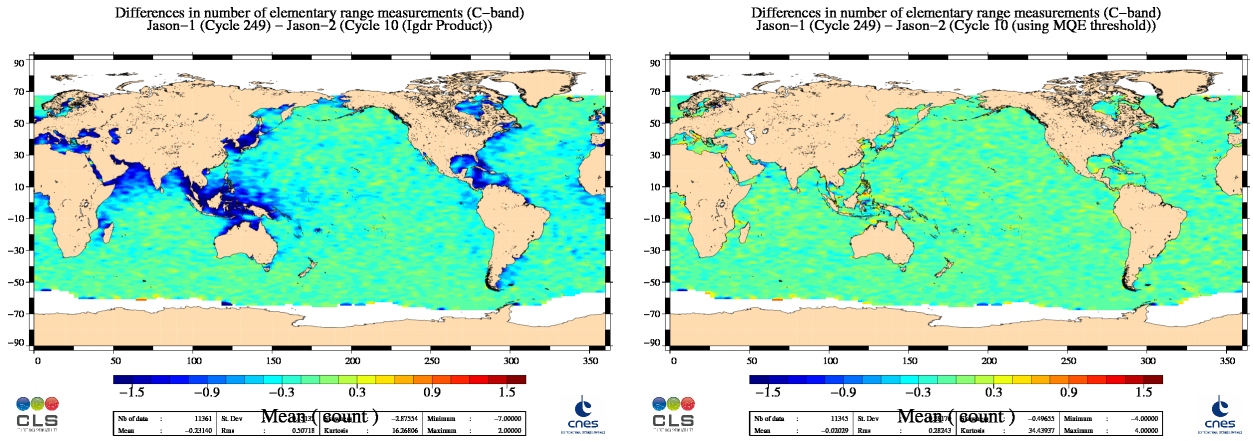

Figure 55: *Map showing mean of JA1-JA2 residus difference of number of elementary C-band range measurements. Left: original JA2 product, right recomputed JA2.*

7.2.1.3. C-band significant wave height

Using MQE threshold for Jason-2 increases the global bias of C-band SWH between Jason-1 and Jason-2 from -0.8 cm to -3.5 cm, but local biases are reduced.

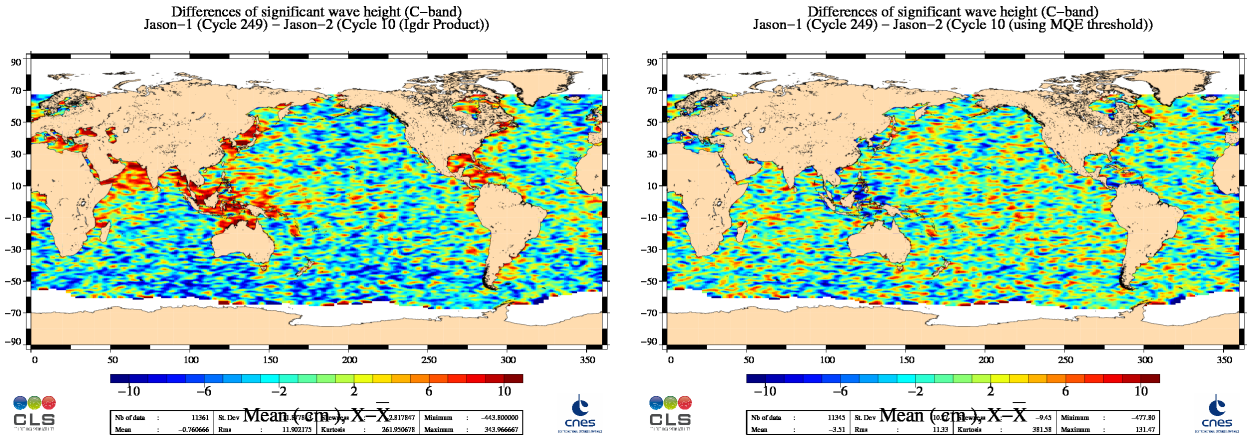

Figure 56: *Map showing mean of JA1-JA2 residus difference of C-band significant wave height. Left: original JA2 product, right recomputed JA2.*

The following table reminds the value around which the maps are centered.

parameter	JA1-JA2 mean (product)	JA1-JA2 mean (JA2 recomputed)
SWH Ku	-1.36 cm	-1.521 cm
SWH C	-0.760 cm	-3.51 cm
Rms of 20 Hz SWH Ku	0.146 cm	0.149 cm
Rms of 20 Hz SWH C	0.809 cm	0.803 cm
Rms of 20hz Ku range	-0.011 cm	-0.006 cm
Rms of 20hz C range	-0.003 cm	0.031 cm
Nb of 20hz Ku range	-0.117	-0.088
Nb of 20hz C range	-0.231	-0.020
altimeter ionosphere	-0.860	-0.835

7.2.2. Conclusion

The lack of MQE threshold on Jason-2 explains the local differences visible in Jason-1 - Jason-2 residus differences for number of elementary C-band range and C-band significant wave height. More detailed studies on MQE threshold can be found at [28].

7.3. AMR incident during cycle 19

During cycle 19, brightness temperatures and radiometer wet troposphere correction were at default values two times:

- from 2009-01-07 11:00:35 to 2009-01-08 03:23:34 impacting passes 24 to 42
- from 2009-01-11 03:56:38 to 2009-01-12 19:26:14 impacting passes 119 to 161

The first time brightness temperatures went to default values on pass 24 at land/ocean transition, the second time on pass 119 over pacific ocean (figure 57). Both times, brightness temperatures did not show any anomaly before going to default values, as visible on figure 58, where Jason-2 and Jason-1 34 GHz brightness temperature are shown.

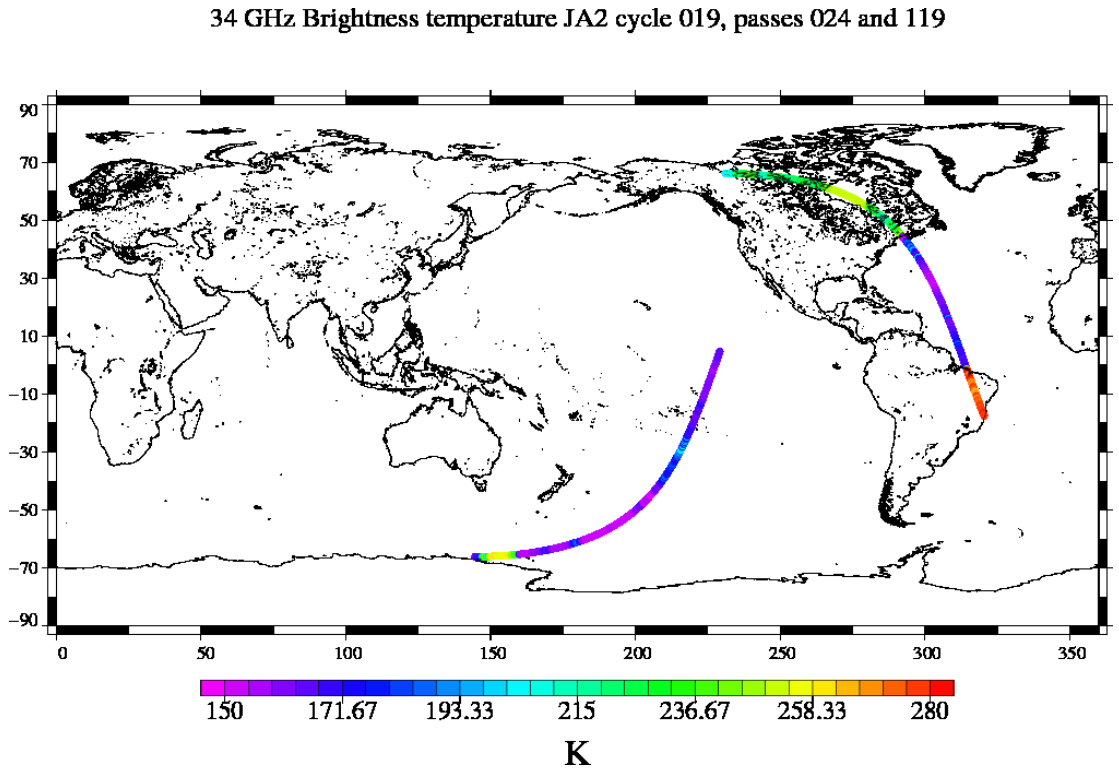

Figure 57: *Map of 34 GHz brigthness temperature for Jason-2 cycle 19 showing location of passes 24 and 119 (passes where incidents started).*

Note that the unavailability of AMR has also a small impact on editing of measurements, other than radiometer wet troposphere correction. Indeed, ice flag also uses brightness temperatures. When they are at default value, a backup is used (based on climatological data). This backup is the same ice flag as used in GDRs version "b" of Jason-1 data. It has the drawback to never detect ice in the far left side of Hudson bay. During the passes with brightness temperatures at default value, ice flag does not detect ice in the far left side of Hudson bay (see figure 59). Nevertheless, these measurements - due to their non-ocean waveforms - are edited by other criteria, such as number of elementary 20 Hz measurements, backscattering coefficient, ocean tide, orbit minus range, ... Therefore for cycle 19, percentage of edited measurements is higher than usual for several threshold criteria (see section 3.2.).

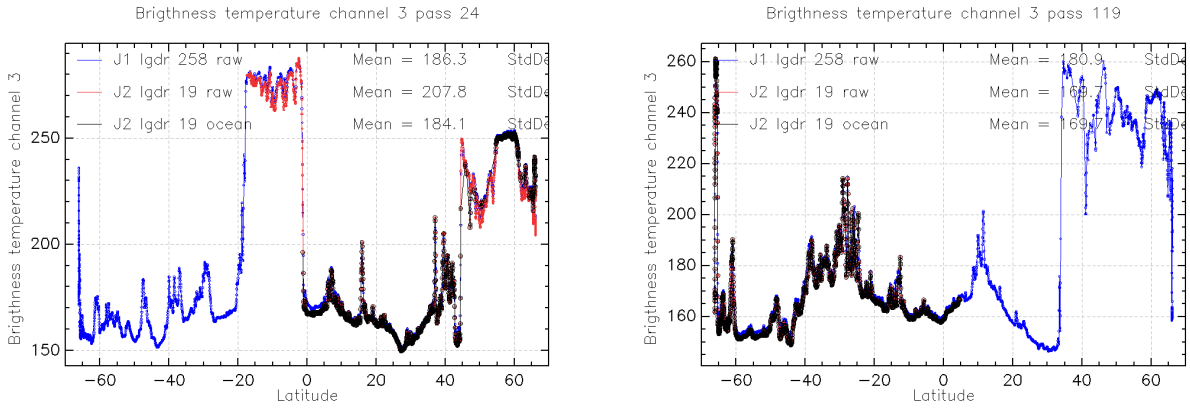

Figure 58: *34 GHz brigthness temperature for Jason-2 in red and black (and Jason-1 in blue) cycle 19 along passes 24 (left) and 119 (right).*

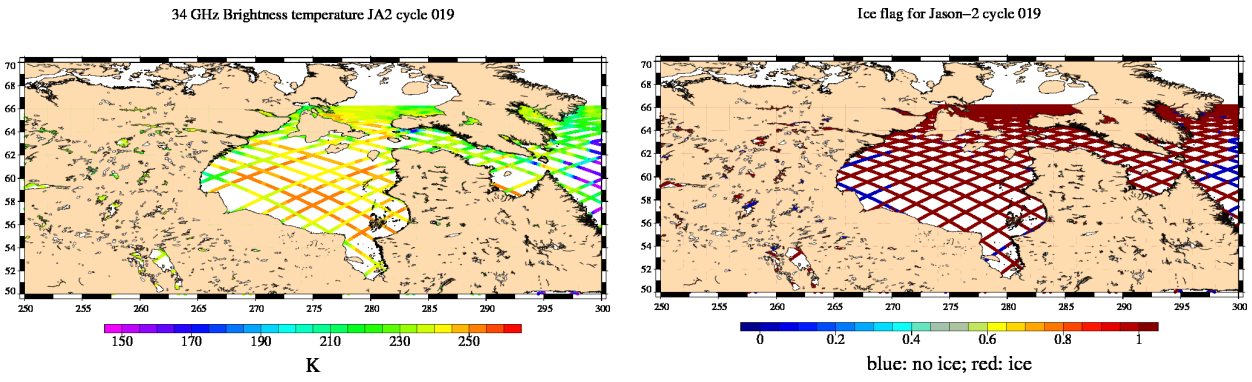

Figure 59: *Map of 34 GHz brightness temperature (left) and map of ice flag (right) in Hudson bay for Jason-2 cycle 19.*

7.4. Impact of different orbit solutions on mean SSH differences at crossovers

Cyclic monitoring of mean SSH differences at crossovers showed for Jason-2 GDRs (figure 60):

- that it mostly has negatif values
- that cycles 33,35, and 36 had particulary negatif values
- that there seems to be a negatif tendancy

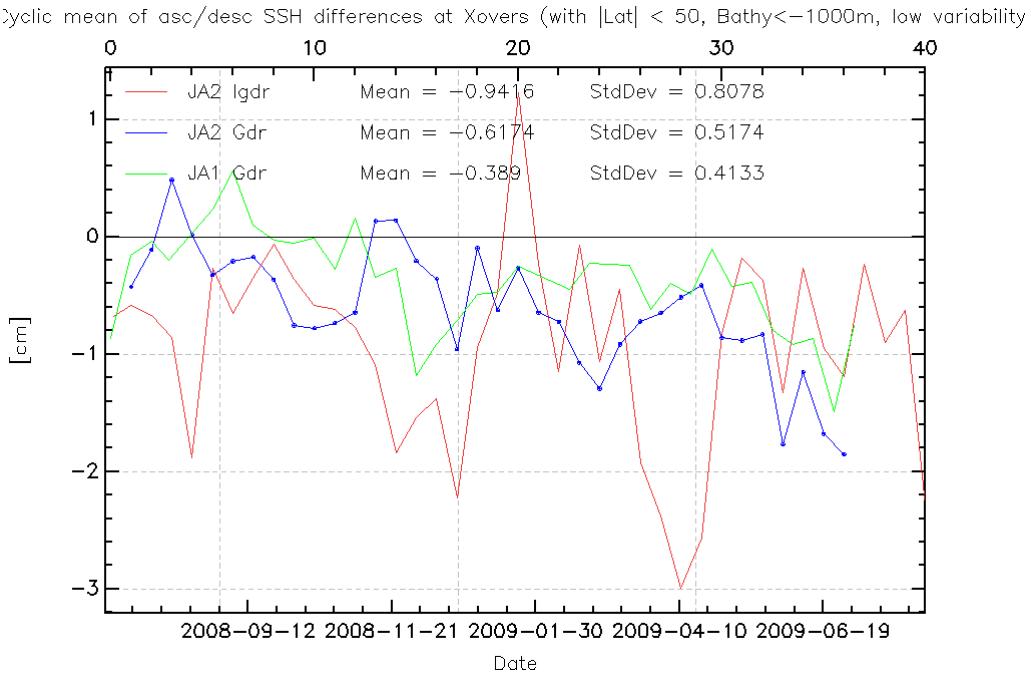

Figure 60: *Cyclic monitoring of mean SSH differences at crossovers for Jason-2 I/GDR and Jason-1 GDR.*

Several GPS only precise orbit solutions provided by CNES and JPL were used to study the impact on mean SSH differences at ascending/descending crossovers. They are listed in table 7.

Orbit	Type	Cycles
POE from GDR product	using Doris, GPS and laser	1 to 40
CNES_g_std040	GPS only standard dynamic	1 to 40
CNES_g_dynred	GPS only reduced dynamic	1 to 32
JPL_rlse09a	GPS only reduced dynamic	1 to 40

Table 7: *Used orbits*

Orbits of Jason-2 GDR products are fully compliant with requirement. Nevertheless, small geographical correlated patterns of amplitudes up to ± 2 cm are visible on maps of mean SSH differences at crossovers (see top left of figure 61). Using reduced dynamic GPS only orbits reduces these small geographical correlated pattern, especially for JPL orbit (see bottom left and right of figure 61). The map highlights only a small hemispheric signal lower than 1 cm between northern and southern hemisphere. This comes from a small pseudo time tag bias (-0.28 ms).

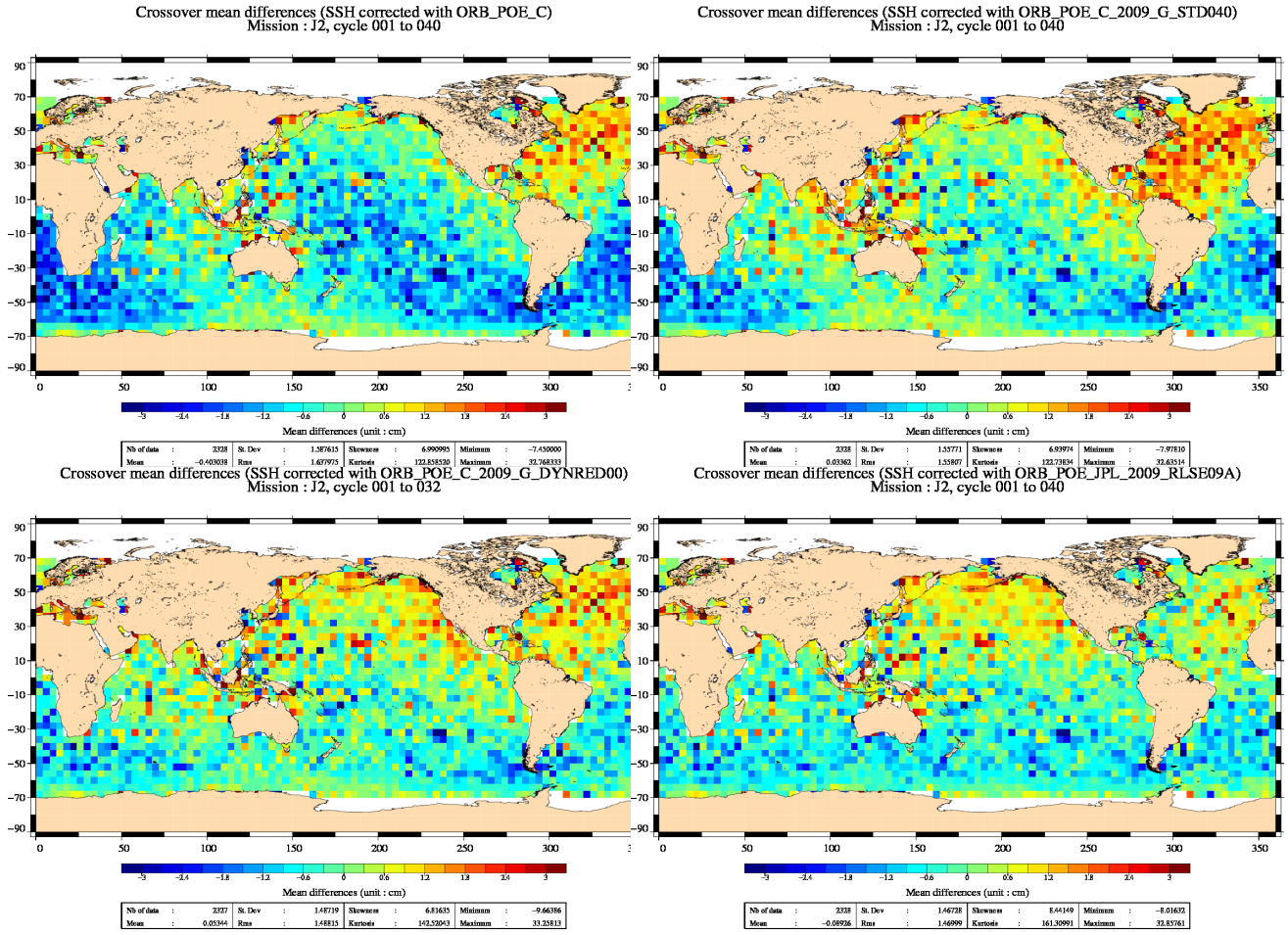

Figure 61: *Map of mean of SSH crossovers differences for Jason-2 using POE from GDR product (top left), CNES GPS only standard dynamic POE (top right), CNES GPS only reduced dynamic POE (bottom left), and JPL GPS only reduced dynamic POE (bottim right). Data cover Jason-2 cycles 1 to 40, except for CNES GPS reduced dynamic POE, which covers cycles 1 to 32.*

Figure 62 shows temporal evolution of mean SSH differences at crossovers. It highlights a 120 day signal for CNES GPS only orbits, whereas JPL GPS only orbits are more stable in time.

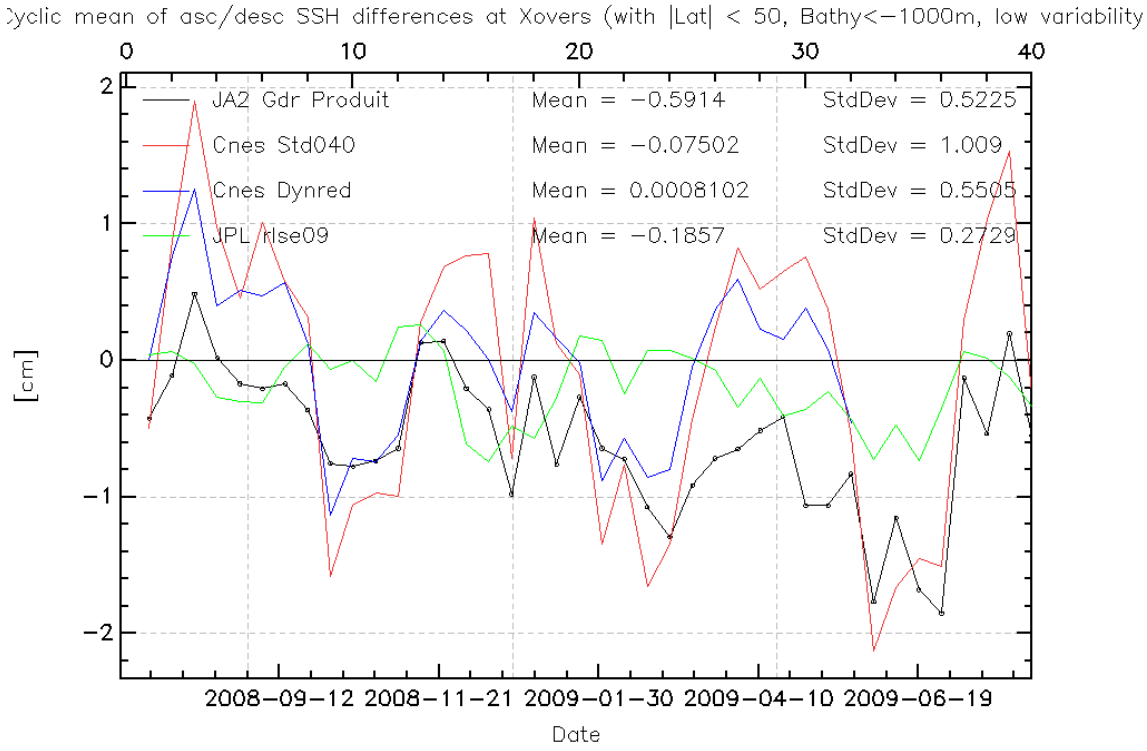

Figure 62: *Cyclic monitoring of mean SSH differences at crossovers for Jason-2 using different POEs.*

8. Conclusion

Jason-2 is in orbit since 20th of June, 2008 flying during the verification phase in tandem with Jason-1 (55s apart) over the same historical TOPEX/Poseidon ground track (till cycle 20). This allows extensive verification and validation of the data, as both satellites observe the same geophysical phenomena. OGDR and IGDR data quality was already approved during OSTST 2008 meeting in Nice. OGDR products were distributed to users since mid-December 2008 and IGDR since mid-January 2009. In addition, the GDR production started end of February 2009 and was released to users since August 2009.

The verification phase has shown that Jason-2 data quality is excellent, at least of the same order as the Jason-1 one. The raw data coverage is similar to Jason-1's over ocean and improved in coastal areas. Thanks to the new altimeter tracking modes, the availability of land measurements is significantly improved. Over ocean, the valid data coverage is similar since the additional Jason-2 raw measurements are removed by the editing procedure. But thanks to studies on going (in PISTACH ans SLOOP projects), we can benefit from these new measurements to calculate the SSH especially in coastal areas and over the rivers and lakes.

The altimetric parameter analysis has shown a similar behavior compared to Jason-1. Some biases exist as between dual-frequency ionosphere correction, but they are stable. Though Advanced Jason-2 radiometer performances are improved especially near coasts, potential stability problems are observed in Jason-2 IGDR product (small jumps (versus JMR) occurred in 34 GHz channel). These potential stability problems are corrected thanks to new ARCS system applied for GDR.

The SSH performances analyzed at crossovers or along-track highlight similar performances between Jason-1 and Jason-2. The consistency between both SLA is remarkable with a small hemispheric signal lower than 0.5 cm. This signal is removed using GSFC orbits proving the sensibility of the orbit calculation for the detection of geographically correlated biases.

The verification phase between Jason-1 and Jason-2 allowed us to check accurately the Jason-2 mission. As during the Jason-1/TOPEX verification phase, we also learned a lot from Jason-1 measurement quality. To balance all these excellent results and especially the quasi-perfect SSH consistency between both missions, both systems can contain similar errors undetectable with the analyzes performed here. Comparisons with external and independent datasets (Tide gauges, Temperature/Salinity profiles, ...) are thus essential to detect potential errors.

Given the very good Jason-2 data quality, the Jason-2 verification phase with Jason-1 ended on 26th of January. At this time, Jason-1 was moved to the interleaved ground track already used by TOPEX. Scientific studies and operational applications therefore benefit from the combination of Jason-2, Jason-1, and Envisat data.

9. References

References

[1] Ablain, M., A. Cazenave, G. Valladeau, and S. Guinehut. 2009 : A new assessment of the error budget of global mean sea level rate estimated by satellite altimetry over 1993-2008. *Ocean Sci*, **5, 193-201**. Available at http://www.ocean-sci.net/5/193/2009/os-5-193-2009.pdf

[2] AVISO and PODAAC User Handbook. IGDR and GDR Jason-1 Products. Edition 4.1, October 2008. SMM-MU-M5-OP-13184-CN (AVISO), JPL D-21352 (PODAAC). Available at http://www.aviso.oceanobs.com/fileadmin/documents/data/tools/hdbk_j1_gdr.pdf.

[3] Bertiger, W., I., Desai, S., Dorsey, A., Haines, B., Harvey, N., Kuang, D., Sibthorpe, A., Weiss, J. 2011. Sub-centimeter Precision Orbit Determination With GPS For Ocean Altimetry. *Marine Geodesy*. Submitted.

[4] Brown G.S., "The average impulse response of a rough surface and its application", *IEEE Transactions on Antenna and Propagation*, Vol. AP 25, N1, pp. 67-74, Jan. 1977.

[5] Brown S., S. Desai, and W. Lu "Initial on-orbit performance assessment of the advanced microwave radiometer and performance of JMR GDR-C", *Oral presentation at OSTST meeting, Nice, France, 9-12 november 2008*. Available at http://www.aviso.oceanobs.com/fileadmin/documents/OSTST/2008/oral/brown_calval.pdf

[6] Brown, S., S. Desai, W. Lu, and A. Sibthorpe. 2009. Performance Assessment of the Advanced Microwave Radiometer after 1 Year in Orbit. *Oral presentation at OSTST meeting, Seattle, USA*. Available at: http://www.aviso.oceanobs.com/fileadmin/documents/OSTST/2009/oral/Brown.pdf

[7] Cerri L., Berthias J.P., Bertiger W., Haines B., Lemoine F.G., Mercier F., Ries J.C., Willis P., Zelensky N.P., Ziebart M., 2010. Precision Orbit Determination Standards for the Jason Series of Altimeter Missions. *Marine Geodesy*. Submitted.

[8] Chambers, D., P., J. Ries, T. Urban, and S. Hayes. 2002. Results of global intercomparison between TOPEX and Jason measurements and models. *Paper presented at the Jason-1 and TOPEX/Poseidon Science Working Team Meeting, Biarritz (France), 10-12 June.*

[9] Commien, L., S. Philipps, M. Ablain and N. Picot. 2009. SSALTO CALVAL Performance assessment Jason-1 GDR "C"/GDR "B". *Poster presented at OSTST meeting, Seattle, USA*. Available at: http://www.aviso.oceanobs.com/fileadmin/documents/OSTST/2009/poster/commien.pdf

[10] DeCarvalho, R., S. Brown, B. Haines and S. Desai. 2009. Global cross calibration and validation of the Jason-1 and Jason-2/OSTM data products. *Oral presentation at OSTST meeting, Seattle, USA*. Available at: http://www.aviso.oceanobs.com/fileadmin/documents/OSTST/2009/oral/deCarvalho.pdf

[11] Desjonqueres, J.-D., G. Carayon, J.-L. Courriere, and N. Steunou "POSEIDON-2 In-Flight results", *Oral presentation at OSTST meeting, Nice, France, 9-12 november 2008*. Available at http://www.aviso.oceanobs.com/fileadmin/documents/OSTST/2008/oral/desjonqueres.pdf

[12] Desjonqueres, J.-D., 2010. POSEIDON-3 altimeter : design, tracking modes. *Marine Geodesy*. Submitted.

[13] Dorandeu.,J., M. Ablain, Y. Faugère, F. Mertz, 2004 : Jason-1 global statistical evaluation and performance assessment. Calibration and cross-calibration results. *Marine Geodesy***27: 345-372.**

[14] Faugère, Y. et al. 2009. The SLOOP project: preparing the next generation of altimetry products for open ocean. *Poster presented at OSTST meeting, Seattle, USA*. Available at: http://www.aviso.oceanobs.com/fileadmin/documents/OSTST/2009/poster/Faugere2.pdf

[15] Jason-2 Version "T" Geophysical Data Records : Public Release, August 2009. Available at : http://www.aviso.oceanobs.com/fileadmin/documents/data/products/Jason-2_GDR_T_disclaimer.pdf

[16] Gourrion, J., Vandemark, D., Bailey, S., Chapron, B., Gommenginger, G.P., Challenor, P.G. and Srokosz, M.A., 2002: A two-parameter wind speed algorithm for Ku-band altimeters, *Journal of Atmospheric and Oceanic Technology*. **19(12) 2030-2048**.

[17] Dumont, J.-P., V. Rosmorduc, N. Picot, S. Desai, H. Bonekamp, J. Figa, J. Lillibridge, R. Sharroo, 2008: OSTM/Jason-2 Products Handbook. CNES: SALP-MU-M-OP-15815-CN. EUMETSAT: EUM/OPS-JAS/MAN/08/0041. JPL: OSTM-29-1237. NOAA/NESDIS: Polar Series/OSTM J400. Available at http://www.aviso.oceanobs.com/fileadmin/documents/data/tools/hdbk_j2.pdf

[18] Hernandez, F. and P. Schaeffer, 2000: Altimetric Mean Sea Surfaces and Gravity Anomaly maps inter-comparisons. AVI-NT-011-5242-CLS, 48 pp. CLS Ramonville St Agne.

[19] Imel, D.A. 1994. Evaluation of the TOPEX/POSEIDON dual-frequency ionospheric correction. *J. Geophys. Res.*, **99, 24,895-24,906**.

[20] Le Traon, P.-Y., J. Stum, J. Dorandeu, P. Gaspar, and P. Vincent, 1994: Global statistical analysis of TOPEX and POSEIDON data. *J. Geophys. Res.*,**99, 24619-24631.**

[21] Ollivier A., Faugere Y., Granier N., 2008: Envisat RA-2/MWR ocean data validation and cross-calibration activities. Yearly report. Technical Note CLS.DOS/NT/09.10, Contract N° SALP-RP-MA-EA-21633-CLS http://www.aviso.oceanobs.com/fileadmin/documents/calval/validation_report/EN/annual_report_en_2008.pdf

[22] Ollivier A., Faugere Y., P. Thibaut, G. Dibarboure, and J.-C. Poisson, 2008: Investigation on the high frequency content of Jason-1 and Jason-2. CLS.DOS/NT/09-027

[23] Peltier, 2004, Global Glacial Isostasy And The Surface of The Ice-Age Earth: The ICE-5G (VM2) Model and GRACE. *Annual Review of Earth and Planetary Sciences*, May 2004, **Vol. 32, Pages 111-149**, doi: 10.1146/annurev.earth.32.082503.144359

[24] Philipps, S., M. Ablain, J. Dorandeu, P. Thibaut, N. Picot and J. Lambin. 2006. SSALTO CALVAL Performance assessment Jason-1 GDR ?B?/GDR ?A?. *Poster presented at OSTST meeting, Hobbart, Australia*. Available at: http://www.aviso.oceanobs.com/fileadmin/documents/OSTST/2006/ablain1.pdf

[25] Thibaut, P. O.Z. Zanifé, J.P. Dumont, J. Dorandeu, N. Picot, and P. Vincent, 2002. Data editing : The MQE criterion. *Paper presented at the Jason-1 and TOPEX/Poseidon Science Working Team Meeting, New-Orleans (USA), 21-23 October.*

[26] Thibaut, P., J.-C. Poisson, A. Ollivier, S. Philipps, and M. Ablain: "Jason-2 waveforms, tracking and retracking analysis", *Oral presentation at OSTST meeting, Nice, France, 9-12 november 2008*. Available at http://www.aviso.oceanobs.com/fileadmin/documents/OSTST/2008/oral/thibaut.pdf

[27] Moreau, T., P. Thibaut, 2009. Etude dépointage Poseidon-3: optimisation de l'angle d'ouverture d'antenne. CLS-DOS-NT-09-028. 15 pp, CLS Ramonville St. Agne.

[28] P. Thibaut. Bilan des activités d'expertise altimétriques menées en 2009 : Lot 2D. SALP-RP-MA-EA-21808-CLS, CLS-DOS-NT-10-029.

[29] Tran, N. et al. 2010. Sea State Bias. *Marine Geodesy*. Submitted.

[30] Valladeau, G., S. Philipps. Jason-1 validation and cross calibration activities (Annual report 2009).SALP-RP-MA-EA-21795-CLS, CLS.DOS/NT/10-005.

[31] Zlotnicky, V. 1994. Correlated environnemental corrections in TOPEX/POSEIDON, with a note on ionomospheric accuracy. *J. Geophys. Res.*, **99, 24,907-24,914**

10. Annex

This annex contains posters presented at OSTST meeting in 2009.

10.1. Poster presented at OSTST meeting 2009

The following posters, presented at OSTST meeting 2009 in Seattle (USA), are also available on Aviso web-site: http://www.aviso.oceanobs.com/en/courses/ostst/ostst-2009-seattle/index.html.

(A) GLOBAL Statistical Jason-2 assessment and cross-calibration with Jason-1 Parameter Analysis

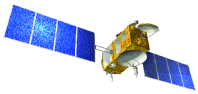

S.Philipps[1], M. Ablain[1], P.Thibaut[1], N.Picot[2]
[1]CLS, Space Oceanography Division, Toulouse, France
[2]CNES, Centre National d'Etudes Spatiales, Toulouse, France

1 Overview

The OSTM/Jason-2 (JA2) satellite was successfully launched on June, 20th 2008. From July, 4th 2008 to January, 26th 2009, Jason-2 was flying in tandem with Jason-1 (JA1), only 55s apart, before JA1 was moved to its new interleaved orbit. This poster assesses the JA2 data quality. Missing and edited measurements are monitored (part 2). Furthermore relevant parameters derived from instrumental measurements and geophysical corrections are analyzed (part 3 to 8). Analyzes are focused on JA1/JA2 cross-calibration since both missions were on the same orbit during the Calibration/Validation phase. This allows us to precisely assess parameter discrepancies between both missions in order to detect geographically correlated biases, jumps or drifts. The SLA performances and consistency with JA1 are described in poster (B).

Used data

The study is conducted for JA2 cycles 1 to 20, corresponding to JA1 cycles 240 to 259. For both satellites GDR (Geophysical Data Records) 1 Hz data are used. For some parameters results from IGDR (Interim Geophysical Data Records) are also presented.

IGDR/GDR

The main differences between Jason-2 IGDR and GDR products are:

	IGDR	GDR
Orbit	MOE (Medium Orbit Ephemeris)	POE (Precise Orbit Ephemeris)
DAC (Dynamical Atmospheric Correction)	Uses non-centered window for filtering	Uses centered window for filtering
Radiometer wet troposphere correction	New AMR characterization file since cycle 023	Same AMR characterization file for entire period
Poseidon-3 AGC tables	New Poseidon-3 characterization file since cycle 023	Same Poseidon-3 characterization file for entire period

Altimeter tracking modes

For Jason-2, two modes of on board tracking are used: Median tracker (for cycles 1,2,4,6,8,9,10,...) and Diode/DEM tracker (for cycles 3,5,7). Cycle 0 and half of cycle 1 was in SGT mode. Most of the following plots integrate all the cycles from 1 to 20. Indeed analysis of parameters obtained during cycles with different tracking modes does not reveal any particular behavior linked to the tracking mode.

2 Missing and Edited measurements

Over open ocean, JA2 and JA1 data coverage are very similar. Few missing measurements are however detected for Jason-2 over ocean, mostly due to station acquisition problems (cycle 001 pass 44-46, cycle 003 pass 33-34, cycle 005 pass 237-240). Note that from 7th to 20th of August 2008 and 26th of January to 10th of February 2009, no measurements are available for Jason-1. Over ice, coastal and hydrological zones, JA2 is much better than JA1 due to new tracker algorithms (Median and Diode/DEM).

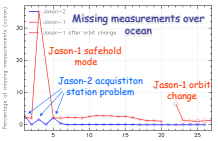

For open ocean calval, the same editing procedure is applied for both satellites. Percentage of edited measurements is very similar, since approximately 16% (~12% due to ice flag and ~3% due to parameters out of thresholds) of ocean Jason-2 measurements are edited for each cycle. Till upload (during cycle 016) of correction for low signal tracking anomaly, small portions of a pass were sometimes edited in median mode, due to AGC, Sigma0, waves and apparent mispointing out of threshold.

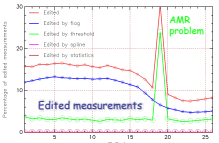

3 Backscattering coefficient

The JA2 backscattering coefficient (Sig0) shows good agreement with JA1 in Ku and C bands as plotted in map of mean differences (fig. 1) and in daily monitoring (fig. 2). The global bias with JA1 is weak (0.14 dB in Ku-band and 0.2 dB in C-band). Bias is slightly higher for GDR than for IGDR, as altimeter characterization file has changed (part 1). In comparison, the global bias between JA1 and T/P was about 2.4 dB. Notice that a small signal (0.1 dB) in both Ku- and C-band differences is detected in daily monitoring (fig. 2). It is correlated to increased JA1 mispointing (fig. 9).

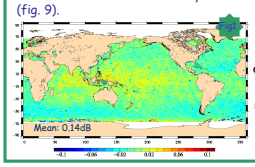

Map of JA1-JA2 Ku-band Sigma0 differences (mean over cycles 1 to 20) (fig. 1). Daily monitoring showing mean of JA1 - JA2 Sig0 difference (fig. 2).

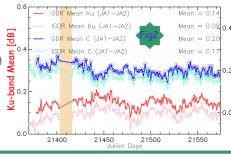

4 Wet troposphere correction

JA2 radiometer wet troposphere correction in GDR product is very stable and without drift versus ECMWF model, as visible on fig. 3. Behavior of AMR (JA2) and JMR (JA1) far away from coast is similar (fig.4), with AMR staying more stable than JMR when approaching coast related to different antenna properties.

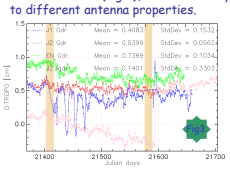

Mean of radiometer - model wet troposphere correction per day (fig.3) and in function of coast distance (fig.4).

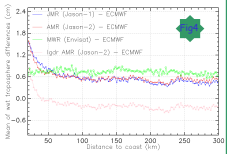

After the Jason-1 safehold, difference of JMR - AMR radiometer wet troposphere correction (fig. 5) shows a signal up to 7 mm amplitude. The reason is unknown, but caused by JMR, as visible when comparing with ECMWF model (fig. 3). For IGDR, JMR-AMR difference showed a drift, which was probably caused by AMR 34 GHz channel (fig. 6). 34 GHz JA1 -JA2 difference shows jumps which are often, but not always correlated with yaw maneuvers. In GDR products, a different AMR characterization file than for 22 first IGDR (part 1), as well as ARCS system was used. Therefore drift of 34 GHz channel is removed and AMR radiometer wet troposphere correction put at the level of JMR. But there might be a risk that real geophysical signals are removed, when correcting AMR in GDRs.

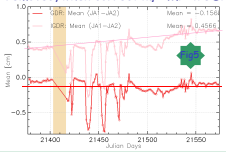

Daily monitoring of JA1-JA2 radiometer correction (fig.5) and JA1-JA2 34GHz brightness temperature (fig. 6).

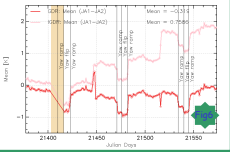

5 Significant Wave Height

The Significant Wave Height (SWH) shows very good agreement between JA2 and JA1 (fig. 7). Daily monitoring (fig. 8) of mean and std of JA1-JA2 SWH differences shows no drift neither for Ku-band nor for C-band. Waves between JA1 and JA2 are more coherent in Ku-band than in C-band. Mean of JA1-JA2 SWH differences are : -1.1 cm (Ku-band) and -0.7 cm (C-band). Std of JA1-JA2 SWH differences are : 17.2 cm (Ku-band) and 43.2 cm (C-band). Mean Ku-band SWH difference between T/P and JA1 was 8.9 cm. Weak regional differences around Indonesia (fig. 7) are very likely explained by the difference of MQE editing criteria used for both missions during 20 Hz to 1 Hz compression.

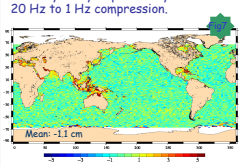

Map of JA1-JA2 Ku-band Sigma0 differences (mean over cycles 1 to 20) (fig.7). Daily monitoring showing mean of JA1 - JA2 SWH difference (fig.8).

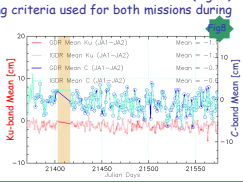

6 Apparent squared mispointing from waveforms

Daily monitoring of apparent squared mispointing from JA2 waveforms is much more stable than JA1 (see fig.9). This is due to reduced star tracker availability for JA1 which leads to a poorer pointing of the satellite. The JA2 satellite has no real mispointing, but mean value of apparent squared mispointing is around 0.012 deg2 (0.11 deg). This value is understood and can be updated in a next product version (see P.Thibaut talk: Jason-2 instrumental and processing status)

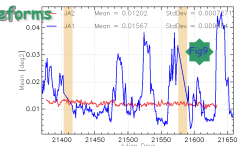

Daily monitoring of JA1 and JA2 apparent squared mispointing (from waveforms) (fig. 9).

7 Altimeter ionospheric correction

The map of mean differences over cycles 1 to 20 (fig. 10) shows that altimeter ionospheric correction of JA1 and JA2 are in good agreement. Note that the global bias is -0.9 cm (under investigation), but it is stable (fig. 11) with small variations up to 2 mm from one day to another. As for other altimeter parameters, differences are slightly higher in some regions like Indonesia (MQE criteria are not the same for JA1 and JA2).

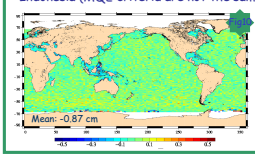

Map of JA1 - JA2 ionospheric correction, mean over cycles 1 to 20, except for cycle 4 (fig. 10). Daily monitoring of JA1-JA2 (filtered) altimeter ionospheric correction (fig. 11).

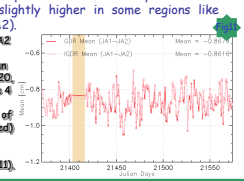

8 Altimeter wind speed

Difference of JA1-JA2 altimeter wind speed is quite stable with only small variations (fig.12). But wind speed histograms for JA1, JA2 altimeter and ECMWF model show different shapes (fig.13). JA1 and JA2 have slightly different backscattering coefficients (part 3), which impacts altimeter wind speed. This behavior should be investigated in more detail. Note that differences between JA2 IGDR and GDR are due to different altimeter characterization files (part 1).

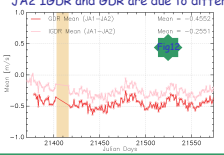

Daily monitoring of JA1-JA2 altimeter wind speed (fig. 12). Histogram of JA1, JA2 altimeter and ECMWF model wind speed for JA2 cycle 20 (fig.13)

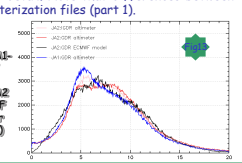

Conclusion

This study, using 20 cycles of Jason-2 flying in tandem with Jason-1, shows the very good consistency between altimetric parameters of JA1 and JA2.

Thanks to new AMR characterization files and ARCS system, drifts in JA2 radiometer (AMR) are corrected in GDRs, improving the stability of radiometer wet troposphere correction. Nevertheless, there is a risk that real geophysical signals might be removed. Furthermore, the new JA2 DEM tracking mode (used during cycles 3, 5, and 7) shows no impact on parameter analysis of 1 Hz ocean measurements. The very small differences observed do not impact the SSH computation (see poster B).

Finally, from the Cal/Val parameter analysis point of view, JA2 has excellent data quality.

Collecte Localisation Satellites
8-10 rue Hermes
31520 Ramonville Saint-Agne - France

OSTST
Seattle, June 2009

Figure 63: *Poster presented at OSTST meeting, Seattle 2009*

(B) GLOBAL Statistical Jason-2 assessment and cross-calibration with Jason-1 SLA Performances and Consistency

M. Ablain[1], S. Philipps[1], N.Picot[2]

[1]CLS, Space Oceanography Division, Toulouse, France
[2]CNES, Centre National d'Études Spatiales, Toulouse, France

Overview

This study aims at presenting the Jason-2 (JA2) and Jason-1 (JA1) SLA performances and consistency. Analysis are concentrated on first 20 cycles, when JA1 and JA2 were on the same orbit, only 55 seconds apart. On the one hand, SSH crossovers analyses provide the global performances of the Jason-2 system using IGDR and GDR products. Performances with similar Jason-1 statistics are compared. On the other hand, along-track analyses allow us to check the SLA consistency between both missions. Peculiar attention is paid on the global SSH bias and correlated geographically SSH bias using MOE and POE orbits.

Data used for Jason-1 and Jason-2		
Products	Jason-1	Jason-2
IGDRs	Cycles 240 to 259/267/272	Cycles 1 to 20/28/33
GDRs	Cycles 240 to 259/267	Cycles 1 to 20/28

Along track SLA analyses

Cycle by Cycle monitoring

The global SSH bias between Jason-1 minus Jason-2 is -8.3 +/- 0.2 cm using MOE or POE orbits for both satellites (Fig. 1), and without using any correction in SSH calculation. It is very stable with weak variations around 0.2 cm. Applying all the usual correction (not shown here), the bias is reduced close to -7.5 cm, mainly due to the altimeter ionospheric bias between Jason-1 and Jason-2.
The standard deviation of global SLA differences is also very stable and weak over all the Jason-2 period (fig.2) with figures close to 4.0 cm RMS using MOE orbits and 3.5 cm RMS using POE orbits.

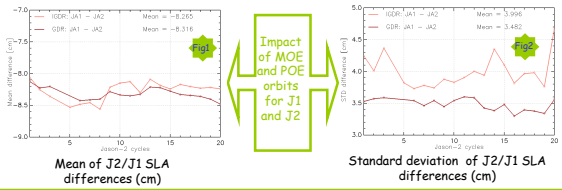

Mean of J2/J1 SLA differences (cm)

Standard deviation of J2/J1 SLA differences (cm)

Spatial Analyses

The map of mean of Jason-1/Jason-2 SLA differences over cycles 1 to 20 from IGDR products highlight correlated geographical biases as plotted in figure 3, ranging between +/- 3 cm. As expected, these patches are almost completely removed using POE orbits (fig. 4), showing the very good consistency between both missions. However, very weak hemispheric structures remain with an amplitude close to 1 cm (fig. 8). They are very likely related to the orbit calculation. In addition, the structures observed using MOE orbit vary in space and in amplitude from one cycle to another as shown by the analyze of the temporal variability of the SLA differences (fig. 5). Using POE orbit, these variations are significantly reduced (fig. 6).

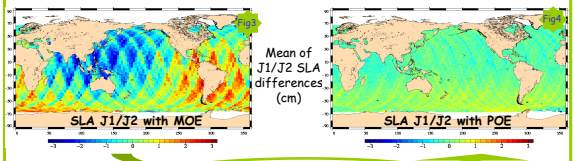

Mean of J1/J2 SLA differences (cm)

Impact of Jason-1 and Jason-2 POE orbits

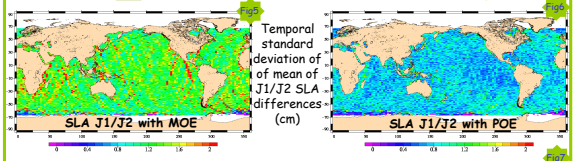

Temporal standard deviation of of mean of J1/J2 SLA differences (cm)

The standard deviation of SLA difference is, as expected, mainly depending on the SWH (fig. 7). This is explained by the 1-Hz SSH noise higher in strong SWH area due the ground processing. No abnormal feature is highlighted, showing the good consistency of both SLA between 3 and 5 cm RMS.

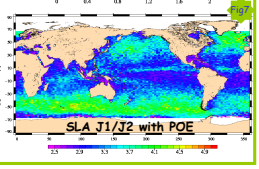

Standard deviation of J1/J2 SLA differences (cm)

Small hemispheric bias between JA2 and JA1 GDR

POE of JA1 and JA2 are in good agreement, there is however a small hemispheric bias (+/- 1cm) in the map of JA1 - JA2 SLA differences (fig. 8). This bias is also visible on cyclic monitoring separated for hemispheres (fig. 9). This bias, relatively strong during first cycles, varies with time. It is probably caused by differences in orbit solutions (no more GPS data for Jason-1).

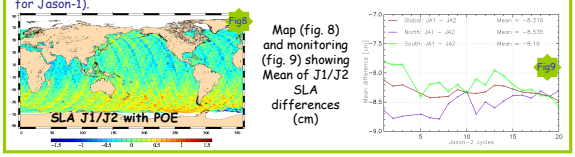

Map (fig. 8) and monitoring (fig. 9) showing Mean of J1/J2 SLA differences (cm)

SSH Crossovers analyses

Cycle by Cycle monitoring

The monitoring of Jason-2 (corrected) SSH statistics at crossovers are very good. A slight improvement is observed using Jason-2 IGDRs in comparison with Jason-1 : SSH crossover mean is equivalent (fig 1), but SSH crossover standard deviation is reduced (5.4 cm RMS for JA2 instead of 5.5 cm RMS for JA1 (fig.3)). Nevertheless, standard deviation of Jason-2 seems to show an increasing trend. Results for GDR products are equivalent for Jason-2 and Jason-1 with SSH crossover mean more homogeneous than for IGDR and standard deviation close to 5.0cm.
Concerning multi-mission SSH crossovers (JA1 - JA2), coherence between the two missions is improved for GDR (5.1 cm) versus IGDR (5.6 cm) (fig. 4). Note that mean of IGDR SSH crossovers displays a jump at cycle 23, due to new AMR characterization files (see poster A).

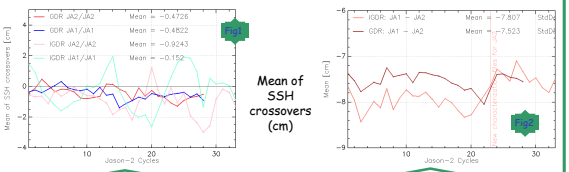

Mean of SSH crossovers (cm)

Impact of MOE and POE orbits for J1 and J2 (Mono-mission)

Impact of MOE and POE orbits for J1 and J2 (Multi-mission)

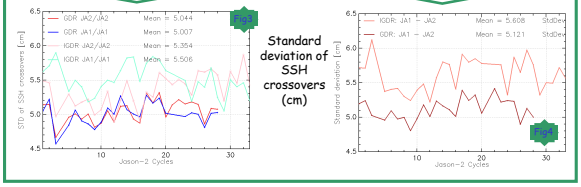

Standard deviation of SSH crossovers (cm)

Spatial Analyses over all the period

The map (over cycles 1 to 28) of SSH crossovers mean is more homogeneous for Jason-2 (fig. 5) than for Jason-1 (fig.6) using IGDR products. Concerning GDR products, maps of SSH crossovers mean are very similar for both Jason-2 and Jason-1 (fig. 7 and 8), with a weak geographical pattern in North Atlantic. These items bring out the very good quality of Jason-2 SSH for both GDR and IGDR products, as well as the good consistency between POE of Jason-1 and Jason-2.

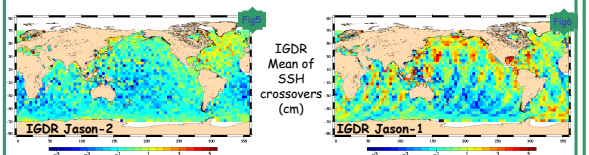

IGDR Mean of SSH crossovers (cm)

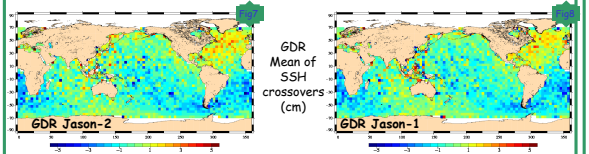

GDR Mean of SSH crossovers (cm)

Conclusion

In this study, we show the good performances of Jason-2 SSH in the same order (GDR) or better (IGDR) than Jason-1 ones. In addition, the SLA consistency between both missions is very good. The weak remaining SLA differences observed by hemisphere using the POE orbits (around 1 cm) are likely due to the orbit calculation differences between both missions. The ageing of Jason-1 (no more GPS data) explains very likely these differences.
The excellent data quality of Jason-2 allows to continue studies of Mean Sea Level evolution and assures a seamless transition with Jason-1 data.

Collecte Localisation Satellites
8-10 rue Hermes
31520 Ramonville Saint-Agne - France

OSTST
Seattle, June 2009

Figure 64: *Poster presented at OSTST meeting, Seattle 2009*

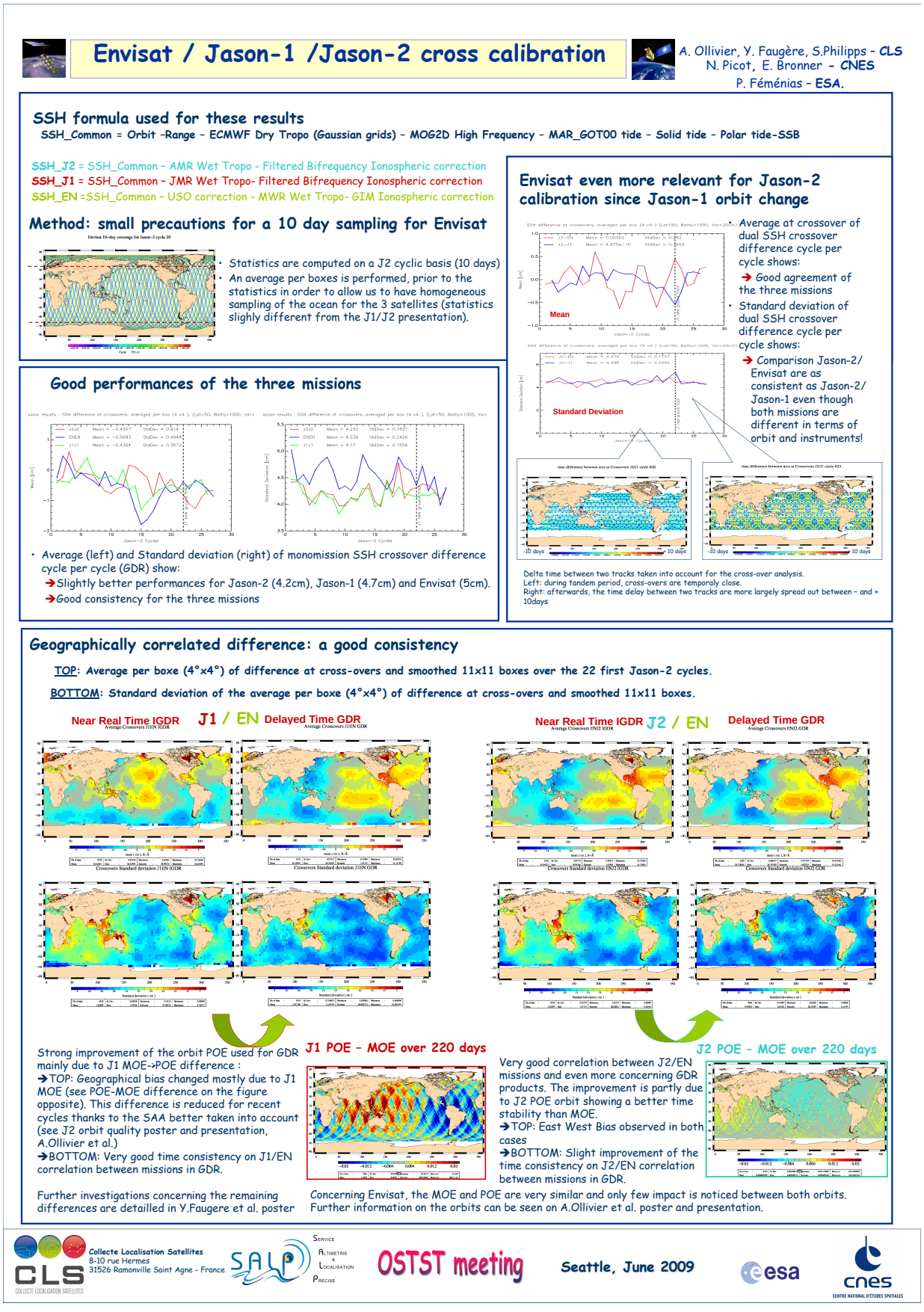

Figure 65: *Poster presented at OSTST meeting, Seattle 2009*

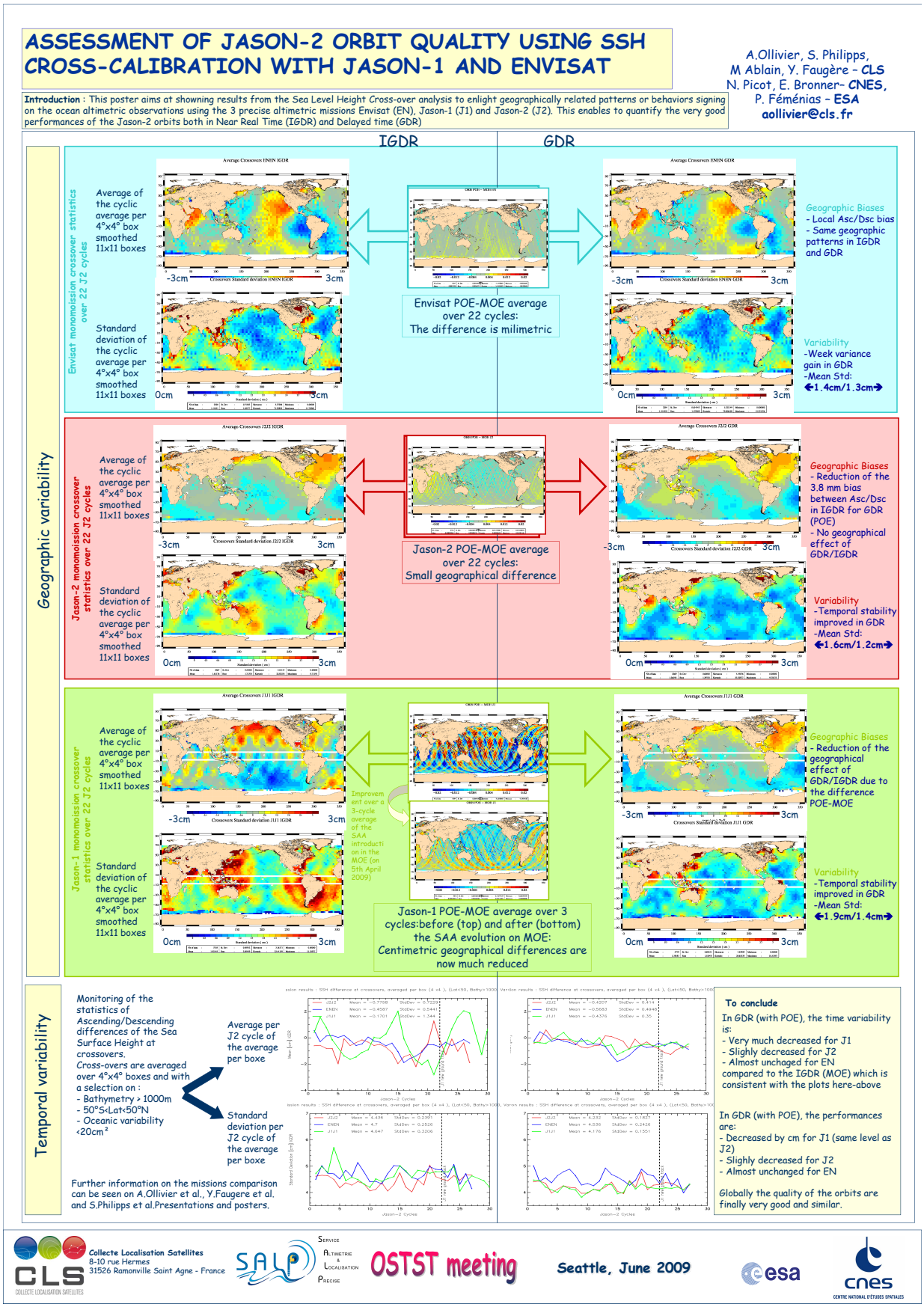

Figure 66: *Poster presented at OSTST meeting, Seattle 2009*